People's Democratic Republic of Algeria
وزارة التعليم العالي والبحث العلمي
Ministry of Higher Education and Scientific Research
جامعة الشهيد شيخ العربي التبسي تبسة
Echahid Cheikh Larbi Tebessi University – Tebessa
معهد المناجم
Mining Institute
قسم المناجم والجيوتكنولوجيا
Department of mines and geotechnology
A dissertation submitted in partial fulfilment of the requirement for
the award of the degree of Master in mining engineering
Specialty: Geotechnics

Slope Benches Stability Assessment and Hydrological Effects in Large Open pit mine, kef Essnoun case study.

Presented by: BOUTRA Abir

Jury Members

HAMDANE Ali	**Chairman**	**MAA**	**Echahid Cheikh Larbi Tebessi University – Tebessa**
BRAHMI Serhane	**Supervisor**	**MCB**	**Echahid Cheikh Larbi Tebessi University – Tebessa**
BERRAH Yacine	**Co-supervisor**	**MCA**	**Echahid Cheikh Larbi Tebessi University – Tebessa**
BENGHAZI Zied	**Examiner**	**MCB**	**Echahid Cheikh Larbi Tebessi University – Tebessa**

2023/2024

Année universitaire : 2023/2024   Tébessa le : 06/06/2024

Lettre de soutenabilité

Noms et prénoms des étudiants : **BOUTRA Abir**

Niveau : **Master 2**   Option : **Géotechnique**

Thème : **Slope bench stability assessment and hydrological effects in large open pit mine, Kef Essnoun case study.**

Nom et prénom de l'encadreur : Dr **BRAHMI Serhene** et Dr **BERRAH Yacine**.

Chapitres réalisés	Signature de l'encadreur
Slope stability causality and effects	
Geology, hydrogeology and climatic conditions	
Geotechnical investigation and data collection	
Geological and geotechnical modeling and safety analysis	

i

الجمهورية الجزائرية الديمقراطية الشعبية
وزارة التعليم العالي والبحث العلمي

مؤسسة التعليم العالي : جامعة الشهيد الشيخ العربي التبسي – تبسة

تصريح شرفي
خاص بالالتزام بقواعد النزاهة العلمية لانجاز بحث

أنا الممضي أدناه،

السيد (ة).......بوتوبنت كبير.......الصفة : طالب، أستاذ باحث، باحث دائم : ....طالب السيد........

الحامل لبطاقة التعريف الوطنية رقم : ......4a.14.3.1.17.9...... و الصادرة بتاريخ .....14..04..2022..
المسجل بمعهد ......المناجم....... قسم...المناجم والجيوتكنولوجيا....
و المكلف بانجاز أعمال بحث (مذكرة التخرج، مذكرة ماستر، مذكرة ماجستير، أطروحة دكتوراه)، عنوانها :

.......safe bench stability assessment and hydrological.......
.......effects in large open pit mine kef Essnoun case study.......

أصرح بشرفي أني ألتزم بمراعاة المعايير العلمية و المنهجية و معايير الأخلاقيات المهنية و النزاهة الأكاديمية
المطلوبة في انجاز البحث المذكور أعلاه.

التاريخ:............

إمضاء المعني (ة)

UNIVERSITÉ LARBI TEBESSI - TÉBESSA   جامعة العربي التبسي-تبسة

INSTITUT des Mines   معهد المناجم

تبسة في: ...../...../2020   رقم: 5.36..../ج.ع.ت.ت/م.م/2020
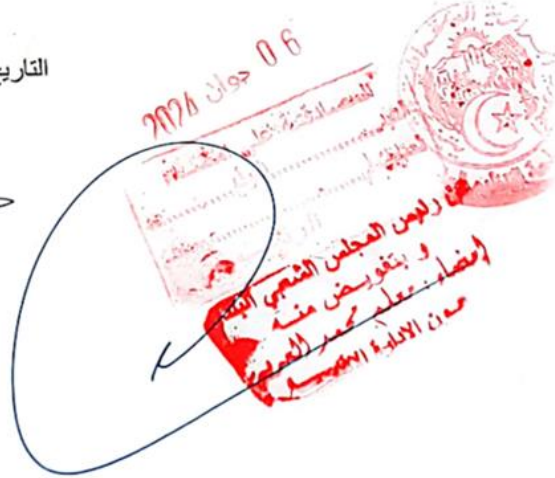
رفـــــع التحفظـــــات

اسم و لقب الأستاذ المنــــاقش : .... حميادي علي ....

عنــــوان المذكرة : Safe benches Stability assessment and hydrological effects in large open pit mine, Kef Essennoun case study

الطلبة :

1- .... عبير بوبكر ع ....

2- .... ✓ ....

التخصص : .....جيوتقنية.....، القسم: ....المناجم و الجيوتكنولوجيا.....

☑ موافق على وضع المذكرة في المكتبة بعد إجراء التصحيح المطلوب

☐ موافق على وضع المذكرة في المكتبة و هي معفية من التصحيح

إمضاء الأستاذ المناقش

الجمهورية الجزائرية الديمقراطية الشعبية

وزارة التعليم العالي والبحث العلمي

جامعة العربي التبسي- تبسة

مقرر رقم : ١٦١٤ مؤرخ في : 0 9 جوان 2024

يتضمن تعيين لجنة مناقشة مذكرة الماستر

إن مدير جامعة العربي التبسي بتبسة.

- بموجب القرار الوزاري رقم 318 و المؤرخ في 05 ماي 2021 المتضمن تعيين السيد "قواسمية عبد الكريم" مديرا لجامعة العربي التبسي - تبسة.
- و بمقتضى المرسوم التنفيذي رقم : 12- 363 مؤرخ في 8 أكتوبر 2012، يعدل و يتمم المرسوم التنفيذي رقم 09 - 08 المؤرخ في : 04 جانفي 2009 و المتضمن إنشاء جامعة العربي التبسي بتبسة.
- ويمقتضى المرسوم التنفيذي رقم 08-265 المؤرخ في 17 شعبان عام 1429 الموافق 19 غشت سنة 2008 الذي يحدد نظام الدراسات للحصول على شهادة الليسانس وشهادة الماستر وشهادة الدكتوراه. لاسيما المادة 9 منه.
- وبموجب القرار رقم 362 المؤرخ في 09 جوان 2014 الذي يحدد كيفيات إعداد ومناقشة مذكرة الماستر. لاسيما المادتان 10 و11 منه.
- وبموجب القرار رقم 1080 المؤرخ في 13 أكتوبر 2015 والمتضمن تأهيل ماستر الفروع ذات تسجيل وطني بجامعة تبسة.
- وبموجب القرار رقم 375 المؤرخ في 15 جوان 2020 المعدل للملحق القرار 1080 المؤرخ في 13 أكتوبر 2015 والمتضمن تأهيل ماستر الفروع ذات تسجيل وطني بجامعة تبسة. اختصاص
- وبعد الاطّلاع على محضر المجلس العلمي لمعهد المناجم المؤرّخ في : ....1.....2...جانفي....... 2024

يقرر ما يأتي:

المادة الأولى: نُعيّن بموجب هذا المقرر لجنة مناقشة مذكرة الماستر المحضّرة من طرف الطّالب :

بوترعة عبير. المولود (ة) بتاريخ: 1999/07/01-تبسة

والموسُومة ب

Slope bench stability assessment and hydrological effects in large open pit mine, kef Essenoun case study

والمسجّل (ة) بمعهد **المناجم**

المادة 2: تتشكّل اللجنة المشار إلها في المادة الأولى من الأعضاء الآتي ذكرهم:

الصّفة	مؤسّسة الانتماء	الرّتبة	الاسم واللّقب	رقم
رئيسا	جامعة العربي التبسي - تبسة	أستاذ مساعد أ	حمدان علي	1
المؤطر	جامعة العربي التبسي - تبسة	أستاذ محاضر ب	براهمي سرحان	2
ممتحنا	جامعة العربي التبسي – تبسة	أستاذ محاضر ب	بن غازي زياد	3

المادة 3: يكلّف رئيس قسم المناجم والجيوتكنولوجيا بتنفيذ هذا المقرر الذي يُسلّم عنه نسخةٌ إلى كلّ من الطّالب المعني والمشرف على المذكرة وأعضاء لجنة المناقشة فور توقيعه.

المادة 4: تحفظ نسخة عن هذا المقرر في الملفّ البيداغوجي للطالب المعني، وينشر في النّشرة الرّسمية لجامعة العربي التبسي.

حُرّر ب تبسة، في : ....0 9 جوان...... 2024

عن المدير ، وبتفويض منه

مدير معهد المناجم

الجمهورية الجزائرية الديمقراطية الشعبية

وزارة التعليم العالي و البحث العلمي

جامعة العربي التبسي- تبسة

مقرر رقم: ٦٦١ ٱ مؤرخ في 9 0 جوان 2024

يتضمن الترخيص بمناقشة مذكرة الماستر

ان مدير جامعة العربي التبسي بتبسة.

- بموجب القرار الوزاري رقم 318 و المؤرخ في 05 ماي 2021 المتضمن تعيين السيد "قواسمية عبد الكريم" مديرا لجامعة العربي التبسي - تبسة.

- وبمقتضى المرسوم التنفيذي رقم : 12- 363 مؤرخ في 8 أكتوبر 2012. يعدل و يتمم المرسوم التنفيذي رقم 09 - 08 المؤرخ في : 04 جانفي 2009 و المتضمن إنشاء جامعة العربي التبسي بتبسة.

- وبمقتضى المرسوم التنفيذي رقم 08-265 المؤرخ في 17 شعبان عام 1429 الموافق 19 غشت سنة 2008 الذي يحدّد نظام الدراسات للحصول على شهادة الليسانس وشهادة الماستر وشهادة الدّكتوراه. لاسيما المادة 9 منه.

- وبموجب القرار رقم 362 المؤرّخ في 09 جوان 2014 الذي يحدّد كيفيات إعداد ومناقشة مذكرة الماستر. لاسيما المادة 7 منه.

- وبموجب القرار رقم 1380 المؤرّخ في 09 أوت 2016 والمتضمّن تأهيل مؤسسات التعليم العالي لضمان التكوين لنيل شهادة الماستر اختصاص جيوتقني بعنوان السّنة الجامعية 2024/2023،

- وبموجب المقرر رقم 485 المؤرّخ في 9 0 جوان 2024 والمتضمّن تعيين لجنة مناقشة مذكرة الماستر.

- وبعد الاطّلاع على مقرر تعيين لجنة مناقشة مذكرة الماستر المؤرّخ في 9 0 جوان 2024

يقرر ما يأتي:

المادة الأولى: يُرخّصُ للطالب(ة) بوترعة عبير. المولود (ة) 1999/07/01 تبسة .بمناقشة مذكرة الماستر والموسومة ب

Slope bench stability assessment and hydrological effects in large open pit mine, kef Essenoun case study

المادة 2: يكلّف رئيس قسم المناجم و الجيوتكنولوجيا بتنفيذ هذا المقرّر الّذي يسلّم عنه نسخة إلى الطّالب المعني بالمناقشة وأعضاء لجنة المناقشة فور توقيعه. وبضمان نشره عبر فضاءات المؤسّسة المادية والرقمية.

المادة 3: تُحفظ نسخة عن هذا المقرر ضمن الملفّ البيداغوجي للطّالب المعني وينشر في النّشرة الرّسمية لجامعة العربي التبسي.

حُرّر ب تبسة، في: 9 0 جوان 2024

عن المدير ، وبتفويض منه

مدير معهد المناجم

Abstract

The stability of slope benches in large open-pit mines is paramount to ensuring mine safety and operational efficiency. This study aims to investigate the safety of slope benches in the Kef Essnoun phosphate deposits, extracted from a large open-pit mine, by examining the interaction between geological, geotechnical, and hydrological factors that affect slope stability. Through a comprehensive methodology, the structural geology and tectonics of the area are analyzed, emphasizing the main lineaments, beddings, joints, and other discontinuities. Advanced techniques such as stereographic projection, rosette plot analysis, and kinematic analysis are employed to classify discontinuities and identify potential slope movements. The study also evaluates the hydrological impacts, particularly rainfall, on open-pit mine stability. Geomechanical rock classification with different methods and system and various mapping techniques using ArcGIS are utilized to visualize geological and hydrological features. Additionally, 3D and 2D geological modeling with GEOVIA Surpac and numerical simulation using PLAXISv23 (2D and 3D) provide detailed visualization facilitating all description, and introducing exceptionally rainfall models as main parameters for stability analysis and mechanical behavior predictions for any geological cross-section orientation. Different calculations using various input parameters and behavior models allow for the identification of the impact of discontinuities, rainfall, and infiltration on mine slope stability. This integrative methodology and approach offer a thorough assessment of slope stability, aiming to enhance safety and management practices in large open-pit mines.

Keywords: Slope stability, large open-pit mine, geotechnical investigation, hydrological analysis, 3D geological modeling, kinematic and numerical analysis, Kef Essnoun.

Résumé

La stabilité des gradins de pente dans les grandes mines à ciel ouvert est primordiale pour garantir la sécurité de la mine et l'efficacité opérationnelle. Cette étude vise à examiner la sécurité des gradins de pente des gisements de phosphate de Kef Essnoun, extraits d'une grande mine à ciel ouvert, en analysant l'interaction entre les facteurs géologiques, géotechniques et hydrologiques qui affectent la stabilité des pentes. À travers une méthodologie complète, la géologie structurale et la tectonique de la région sont analysées, en mettant l'accent sur les principaux linéaments, couches, joints et autres discontinuités. Des techniques avancées telles que la projection stéréographique, l'analyse des diagrammes en rosette et l'analyse cinématique sont employées pour classifier les discontinuités et identifier les mouvements potentiels des pentes. L'étude évalue également les impacts hydrologiques, en particulier les précipitations, sur la stabilité des mines à ciel ouvert. La classification géomécanique des roches et diverses techniques de cartographie, utilisant ArcGIS, sont utilisées pour visualiser les caractéristiques géologiques et hydrologiques. De plus, la modélisation géologique en 3D et 2D avec GEOVIA Surpac et la simulation numérique utilisant PLAXISv23 2D et 3D fournissent des modèles détaillés de précipitations pour l'analyse de la stabilité et les prédictions de comportement mécanique pour toute orientation de coupe géologique. Différents calculs effectués en utilisant différents paramètres d'entrée et modèles de comportement permettent d'identifier l'effet des discontinuités et des précipitations ainsi l'infiltration sur la stabilité des pentes de la mine. Cette méthodologie et ces approches intégratives offrent une évaluation approfondie de la stabilité des pentes, visant à améliorer les pratiques de sécurité et de gestion dans les grandes mines à ciel ouvert.

Mots clés : Stabilité des pentes, grande mine à ciel ouvert, analyse hydrologique, modélisation géologique 3D, analyse cinématique et numérique, Kef Essnoun.

ملخص

ثبات المدرجات في المنحدرة المناجم الكبيرة المفتوحة هو أمر أساسي لضمان سلامة المنجم وكفاءة عمليات الاستغلال. تهدف هذه الدراسة إلى فحص سلامة المدرجات المنحدرة في رواسب الفوسفات في كاف السنون، المستخرجة من منجم كبير مفتوح، من خلال تحليل التفاعل بين العوامل الجيولوجية والجيوتقنية والهيدرولوجية التي تؤثر على استقرار المنحدرات. من خلال منهجية شاملة، يتم تحليل الجيولوجيا الهيكلية والتكتونية للمنطقة، مع التركيز على التصدعات الرئيسية، التشققات والاسطح الرئيسة للتقسيم الطبقي، الوصلات وغيرها. تُستخدم تقنيات متقدمة مثل الإسقاط الستيريوغرافي، تحليل مخطط الزهري والتحليل الحركي لتصنيف الفواصل وتحديد الحركات المحتملة للمنحدرات. كما تقيم الدراسة التأثيرات الهيدرولوجية، خاصة الأمطار، على استقرار المناجم المفتوحة. تُستخدم تصنيفات الجيوميكانيك للصخور وتقنيات رسم الخرائط المختلفة باستخدام ArcGIS لتصور الخصائص الجيولوجية والهيدرولوجية. بالإضافة إلى ذلك، توفر النمذجة الجيولوجية ثلاثية وثنائية الأبعاد باستخدام GEOVIA Surpac والمحاكاة العددية باستخدام PLAXISv23 2D 3D نماذج مفصلة للأمطار لتحليل الثبات وتنبؤات السلوك الميكانيكي لأي اتجاه للقطاع الجيولوجي. يتم إجراء حسابات مختلفة باستخدام معلمات إدخال مختلفة ونماذج سلوك لتحديد تأثير الفواصل والأمطار وكذلك تسرب المياه على استقرار منحدرات المنجم. توفر هذه المنهجية المتكاملة ومقارباتها تقييماً شاملاً لثبات المنحدرات، بهدف تحسين ممارسات السلامة والإدارة في المناجم الكبيرة المفتوحة.

الكلمات الرئيسية: ثبات المنحدرات، منجم كبير مفتوح، تحليل هيدرولوجي، نمذجة جيولوجية ثلاثية الأبعاد، تحليل حركي وعددي، كاف السنون.

الاهداء

الحمدُ لله على البدء والختام، أُهدي تخرجي هذا إلى نفسي الطموحة، وإلى عائلتي، وسندي ♥ ♥ ملهمي 🖤 صديقاتي.

كما أُهديه إلى زملائي في فلسطين، الذين منعتهم الحرب من أن يكونوا في مكاني. أُهديه أيضًا إلى يوسف، الذي بقي عالقًا في ذاكرتنا، 'عمره 7 سنين، شعره كيرلي، أبيضاني وحلو'. وأُهديه إلى من قال له أبوه في لحظة استشهاده: 'يا با مش كان بدك تطلع صحفي'. الذين جاهدوا وأُسِروا وقاتلوا في سبيل الله.

Thanks

It is with great pleasure that I dedicate these few lines as a sign of gratitude and deep appreciation to all those who, near or far, have contributed to the realization and outcome of this work.

First, I thank Allah Almighty for allowing me to carry out this dissertation and for guiding me on the path of knowledge.

I would then like to extend my warmest thanks to Mr. Brahmi Serhene and Mr. Berrah Yacine for their invaluable supervision, advice, patience, and the confidence they showed in me, which were decisive in the completion of my work. My thanks also go to the members of the jury, Mr. Hamdene Ali and Mr. Benghazi Zied, for the honor they bestowed upon us by agreeing to judge my work.

Special thanks to the class of 2019, my bestie,GTV, El Azeba, Stars and Moon.

Thank you to everyone.

Contents

CHAPTER I: SLOPE STABILITY CAUSALITY AND EFFECTS

CHAPTER II: Geology, Hydrogeology, and Climatic Conditions

CHAPTER III: Geotechnical Investigation and Data Collection

CHAPTER IV: Geological and Geotechnical Modeling and Safety Analysis

List of tables

List of figures

NOTATIONS

3-D	3 Dimension
2-D	2 Dimension
SF	Safety Factor
Φ'	Effective internal friction
Ψp	Dip of slide plane
W	Weight of block
U	Uplift force due to pressure along slide plane
v	Poisson's ratio
V	Force due to pressure in tension crack
H	Slope height
z	Tension crack depth
β	Wedge geometry factors
Ψi	Dip of line of intersection
δ	Wedge geometry factors
Φ	internal degree of friction
S	Effective shear strength
R	Resistant force
N	Normal force
θ	volumetric water content
Sr	saturated degree
K	coefficient of permeability
γ	bulk density
sa	matrix suction
u	pore-water pressure
C'	effective cohesion
H	Hydrostatic thrust from tension crack
R	Length of moment arm
ISO	the International Organization for Standardization
SOMIPHOS	Société des Mines de Phosphates
(R)	rainfall intensity
(I)	effective accumulative infiltration
(k),	permeability capacity
(tr)	duration
min	Minute
N, S, W, E	North, South, West, East
s.p.a.	A company with actions
CERAD	Center for Study, Research and Development Support
S.D.O	Société du Djebel Onk
SONAREM	National company for mining research and exploitation
BRGM	Geological and Mining Research Office
SOFREMINES	French mining studies company
FERPHOS	National Iron and Phosphate Company
MgO	Magnesium oxide
P_2O_5	phosphorus pentoxide
Calcite	$CaCO_3$.
Dolomite	$CaMg(CO_3)_2$.
Quartz	SiO_2.
Km	Kilometer

m	Meter
g	Gram
l	Litre
max	Maximum
min	Mimum
mm	Milimeter
RQD	Rock Quality Designation
(RMR	The Rock Mass Rating
Rc	Unixial Compression resistant
(αj	Joint Dip Direction
βj)	Joint Dip (
(αs)	Slope Dip Direction
(βs)	Slope Dip
SMR	Classification of Rock Mass
GSI	Classification of the Kef Essnoun Rock Mass
UTM	Universal Transverse Mercator
X,Y,Z	3D coordinate systeme
DEM	Digital Elevation Model
USGS	United States Geological Survey
CSV	comma-separated value
S-	Sondage
EREM	Metal Packaging Recycling School
Tr	Tranch
γsat	Saturated Unit weight
γunsat	Unsaturated Unit weight
Kx, Ky	Permeability
E	Young's modulus
α1	Dip (*-180≤ α1≤ 180*)

General introduction

The stability of slope benches in open-pit mines is a critical aspect of mine safety and operational efficiency. Ensuring long-term safety, stability, and sustainability is the most challenging aim of geotechnical engineering in mine operations. In this regard, designing rock slope benches is crucial, as it allows for high-level monitoring, which has a major impact on economic viability. This study focuses on investigating the safety of slope benches in Kef Essnoun phosphate deposits, extracted from a large open-pit mine, addressing the interaction between geological, geotechnical rock mass properties, and hydrological factors that influence slope stability. A comprehensive assessment involves regional settings investigations, which are essential for understanding the structural geology and tectonics of the area. These investigations include the analysis of main lineaments of beddings, joints, and other discontinuities that affect slope stability.

In the context of the Kef Essnoun case study, this research employs stereographical projection and rosette plot techniques to classify and analyze the groups and families of discontinuities present in the mine. Through kinematic analysis, the potential movements along these discontinuities are identified, providing insight into the stability of the slope benches by finding the critical intersections, density concentrations, and the failure probability.

A significant component of this study is the evaluation of hydrological effects, particularly the impact of rainfall on mine stability. besides geomechanical rock classification of the site is performed to categorize the rock mass quality, which is further analyzed using various mapping techniques using ArcGIS mapping software to generate and visualize slope maps, hill shade maps, watershed maps, local geological maps, and hydrological maps also to interpret the spatial distribution of geological and hydrological features.

Moreover, geological modeling using the GEOVIA Surpac software facilitates the creation of 3D models of the Kef Essnoun mine and the entire geological 3D model of the different features, offering a detailed representation of the mine's subsurface conditions. The obtained 3D construction allows for cross-section sketching in every orientation, and geometrical models can be easily employed later to enhance numerical analysis and modeling using different stability calculations. Furthermore, numerical simulation using PLAXIS 2D v20 et 3D v23 software where the jointed rock model is used to analyze the mechanical behavior of rock materials under various stress conditions. This simulation helps visualizing and predict potential

movements and assess the impact of different factors on slope stability in all mine exploitation directions.

This integrative approach allows for a comprehensive assessment of slope bench stability, considering both geological structures and hydrological effects. The findings of this study aim to enhance the understanding of slope stability and safety monitoring in large open-pit mines, providing a foundation for improved safety and management practices in mining operations.

To achieve the objectives of this research, the dissertation has been carefully organized into four detailed chapters, along with a general introduction and a conclusion, as follows:

Chapter 1: Slope Stability - Causality and Effects In this chapter, the concept of slope stability is introduced, explaining its significance. Various factors that cause slope instability are discussed, including geological, hydrological, topographical, and anthropogenic influences. Additionally, specific triggering events, such as heavy rainfall, that can initiate slope failures, are identified. The chapter will also present case studies of slope failures, highlighting the causality and effects observed in each instance.

Chapter 2: Geology, Hydrogeology, and Climatic Conditions This chapter focuses on studying the geological and hydrogeological conditions of the study area. It involves describing the types and characteristics of rocks and soils present in the region, as well as the structural geology, including faults, folds, and fractures, and how these features impact the area. Additionally, hydrogeological and hydrological analyses are conducted, studying the groundwater table, aquifer properties, and rainfall patterns.

Chapter 3: Geotechnical Investigation and Data Collection This chapter involves a comprehensive geotechnical investigation and data collection process. Site surveys are conducted to gather data on soil and rock properties, collecting all existing physical and mechanical characteristics data. All collected geotechnical data will be compiled and organized for subsequent analysis, ensuring a thorough understanding of the site's conditions.

Chapter 4: Geological and Geotechnical Modeling and Safety Analysis In the final chapter, the data is used to create geological and geotechnical models of the study area using specialized software. These models (3D and 2D) help perform stability analyses of the slopes, employing methods like finite element modeling. The safety factors of the slopes will be evaluated, and potential failure zones identified. Based on this analysis, recommendations will be made to address engineering solutions to enhance slope stability and prevent failures, ensuring the safety and stability of the region.

Chapter I

**SLOPE STABILITY
CAUSALITY AND EFFECTS**

I.1. Introduction

The study of ground movements is related to slope stability; this issue, caused by various forms of instability in the superficial layers of the soil, can be exacerbated by factors such as geology, topography, morphology, or more complex natural and artificial influences. Slope instabilities occur when the resistance of the terrain is less than the driving forces generated by gravity, groundwater, or human activities. Their dynamics naturally follow the laws of mechanics. The literature review indicates that these instabilities occur when the driving forces exceed the resisting forces of the soil along a critical failure surface (Ortigao, J et al.2013; Ogila; Stokes, A. et al. 2014; W. A. M. 2021; Lann, T et al.2024).

The stability of slopes, or natural inclines, is influenced by multiple factors, including:

Geology and geomorphology: The geological composition of the terrain and the configuration of the slope play a crucial role. The types of rocks, their strength, and their geometric arrangement can influence stability.

Hydrology: Water is one of the main factors influencing slope stability. Water infiltration into the soil can saturate soil layers, increasing pore pressure and reducing soil cohesion, which can lead to landslides.

Climate: Precipitation, temperature changes, and freeze-thaw cycles can impact slope stability by influencing erosion and soil movement processes.
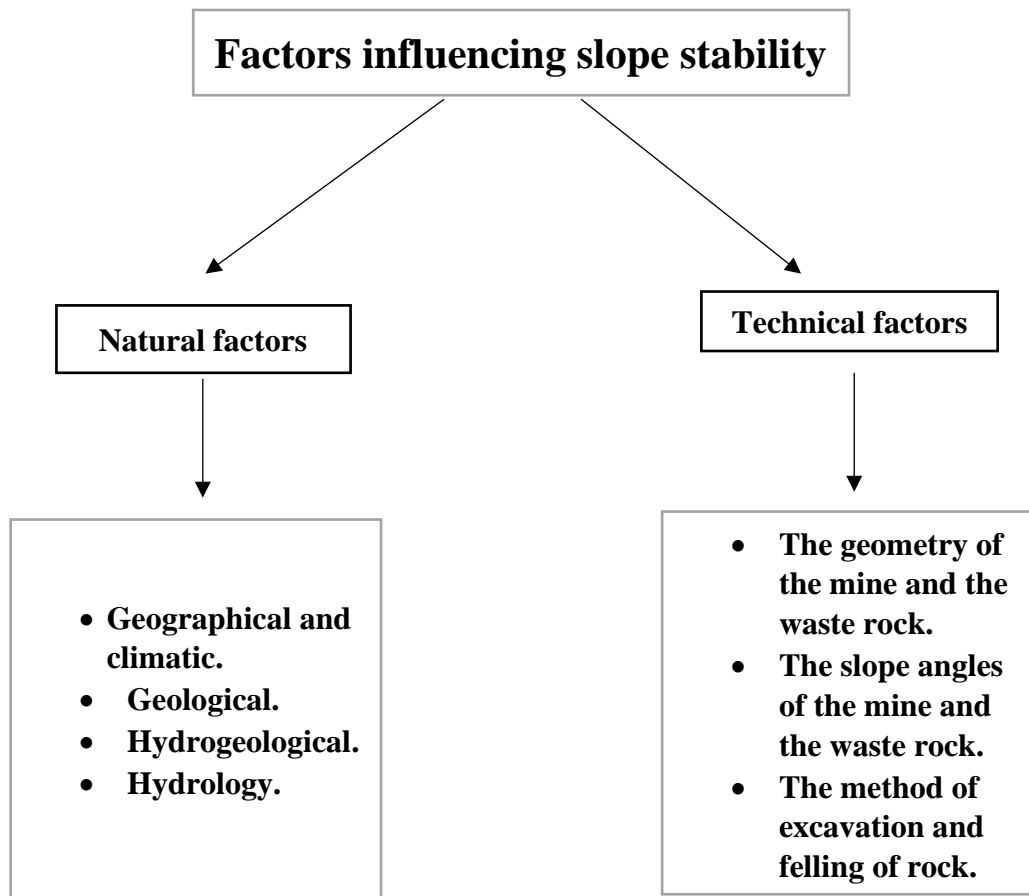
Fig I.1: Factors influencing the slope stability.

I.2. Classification of ground movements:

The term "ground movement" encompasses various phenomena that affect a mass of soil or rock, causing it to transition from one state to another (Nazimko, V., & Zakharova, L. (2017). These movements can occur slowly and superficially due to gravity, or rapidly and deeply due to erosion facilitated by water and human activities. As a result, there are numerous types of ground movements, including landslides, rockfalls, subsidence, and mudflows, each characterized by different rupture mechanisms, materials involved, dynamics, and dimensions (Akpan, A et al. 2016; Huang, D et al.2018; Pánek, T. 2020).

Various classifications exist for ground movements, often categorized based on their speed. Slow movements and rapid movements are two broad categories, with only rapid movements posing direct risks to human safety. The severity of their consequences typically correlates with the scale of the displaced masses. Slow movements, on the other hand, primarily impact socio-economic factors or public interests (Guo, Y et al.2024).

I.2.1. Rapid and discontinuous movements:

a). rockfall:

These are sudden falls of rock masses. The term "rockfall" is used for the detachment of smaller volumes, typically less than 1 cubic decimeter, while "rockslide" is used for larger volumes. The term "collapse" is used when there is a sudden fall of a rock mass that detaches from a wall while disintegrating (Corominas, J et al .2017; Mavrouli, O.et al. 2024).
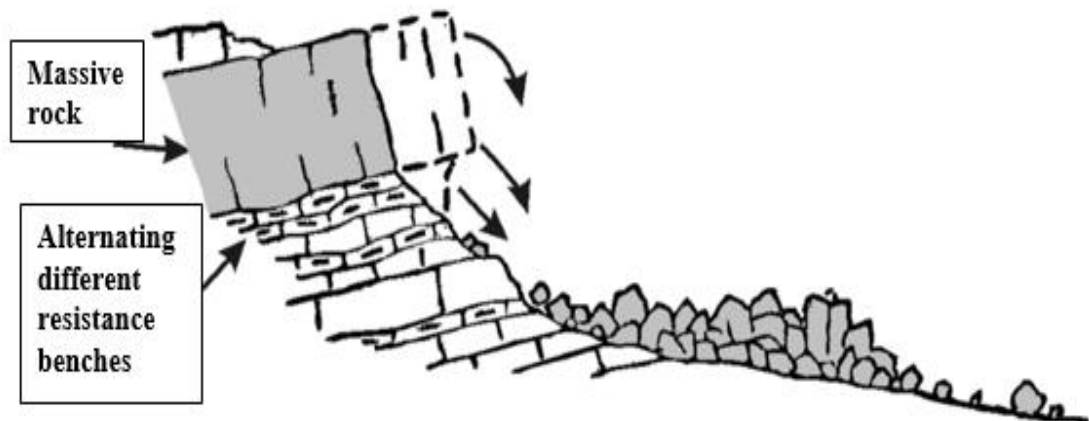
Fig I.2: Rockfall movement (Smith, J., & Doe, A. 2018).

b). Flows:

They occur from loose material, momentarily saturated with water, taking on a more or less viscous consistency, sometimes close to fluidity (Take, W et al.2014; Kang, et al.2017), Several types of flows are distinguished:

-Muddy flows: muddy flows are akin to the flow of a viscous fluid carrying elements of various sizes (from fine particles to boulders) over sometimes significant distances. These phenomena occur in the presence of large quantities of water, such as during heavy rainfall or when dams or levees break (Cageao, P. P. 2014; Coussot, P. 2017).

-Solifluction flows: Solifluction flows refer to the slow movement of soil in periglacial environments, resulting from the instability of the thawed part of the soil surface during summer (Matsuoka, N. 2010; Harris, C et al .2011).
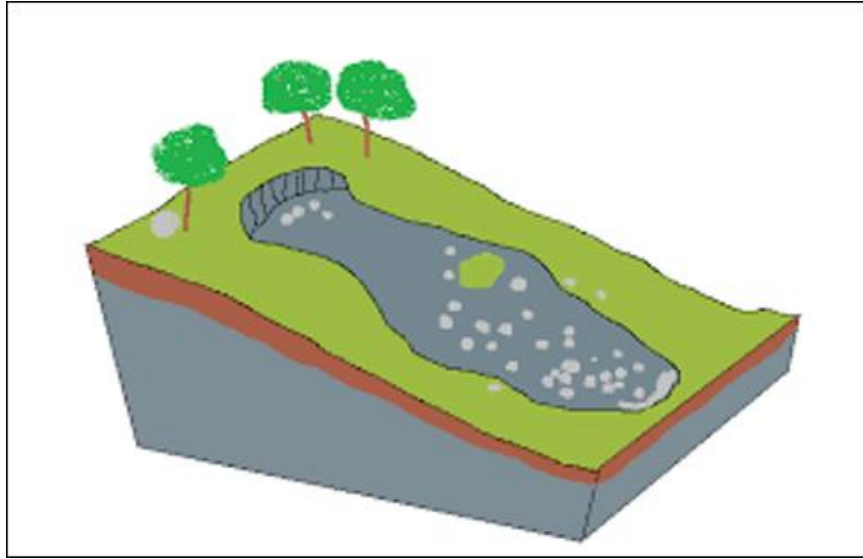
Fig I.3: Flow movement (website 1).

c). Collapses:

Sudden collapses stem from the abrupt rupture of supports or the roof of an underground cavity. This rupture swiftly extends to the surface, resulting in the formation of a roughly cylindrical excavation. The dimensions of this cavity are contingent upon geological factors, the dimensions, and depth of the cavity, as well as the manner of rupture. These collapses can manifest as either localized occurrences (such as sinkholes, typically with a diameter less than 50 meters, occasionally reaching 100 meters) or more widespread events spanning several hectares. (Wei, K et al.2024).

Fig I.4: Collapse mine in China (website 2).

I.2.2. The slow and continuous movements:

a). Creep:

It describes slow movements resulting from stresses nearing the point of rupture (plastic domain). These are gradual viscoplastic deformations under internal shear stress, predominantly observed in clay-rich environments. Nonetheless, the sheer force of gravity alone can also induce the outward displacement of a clay slope (Bhaduri, A., & Bhaduri, A. 2018; Shibkov, A.et al. 2016).
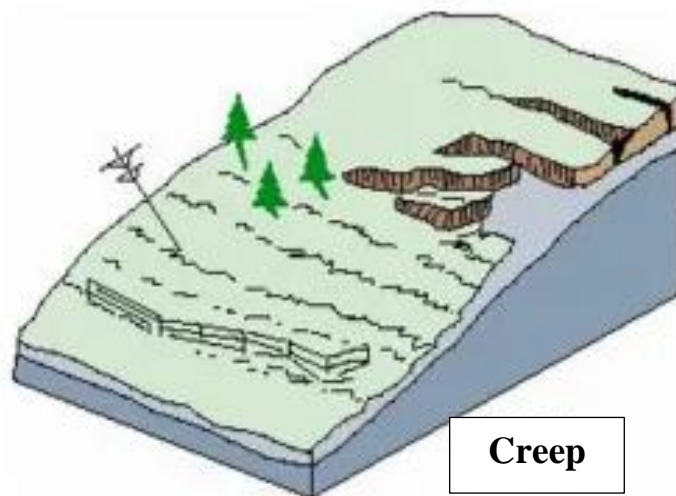
Fig I.5: Creep movement (website 3).

b). Landslides:

Landslides are characterized by downhill movements of terrain, impacting both rock masses and softer ground, along single or multiple rupture surfaces, or through relatively thin zones of intense shear deformation. Typically, the onset of a landslide is influenced by various factors. The magnitude of the phenomenon is governed by three forces (Brideau, M. A., et al.2015; Brideau, M. A., et al.2022).

- **Gravity:** This force pulls material towards the Earth's center and is influenced by the terrain's slope.

- **Frictional force:** This force opposes the movement of loose soil or rock against the underlying layer.

- **Cohesion force:** This force arises from the attraction between soil particles and water stored in the soil.

When resistance forces (friction and cohesion) outweigh the driving force (gravity), the slope remains stable. Conversely, if this balance shifts, a landslide occurs, resulting in a rupture between layers of rock or soil, causing a mass to slide downhill at varying speeds.

Factors contributing to landslide initiation include:

- Terrain characteristics: Clayey soils are prone to landslides.

- Water influence: Water often plays a significant role in terrain movement.

- External mechanical factors: These encompass activities such as earthworks at the slope's base, cutting into stable slopes, and natural or artificial overloading of a slope.
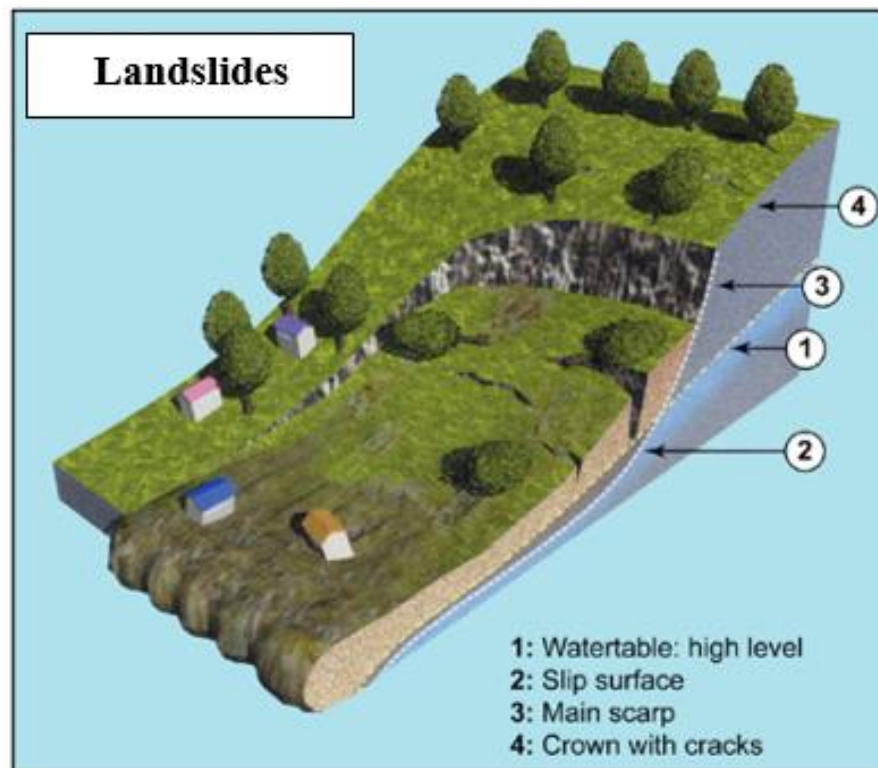
Fig I.6: Landslide movement (website 4).

1.Planar sliding:

It takes place along a defined plane, typically at a geological fault or other discontinuity surface, such as between two materials of different natures or bedding planes. The rupture line follows a thin layer with inferior characteristics, often influenced by water. This layer is commonly referred to as a "slickenside" shown in fig **a** (Smith, J. V., & Arnhardt, C. 2016; Raghuvanshi, T. K. 2019; Biswakarma, P et al .2023).

2.Circular sliding:

Occurs when the terrain moves along a concave surface resembling a spoon shape. Typically, the sliding surface descends almost vertically into the detachment zone. Two types of circular sliding are recognized: simple and complex (compound) shown in fig **b** (De Blasio, F. V. 2011).

a). Simple circular sliding: the rupture surface has a straightforward circular shape, hence the name. It is characterized by significant erosion and detachment of rock masses. Features of such sliding include tension cracks and a cliff at the top marking the beginning of the sliding surface, as well as a bulge formed by materials that have slid at the base (Gu, D., & Huang, D. 2016).

b). Complex circular sliding: This type entails numerous interconnected slides, typically triggered by the removal of the obstruction caused by the preceding slide. Consequently, successive slides occur, moving upstream. This phenomenon is characterized by several small displacements and erosions (Mandal, S & Maiti, R. 2015).
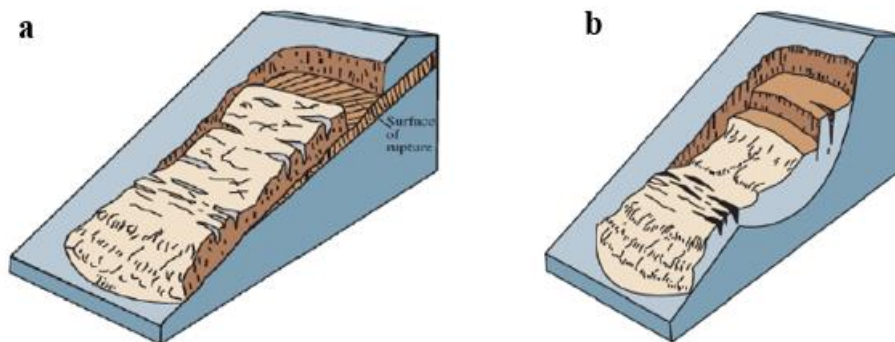
Fig I.7: Sliding types; a) Planar b) Circular (website 5).

3. Corner sliding:

Also known as'' wedge'' sliding, occurs due to the presence of two discontinuity planes oriented in a way that facilitates the sliding of the block towards the open surface (Gischig, V et al.2011; Wolter, A et al 2011; Vick, L 2020).
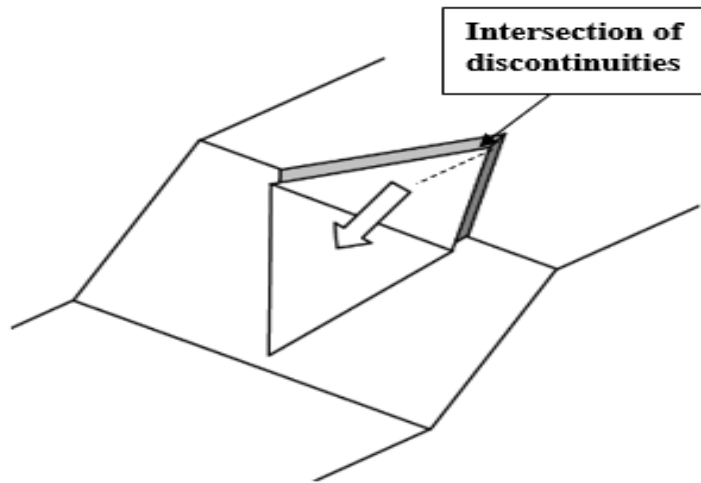
Fig I.8: Corner sliding movement (website 6).

4.Toppling:

Represents a unique type of rock bench movement, akin to a shearing action on the bench heads. It occurs exclusively under particular conditions: the bench dip must be sufficiently steep, the slope steepness of the rocky terrain must be significant, and there must be a close alignment between the bedding and slope orientations. This phenomenon involves the detachment of slabs followed by their tipping over (Marndi, B. 2011; Hungr, O et al .2014).
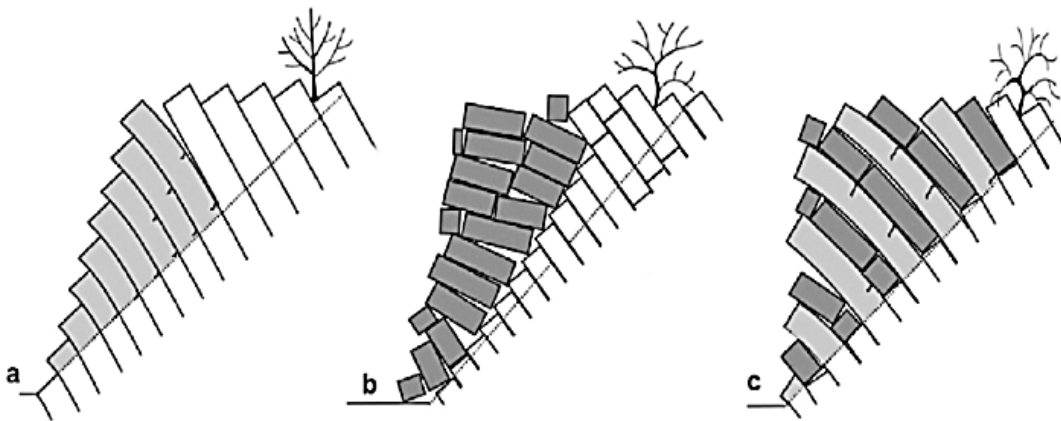
Fig I.9: Schematic diagrams of main toppling failure modes:

a) flexural, b) blocky, c) blocky-flexural (website 7).

I.3. Overview on slope stability calculation methods:

I.3.1. Introduction:

Slope stability analyses are routinely conducted to evaluate the safe and functional design of excavated slopes, such as those found in open-pit mining and road cuts, as well as to assess the equilibrium conditions of natural slopes. The chosen analysis technique depends on site conditions and the potential mode of failure, taking into account the varying strengths, weaknesses, and limitations inherent in each methodology.

A site investigation should precede any stability analysis and include geological and discontinuity mapping to provide essential input data. Ideally, data collection involves rock mass characterization and sampling of rock materials for laboratory analysis (e.g., to determine strength and constitutive behavior), along with field observations and in situ measurements. Monitoring spatial and temporal variations in pore pressures, slope displacements, stresses, and subsurface rock mass deformations provides valuable data for constraining and validating the stability analysis.
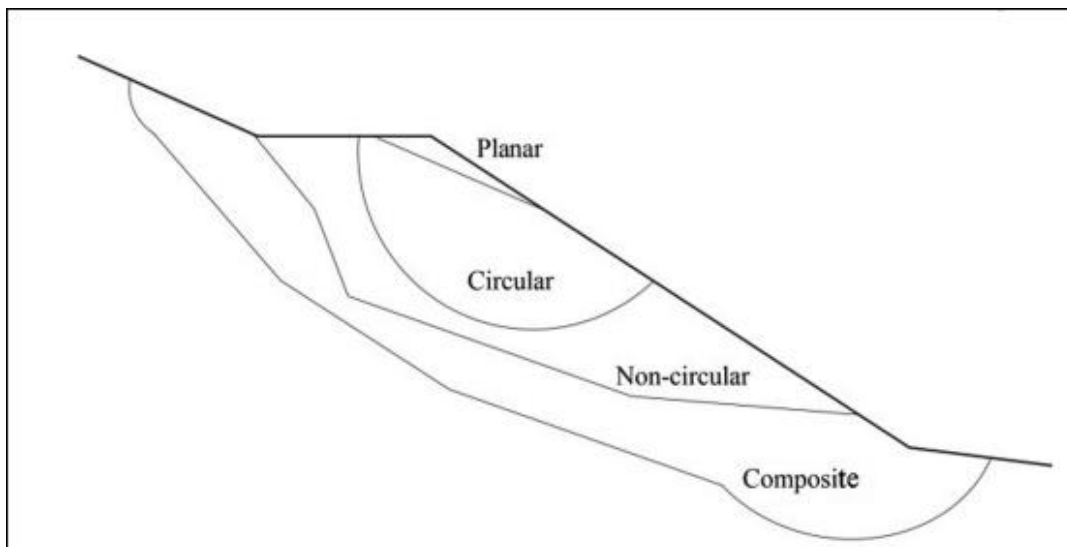
Fig I.10: Various types of slip surfaces in slopes (Azarafza, M et al.2021).

I.3.2. Traditional methods of slope stability analysis:

Traditional methods of rock slope analysis can generally be categorized into kinematic and limit equilibrium techniques. Additionally, analytical computer-based methods, known as rockfall simulators, have been developed to analyze discrete rock block falls (RK, U 2011; Raghuvanshi, T. K. 2019).

Table I.1: Traditional methods of slope stability analysis.

Method	Critical Parameters	Advantages	Limitations
Kinematic (using stereographic interpretation)	Critical slope and discontinuity geometry; representative shear strength characteristics	Relatively simple to use; provides initial indication of failure potential; may allow identification and analysis of critical key-blocks using block theory; can be linked with limit equilibrium methods; can be combined with statistical techniques to indicate probability of failure	Primarily suitable for preliminary design or non-critical slopes; critical discontinuities must be identified; requires representative discontinuity/joint shear strength data; mainly evaluates critical orientations, neglecting other important joint properties
Limit Equilibrium	Representative geometry and material characteristics; soil or rock mass shear strength parameters (cohesion and friction); discontinuity shear strength characteristics; groundwater conditions; support and reinforcement characteristics	Wide variety of commercially available software for different failure modes (planar, wedge, toppling, etc.); can analyze factor of safety sensitivity to changes in slope geometry and material properties; advanced codes allow for multiple materials, 3-D analysis, reinforcement, and groundwater profiles	Mostly deterministic, producing a single factor of safety (though probabilistic analysis is increasing); factor of safety does not indicate instability mechanisms; various techniques with different assumptions; does not consider strains and intact failure; probabilistic analysis requires well-defined input data for meaningful evaluation
Physical Modelling	Representative material characteristics; appropriate scaling factors	Clearly portrays mechanisms; results provide useful constraints for numerical modeling; centrifuge models can examine the effects of time on failure mechanisms	Simplistic groundwater simulation, particularly in rock; techniques do not account for scale effects and in situ stress; centrifuges can be costly
Rockfall Simulators	Slope geometry; rock block sizes and shapes; coefficient of restitution	Practical for siting structures; supports probabilistic analysis; available in 2-D and 3-D versions	Limited experience compared to empirical design charts

1.Kinematic Analysis:

Kinematic methods focus on the feasibility of translational failures caused by the formation of "daylighting" wedges or planes. These methods rely on a detailed evaluation of rock mass structure and the geometry of existing discontinuity sets that may contribute to block instability. This assessment can be conducted using stereonet plots and/or specialized computer software that focuses on planar and wedge formations (Eberhardt, E. 2003; Gischig, V et al.2011).

2.Limit equilibrium:

Limit equilibrium techniques are routinely used to analyze landslides involving translational or rotational movements on distinct failure surfaces. These analyses provide either a factor of safety or, through back-analysis, a range of shear strength parameters at failure. Generally, these methods are the most commonly adopted solution in rock slope engineering, despite many failures involving complex internal deformation and fracturing that bear little resemblance to the 2-D rigid block assumptions required by limit equilibrium analyses (Hungr, O.& Amann, 2011; Utili, S.et al. 2015).

a. Translational analysis:

Limit equilibrium solutions for planar and wedge failures are commonly used to assess discontinuity-controlled rock slope instabilities. These techniques, primarily based on solutions introduced by Hoek & Bray (1991), assume translational sliding of a rigid body either along a single plane or along the intersection of two planes in the case of a wedge. Since the sliding block does not experience any rigid body rotations, all forces are assumed to pass through the centroid of the block (Aksoy, H et al .2007 ; Sari, M. 2019; Liu, G et al.2024).

$$SF = \frac{c'(H-z)\csc\psi_p + (W\cos\psi_p - U - V\sin\psi_p)\tan\phi'}{V\cos\psi_p + W\sin\psi_p}$$

Where:

SF = safety factor
c' = effective cohesion
ϕ' = effective friction angle
ψ_p = dip of slide plane
W = weight of block
U = uplift force due to water pressure along slide plane
V = force due to water pressure in tension crack
H = slope height
z = tension crack depth
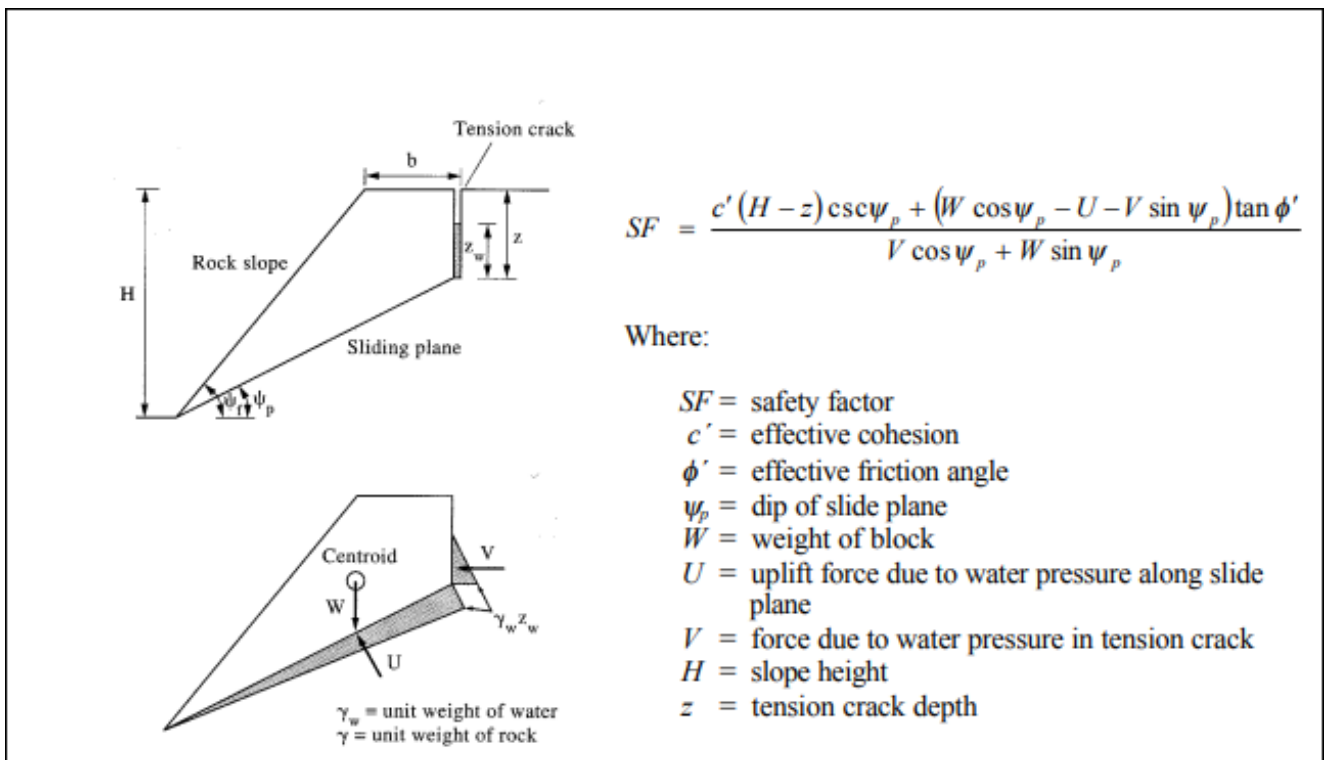
Fig I.11: Limit equilibrium solution for planar failure (Sengani, Fhatuwani &Mulenga, François 2020).
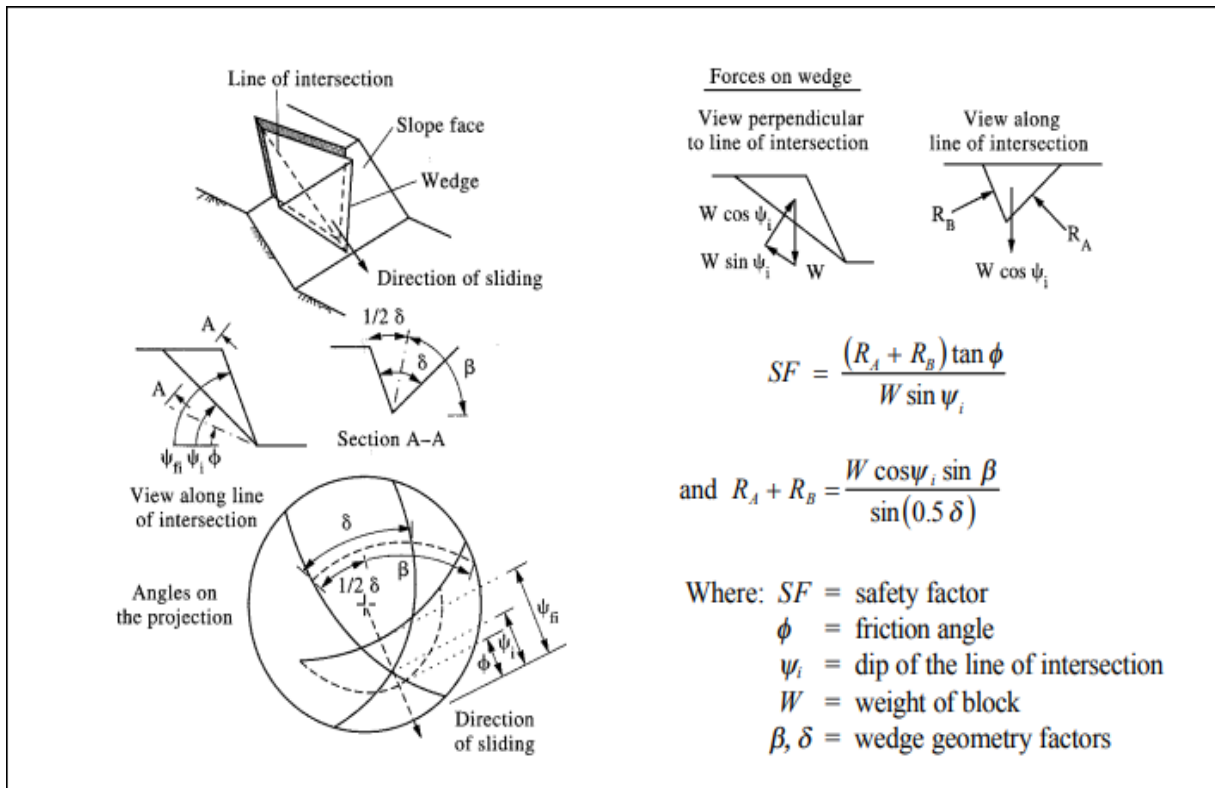
Fig I.12: Limit equilibrium solution for wedge failure under dry conditions and with frictional strength only (Hudson & Harrison 1997).

b. Rotational analysis :

In cases of very weak rock, where the intact material strength is comparable to the induced stresses, the structural geology might not govern stability. Instead, failure modes similar to those observed in soils may occur. These are typically known as circular failures, rotational failures, or curvilinear slips.
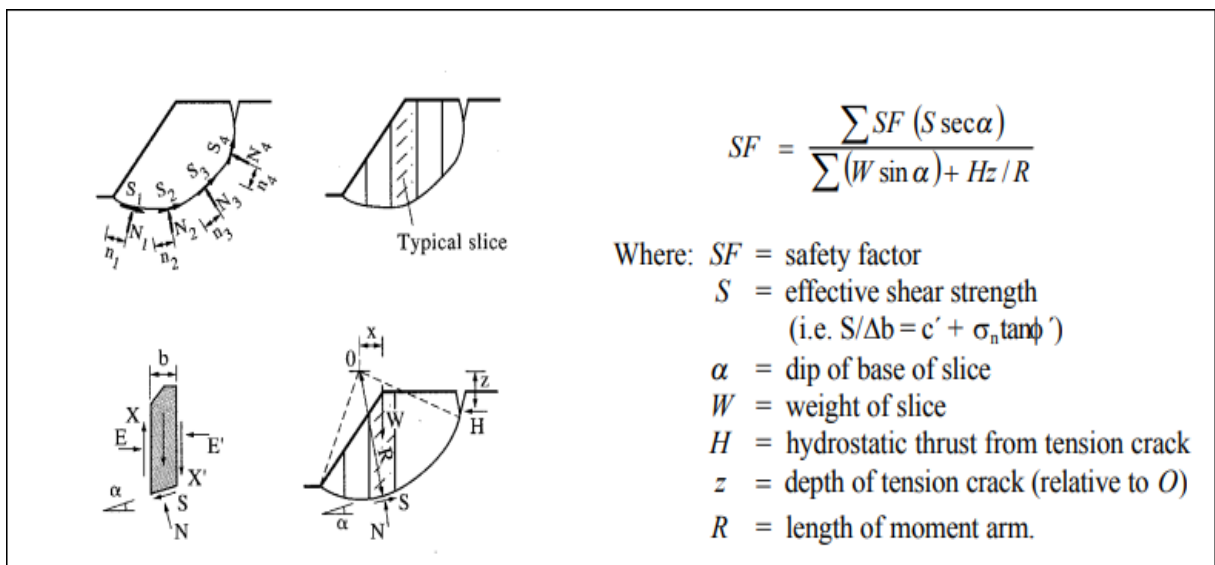
Fig I.13: Limit equilibrium solution for circular failure (Hudson & Harrison 1997).

c. Toppling: Tools are also available for analyzing direct toppling modes of failure. Although solutions exist for flexural toppling, these are less effectively addressed using limit equilibrium techniques due to the involvement of internal block deformations. Direct toppling happens when the center of gravity of a discrete block falls outside its base outline, leading to the development of a critical overturning moment (Nichol, S. L 2000; 范付松. 2015).

$$P_{n-1} = \frac{P_n (M_n - \Delta x \tan\phi) + (W_n/2)(y_n \sin\alpha - \Delta x \cos\alpha)}{L_n}$$

$$P_{n-1} = P_n - \frac{W_n (\tan\phi \cos\alpha - \sin\alpha)}{1 - \tan^2\phi}$$
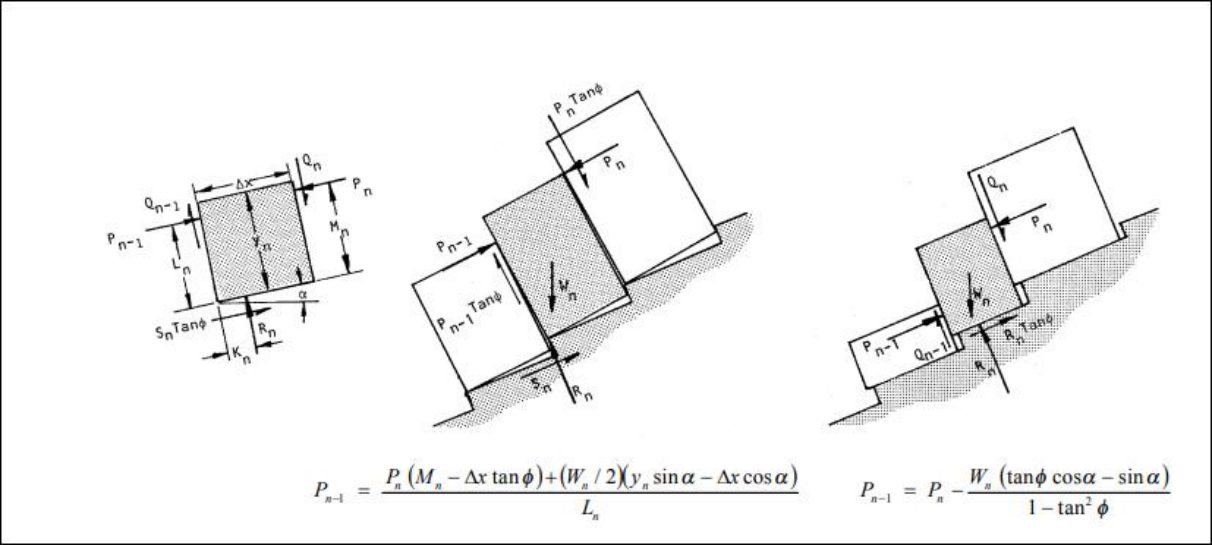
Fig I.14: Limit equilibrium conditions for toppling and sliding, with input variables illustrated in the corresponding diagrams (Hoek & Bray 1991).

Table I.2 : The main limit equilibrium methods used in slope stability analysis.

Method	Equilibrium Conditions Satisfied	Slip Surface	Failure Mechanism	Application	References
OMS/Fellenius method	Moment equilibrium about the circle center	Circular	Rotational	Mass/Slice approach	Fellenius (1936)
Simplified Bishop method	Vertical force equilibrium and moment equilibrium about the center	Circular	Rotational	Mass/Slice approach	Bishop (1955)
Extended Bishop method	Moment equilibrium about the center	Circular	All	Mass/Slice approach	Nonveiller (1965)
Lorimer method	Vertical force equilibrium and moment equilibrium about the center	Circular	All	Slice approach	Fredlund, Krahn, and Pufahl (1981)
Simplified Janbu method	Vertical and horizontal force equilibrium and shear interslice force is assumed ZERO	General shape	All	Mass/Slice approach	Janbu (1954)
Modified Swedish method	Vertical and horizontal force equilibrium	General shape	All	Slice approach	USACE (2003)
USACE's 1970 procedure	Vertical and horizontal force equilibrium and interslice force inclination is parallel with ground	General shape	All	Slice approach	USACE (2003)

Lowe–Karafiath method	Horizontal and vertical force equilibrium and interslice force inclination is equal with slip and ground surfaces	General shape	All	Slice approach	Lowe and Karafiath (1960)
Sarma method I	Vertical and horizontal force equilibrium and shear strength on the interface between adjacent slices	General shape	All	Slice approach	Sarma (1979)
Spencer method	Rigorous limiting equilibrium and interslice force inclination is constant	General shape	All	Slice approach	Spencer (1967)
Morgenstern – Price method	Rigorous equilibrium by interslice force function	General shape	All	Slice approach	Morgenstern and Price (1965)
Sarma method II and III	Rigorous equilibrium of extended Sarma method I	General shape	All	Slice approach	Sarma (1973)
Correia method	Rigorous equilibrium and shear interslice force described by shapes function and force dimension	General shape	All	Slice approach	Correia (1988)
Rigorous Janbu method	All the force and moment conditions are equilibrium	General shape	All	Slice approach	Janbu (1954); Janbu, Bjerrum, and Kjaernsli (1956)
USACE's 2003 procedure	Improvement of USACE's 1970 procedure	General shape	All	Slice approach	USACE (2003)
Wedge method	Fully satisfies the vertical and horizontal force equilibrium	General shape	Wedge Zone	Wedge Zone approach	Abramson et al. (2001)
Infinite slope method	Horizontal and vertical force equilibrium	Planar	Plane	Critical circle	USACE (2003)
Planar failure analysis	Horizontal and vertical force equilibrium	Planar	Plane	Geometry controlled	Hoek and Bray (1981)
Wedge failure analysis	Horizontal and vertical force equilibrium	Wedge	Wedge	Geometry controlled	Brady and Brown (2005)
Circular failure analysis	Horizontal and vertical force equilibrium	Circular	Rotational	Mass/Slice approach	Wyllie and Mah (2004)
Toppling failure analysis	Vertical and horizontal force equilibrium and moment equilibrium	Rotation	Toppling	Geometry controlled	Freitas and Watters (1973)
Block theory	Geometrical equilibrium and force/moment vectors equilibrium	General shape	All	Geometry controlled	Goodman and Shi (1985)

3.Rockfall Simulators:

One aim of analyzing rock slope stability is to develop solutions to mitigate rock mass movements. When dealing with rockfalls, securing every single block is often unfeasible. Thus, it becomes essential to focus on designing protective measures around structures threatened by falling blocks. Therefore, the challenge of rockfall protection primarily revolves around predicting the travel paths and trajectories of unstable blocks that have detached from a rock slope.
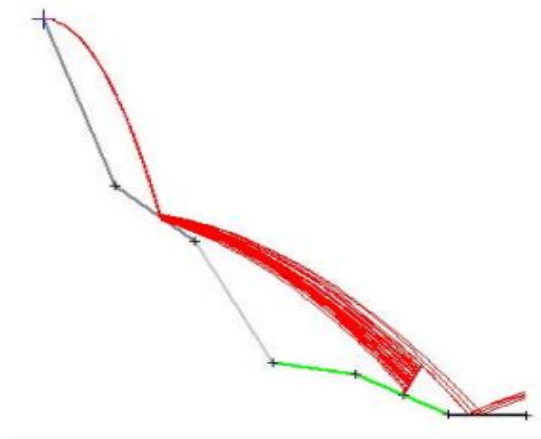
Fig I.15: Rockfall analysis (Erik Eberhardt 2013).

I.4. Effects of Rainfall in Mines:

The presence of rainwater continues to pose significant challenges to mining operations, primarily impacting the stability of mining structures and the safety of operations. Rain-induced landslides are major geotechnical hazards. Additionally, it directly contributes to increased project costs due to the necessity of pumping water to maintain the local water table below the mining zone. In surface mines, particularly those situated in soft sedimentary rock formations like Phosphate mine, rainwater exerts a notable influence on the stability of open-pit slopes. (A Bo et al .2024; Qiao, P 2023; Tien Bui 2016).

Table I .3 : Open pit mining system, impact areas directly affected due to rainfall

Area/System	Impact due to Rainwater
Digging System	Excavation and Loading Process
Slope Stability	Bench and Overall Slope
Transportation System	Haul Roads and Ramps
Dumping Process	Dump Structure degradation
Coal Handling System	Production and Mud accumulation
Dewatering System	Addition of rainwater with Aquifer rechargeable water
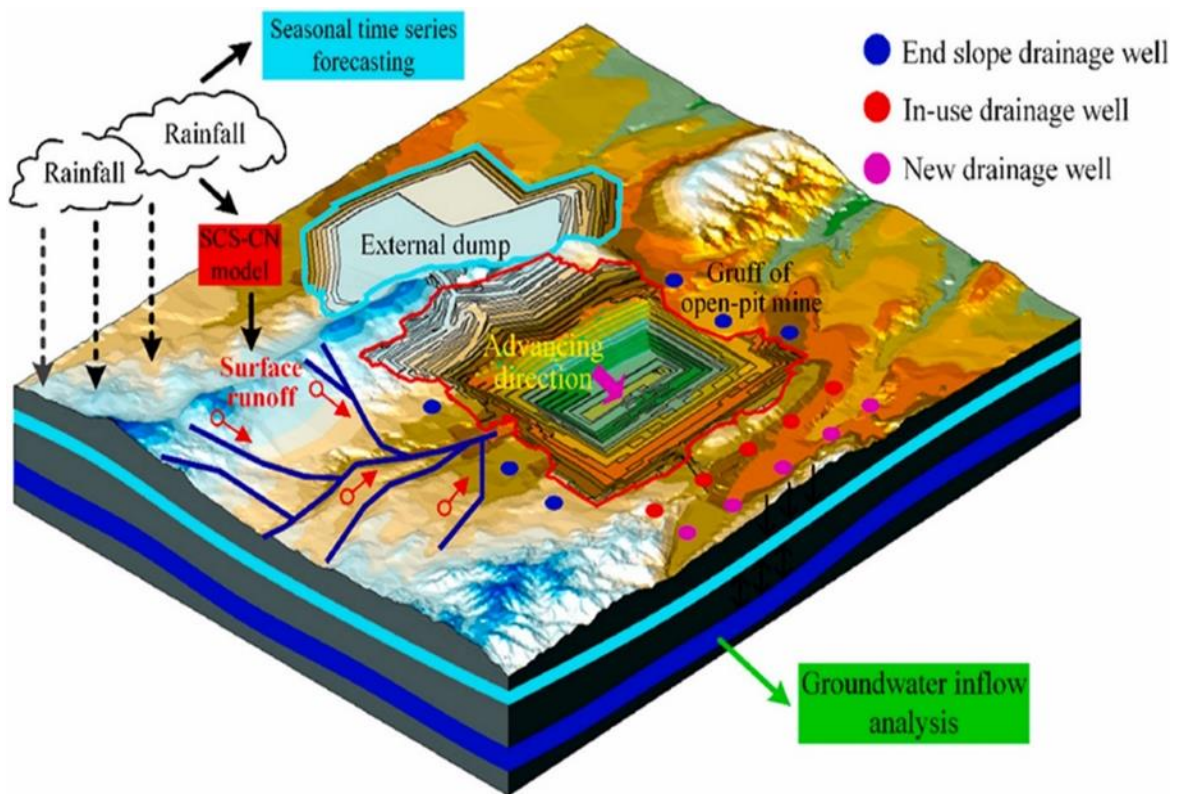
Fig I.16: Impacts on the Stability of Mining Structures (Cao B et al. 2023).

Fig I.17: photo of wastewater stagnation representing the possibility of percolation over the study area.

I.5. Background:

Many researchers had done a lot of work about the analytical method combining the calculation of infiltration with slope stability analysis. Here we summarize some main conclusions.

Rainfall induces the changes of soil behavior, mainly include: the increase of volumetric water content (θ), saturated degree (Sr), coefficient of permeability (k) and bulk density (γ), the decrease of effective cohesion (c) and internal degree of friction (φ), the decrease or even disappearance of matrix suction (sa) and the appearance and increase of pore-water pressure (u) and the development of new strain and displacement in the slope .Therefore, the decrease of c, and φ on the slip surface, the increase of γ in slope and u on the slip surface during rainfall infiltration can cause the decrease of slope stability (Wang, J et al 2024; Feng, K et al .2021; Zhang, L 2016; Yang, K et al 2017; Smith, J., & Doe, A. 2018).
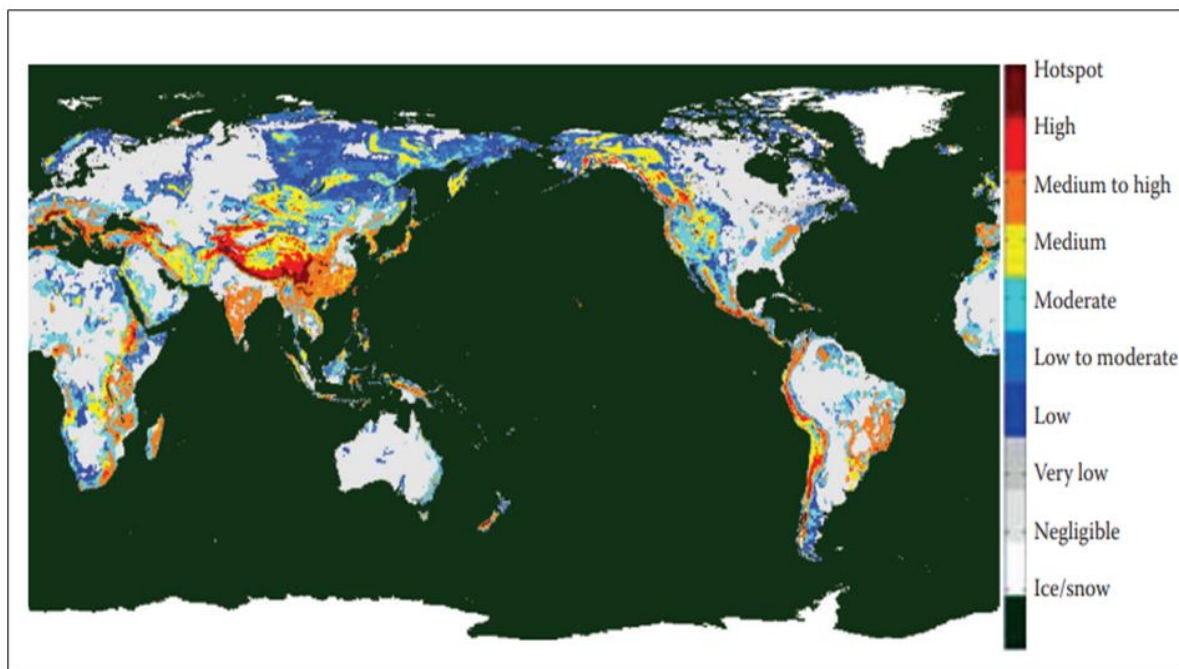
Fig I.18: Global susceptibility map of rainfall-induced landslide (Hong, Y., Adler, R. F.,2008).

Also, rainfall is impact on slope stability hinges on two key factors: effective accumulative infiltration (I) and permeability capacity (k), When solely considering a slope, disregarding other influences, higher rainfall intensity (R) and longer duration (tr) result in increased I and

depth often triggers shallow landslides. Conversely, if infiltration is sufficient to raise the water table, it can induce deep-seated landslides. Moreover, a larger penetration capacity leads to higher I and reduced slope stability. I varies with R: when R is lower than soil penetration capacity, water infiltrates directly, but with higher R, runoff occurs, diminishing I (Gallage, C &al 2021; Chen, J et al 2022; Lee, D. T. T. 2016).
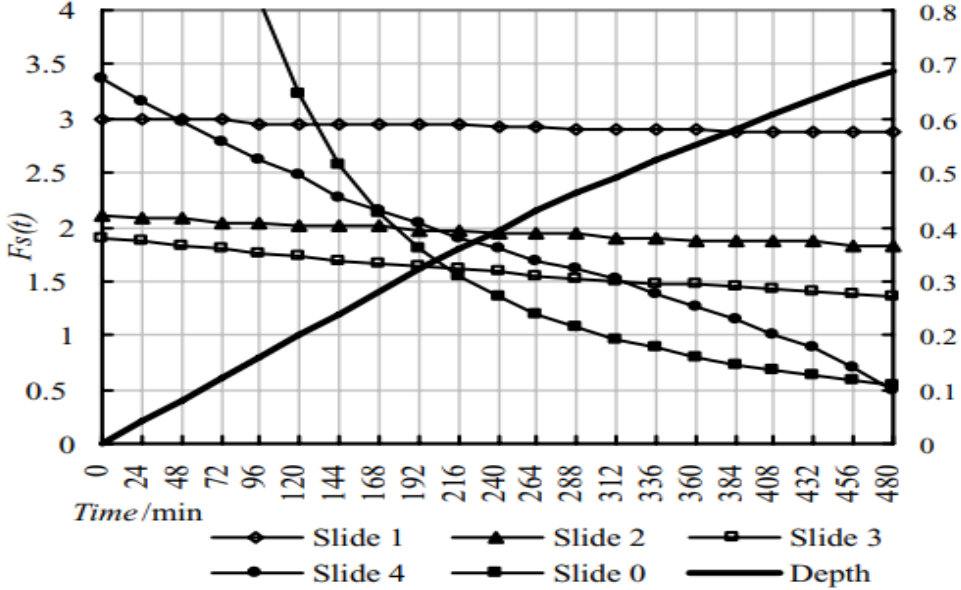
Fig I.19: State of slope under rainfall (Malla, Birasa, Dahal, B K 2022).

Furthermore, landslides due to rainfall happen with an evident delay (Au, S.W.C. 1998, Lumb, P.B., 1975). The delay of shallow landslides (from several hours to days) seems to be smaller than the lag of deepseated ones (several days or more) (Malla, Birasa, Dahal, B K 2022).
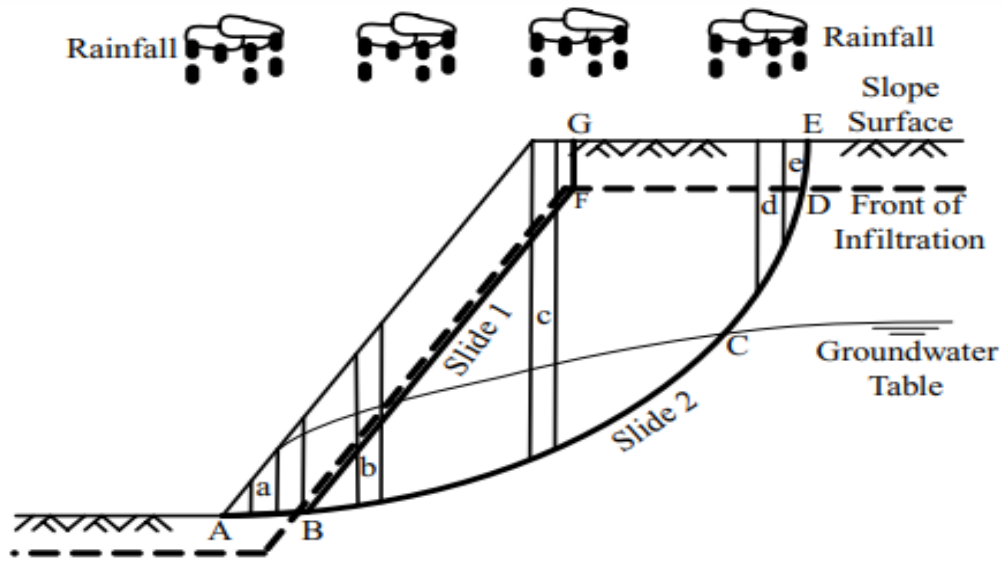
Fig I.20: Safety factor and depth for different slides during 8 hours (Malla, Birasa, Dahal, B K 2022).

For an open-pit coal mine in the Thar Coalfield Pathan et al. (2022) conducted a slope stability analysis to examine the effect of groundwater on slope stability. The study utilized computer models developed using Slide-2D and Phase2 software and performed stability analysis considering local groundwater dimensional limit equilibrium method and a finite element method-based shear strength reduction technique condition.
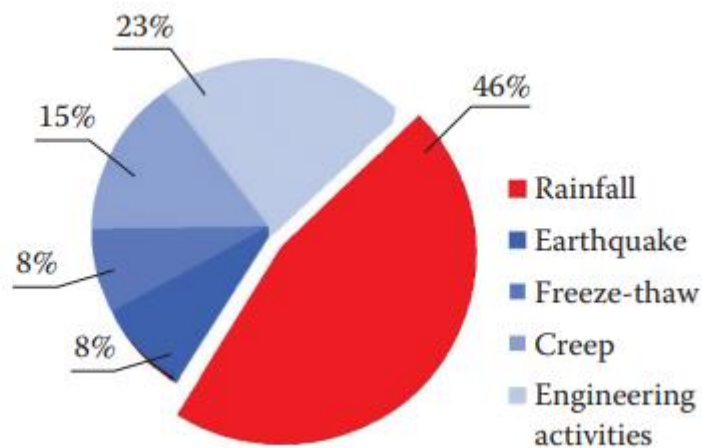
Fig I.21: New Gold mine photo (Malla, Birasa, Dahal, B K 2022).

Heavy rainfall and flooding in the Fort Frances area severely drenched gold production plans at new gold's Rainy River open-pit mine (SB. Hecht, A. Cockburn2010; Koch, K. J. 2024). In China landslides occur frequently, Especially in the western part of China, large-scale landslides are notable for their scale, complex formation mechanism, and serious destruction (Zhao, B et al 2023; Shao, X et al 2024; Zhao, Y et al 2015; Huang, R. 2012).

Fig I.22: Mechanisms of large-scale landslides in China during the twentieth century
(Huang, R. 2012).

It is prone to mention that numerous landslides are commonly initiated by rainfall. As rainwater seeps into the soil, it modifies both the total weight and pore pressure, thereby influencing stress distribution within hillslopes. This highlights the significance of recognizing rainfall-induced landslides as a significant hydromechanical phenomenon (Sidle et al 2016; Roccati, A et al 2020, Amarasinghe, M et al 2024).

I.6. Modeling efforts included:

-**Hydrogeological Modeling:** involves developing detailed models to simulate water movement within the mine site, including groundwater flow patterns and infiltration rates. These models predict changes in pore water pressures, aiding in identifying areas vulnerable to slope failure (Vuille, M et al 2018; Lee, J et al 2012).
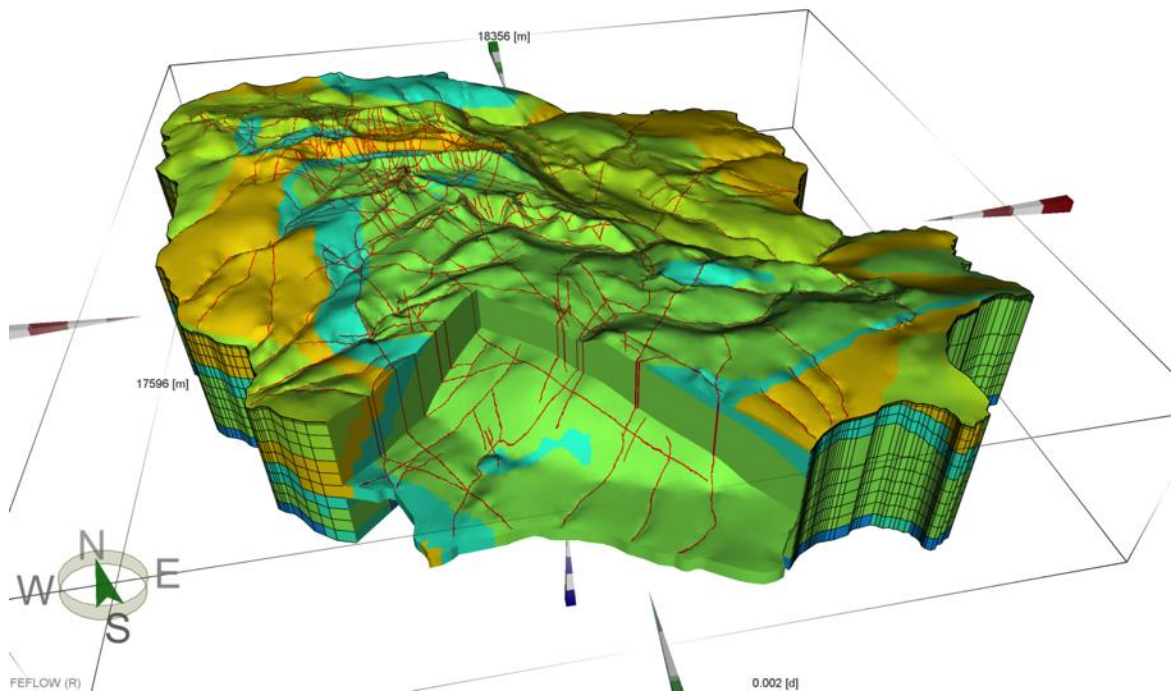
Fig I.23: Example of a finite element grid developed to assess pre-development groundwater flow paths in the vicinity of a proposed tailings storage facility (Leslie Smith, Guelph, Ontario, 2021).

-Geological Modeling:

Landslides constitute a critical geological threat with frequently fatal outcomes. In the ASEAN region, between 2006 and 2018, there were 5305 recorded landslide-related deaths.
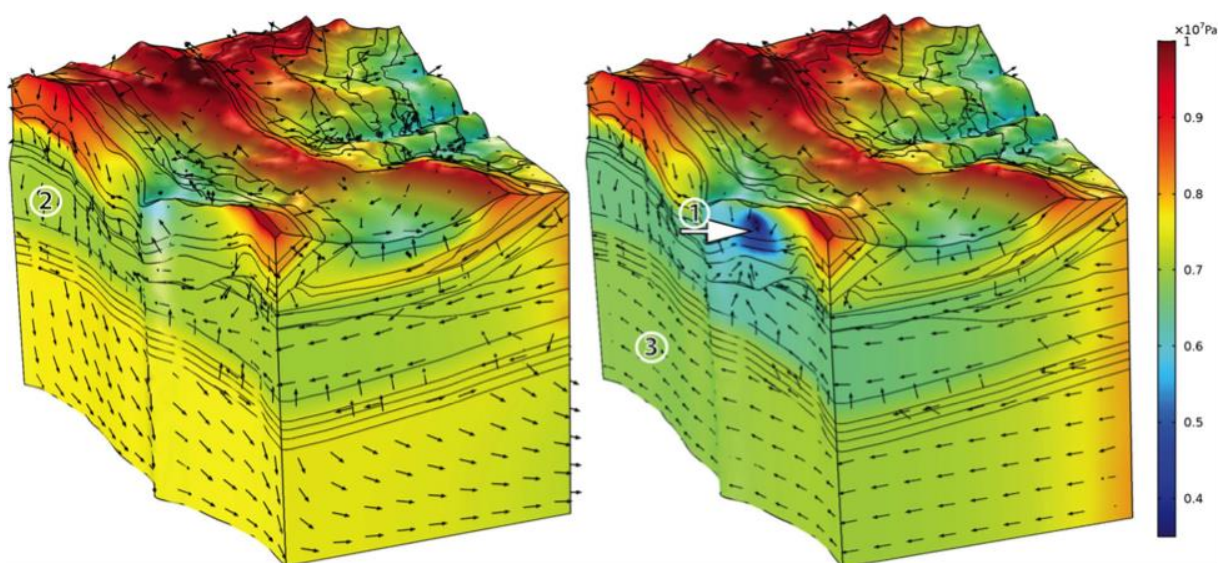
Fig I.24: Result of regional-scale groundwater modeling (Stefan Scheidler 2019).
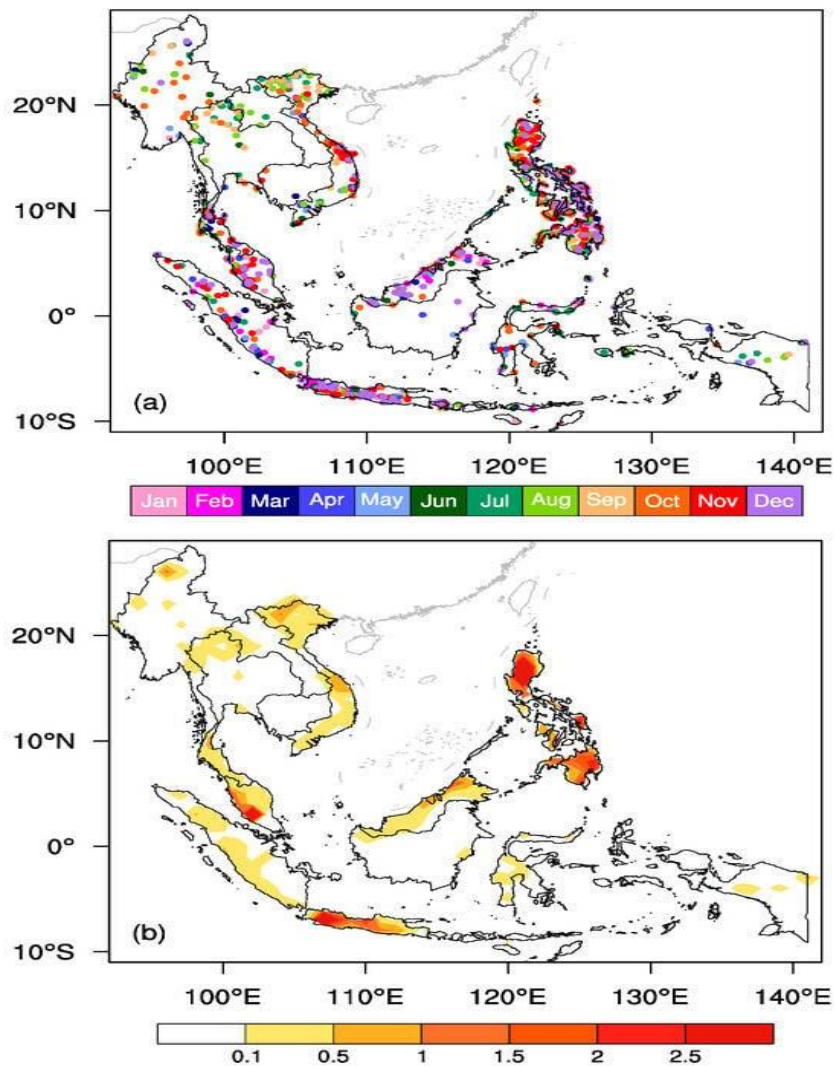
Fig I.25: Spatiotemporal distributions of landslides in ASEAN countries (**a**) and the average annual landslide frequency (**b**); units: times per year (Weiping Lu 2024).

- Geotechnical Modeling:

 utilizes software to analyze slope stability under varying rainfall and flooding scenarios. It considers factors like soil properties and groundwater conditions to assess failure likelihood and propose mitigation measures (Cui, H et al. 2024; Benabid, I.2024).
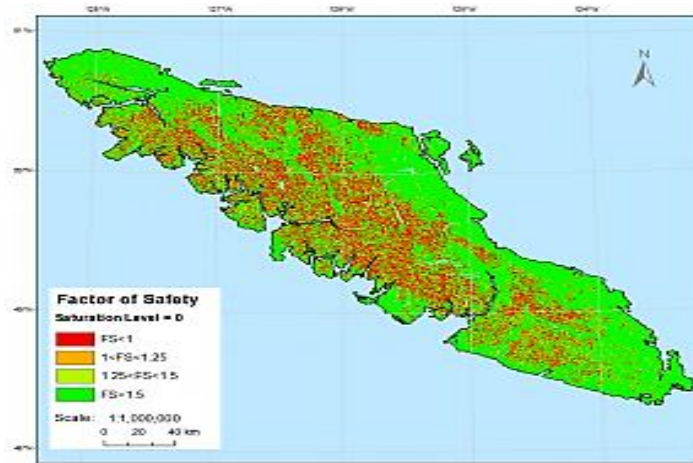
Fig I.26: Safety factor map (Jason Goetz 2015).

-3D Slope Stability Analysis:

Accounts for spatial variability in geological and hydrological conditions, pinpointing unstable areas and guiding targeted mitigation efforts (KS Kalenchuk 2010).
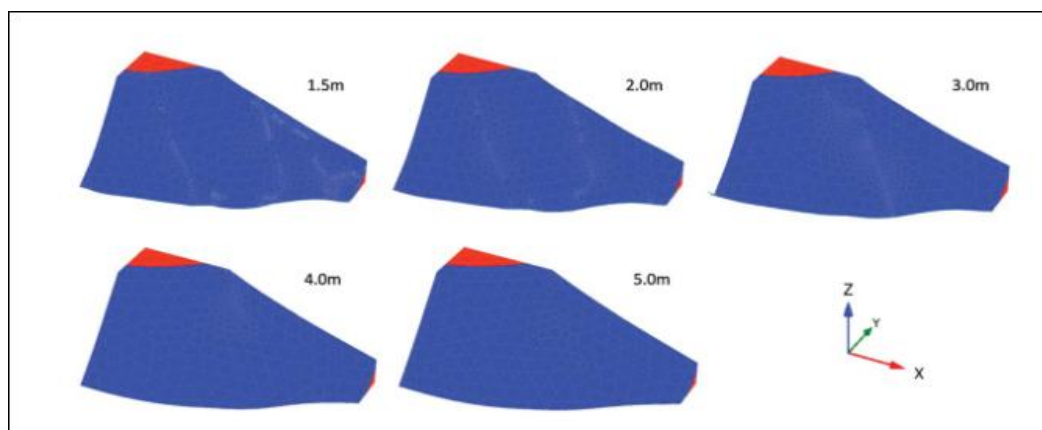
Fig I.27: The numerical model generated in PLAXIS with different point intervals (Wang, M et al.2017).

Overall, the study of ground movements, particularly in the context of slope stability, highlights the various factors that influence the stability of slopes, including geology, hydrology, and climate. Slope instabilities occur when the driving forces, such as gravity and groundwater pressure, exceed the soil's resisting forces. Ground movements can be classified into rapid and slow categories, with rapid movements like rockfalls and mudflows posing direct risks to human safety, while slow movements like creep and solifluction primarily impact socio-economic factors. The overall analysis underscores the importance of understanding and predicting slope stability to mitigate risks associated with ground movements in mining, particularly in large open pit contexts.

Chapter II

Geology, hydrogeology and climatic conditions

II.1. Introduction:

Djebel Onk mining complex serves as SOMIPHOS's main approach to phosphate production within its business units. It holds a crucial position in the national economic and international trade progress, while also enhancing SOMIPHOS's administrative and financial management capabilities, allowing it to more effectively address client needs and preferences. Additionally, the Djebel Onk complex is certified ISO 9001 and ISO 14001 standards by the International Organization for Standardization, ensuring quality and environmental management systems compliance.

Furthermore, the Djebel Onk mining complex operates with state-of-the-art technology and employs sustainable mining practices to minimize environmental impact. It prioritizes safety measures to ensure the well-being of its workforce and adheres to strict regulatory guidelines. Additionally, the complex actively engages in community development initiatives, contributing to local employment opportunities and supporting social welfare programs (Nettour, D et al. 2018; Makhlouf, A et al .2019; Boucif, R et al .2024).

II.2. Presentation of the SOMIPHOS Company:

Company of SOMIPHOS (Société des mines de phosphate) Subsidiary of FERPHOS Group. Established in January 2005, following the reorganization of SOMIPHOS s.p.a. Created for the research, exploitation, enrichment, processing, transportation, and marketing of phosphates.

  SOMIPHOS extracts raw phosphate from the ground through open-pit quarries in the phosphate basin of Djebel Onk. The ore is then screened, washed, and dried. The processed ore is subsequently shipped to the Port Installations of Annaba, either by rail or by road transport. The entire production is exported as raw material to several countries around the world. The Djebel-Onk complex is the main strategic Business Unit of SOMIPHOS for phosphate production (Ornella, T. N., & Fan, Q. 2024).
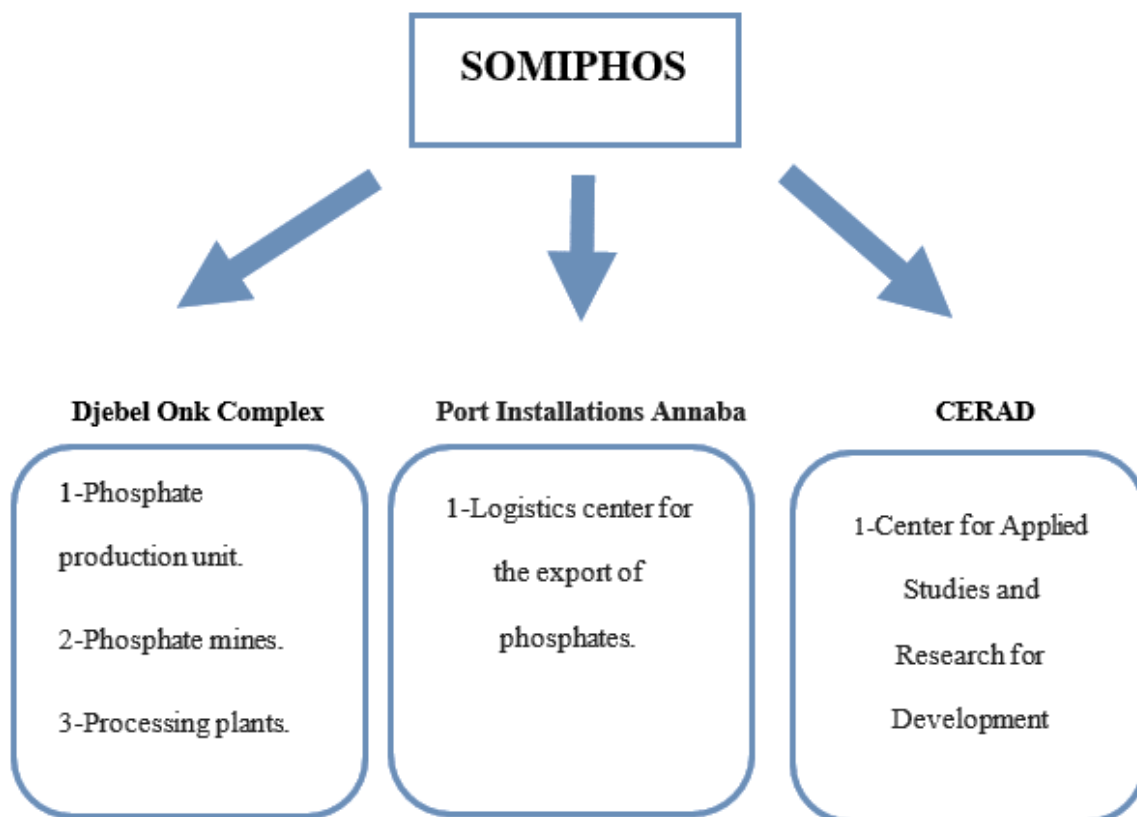
Fig II.1: Compositions of SOMIPHOS Company.

II.3. Background and General Overview of the Mine:

II.3.1. History and methodology of geological research at Djebel Onk:

 According to the EREM report by Cieslinski et al. From 1985 to 1987 are summarized in the following table :(Dass Amiour 2013; Tahri, T et al .2023).

Table II.1: History and methodology of geological research at Djebel Onk.

-In 1873	Laid the foundation for subsequent explorations.
-In 1907–1908	Joleau's identification of the Djebel Onk deposit. with comprehensive insights provided by Dussert, marked a pivotal development.
-In 1924	Dussert D. contributed ethological details concerning the phosphates deposits in Djebel Onk.
-In 1936	A subsidiary was founded: Société du Djebel Onk (S.D.O) in 1936.
-In 1951 and 1952	Visse studied for the S.D.O, the phosphate deposit of Djebel DjemiDjema, the stratigraphy of which he took up in great detail and evaluated the reserves throughout the Djebel Onk area.
- From 1961 to 1963	Airborne radiometric prospecting tests were carried out above the Djebel Onk deposit.
-In 1963	The geological and mining studies preceding the exploitation of the DjemiDjema deposit were carried out by the company SERMI, for the S.D.O. At the same time, the French company SOFREMINES is drawing up a preliminary project for the exploitation of the Kef Essnoun deposit.
- In February 1965	Exploitation of the DjemiDjema deposit began.
-From 1971 to 1974	Research and prospecting work on phosphates in eastern Algeria was relaunched by SONAREM based first on an aeroradiometric survey, then by a prospecting and dissemination campaign. evaluation of the Jebel Onk mining district, in order to highlight additional reserves and better characterize the known deposits.
- In 1986	The Kef Essnoun deposit was recognized in detail by the EREM thanks to 32 core surveys carried out with a mesh size of 250 x 300 m and 22 trenches carried out in the dressings.
- In November 1989	The FERPHOS company made known its specifications for development studies of the Djebel Onk mining complex.
-In 1993	BRGM provided a geological expert report on all the deposits of Djebel Onk-In April 1992, signing of the contract between the company FERPHOS and the consultant BRGM/SOFREMINES concerning the gathering of technical and economic elements making it possible to finalize a project to develop the exploitation of the phosphate deposits of Djebel Onk.

II.3.2. The Phosphate deposits reserves:

The deposit is subdivided into three reserve calculation blocks totaling approximately 317 million tonnes, comprising:

-168 million tonnes of proven reserves.

- 50 million tonnes of probable reserves.

-99 million tonnes of possible reserves.

The attached topographic plan and geological cross-sections clearly depict the quarry's configuration, the thickness of the phosphate layer, as well as the overburden, P_2O_5 and MgO grades, and the inclination of the phosphate layer (Bezzi, N et al. 2012).

II.3.3. Mineralogical composition:

At Djebel Onk and everywhere in other deposits, the mineralized layer (phosphate) is of a stratiform sedimentary type, with a large extent and a thickness estimated at more than 27 meters. The phosphates are of pseudo-lithic type and lithic cut linked by a clayey or dolomitic and siliceous cement (Fantone, I et al .2015).

- Calcite : $CaCO_3$.
- Dolomite : $CaMg\,(CO_3)_2$.
- Quartz: SiO_2.

II.4. General setting:

II.4.1. Geographic Location of Djebel Onk:

The Djebel Onk region is situated approximately 100 km south of the city of Tebessa, 20 km from the Algerian-Tunisian border, and along the road connecting Tebessa to El Oued. This area represents the natural geographic boundary between the Constantine high plateaus and the Saharan domain (G. P. PRIAN, Ph. CORTIEL 1993; Graba, Z et al. 2015). The Djebel Onk massif forms a limestone series spanning 20 km length, with its highest altitude of 1198 m in Djebel Tarfaya, and a lowest elevations of 635 m. This massif constitutes the eastern limit of the Nememcha Mountains.

Fig II.2: Geographic Location of Djebel Onk.

II.4.2. Regional Geology:

The phosphate deposits in the Djebel Onk region are of Upper Thanetian age. The phosphate layer has a thickness of about 30 meters. These terrains are regionally structured into a series of highly asymmetric anticlines and synclines, fractured in their edges, the major faults are oriented N80°E.
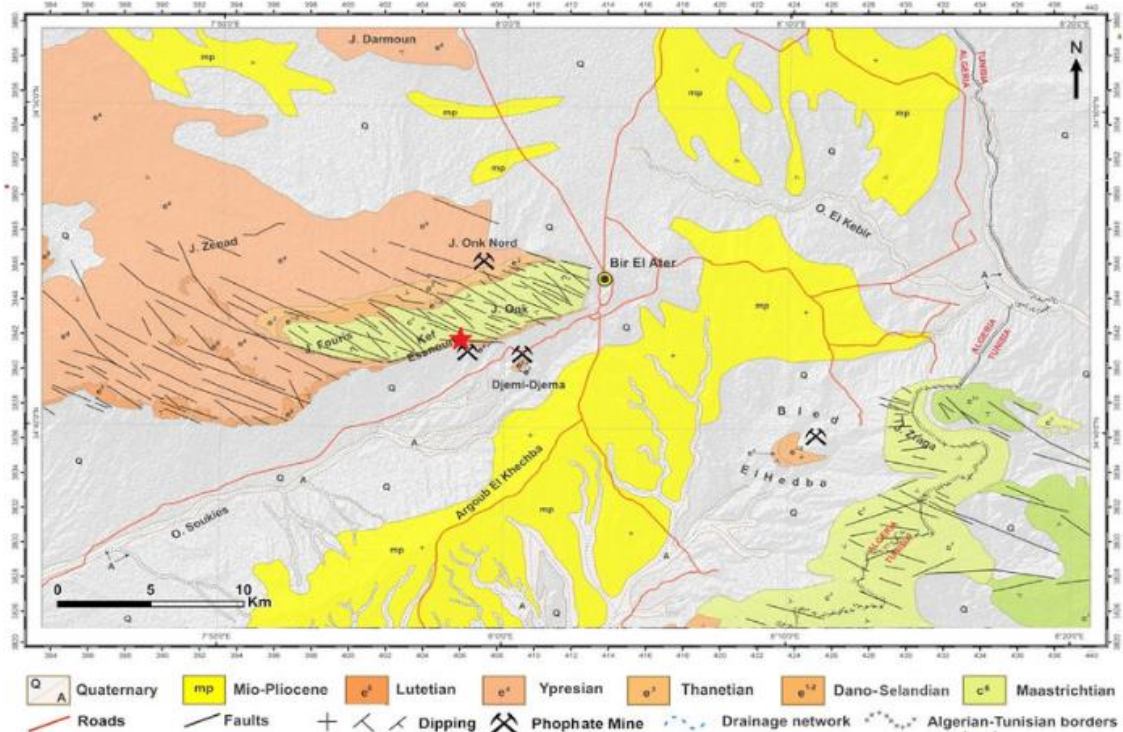
Fig II.3: Regional Geology map of Djebel Onk region.

II.4.3. Stratigraphy:

The stratigraphy of Djebel Onk region was established by Visse, L. D. 1952. The sedimentary series exposed in the region includes a stratigraphic succession ranging from the Upper Cretaceous (Maastrichtian) to the Middle Eocene (Lutetian). This marine series is approximately 500 meters thick. It is unconformably overlain by a thick continental sandy-clayey series of Miocene age, followed by Quaternary deposits filling synclinal structures and fossilizing the pre-Miocene age series.

1.Cretaceous:

   These are the oldest sediments at the core of the Djebel Onk anticline. Tectonically, these formations are highly deformed. Only the deposits from the Maastrichtian are exposed there.

a-Maastrichtian: is represented by massive white limestones with marly intercalations at the core of the Djebel Onk anticline. The top is marked by an iron-rich and weathered surface.

➤**Maastrichtian Limestones:**

-Texture: fine, beige, chalky, and sonorous.

-Content: silica nodules, sometimes in boudins.

-**Transition to the Danian:** Upper layers show alternating marls and marly limestones, topped by conglomeratic monogenetic breccias. Upper marls contain gypsum, with scattered masses and fibers.

Fig II.4: Limestone outcrop represents Maastrichtian unit

This alternation marks the transition from upper Maastrichtian to basal Danian, with a direction of N80°E and an inclination ranging between 45° and 10° S, illustrating regional tectonic effects.
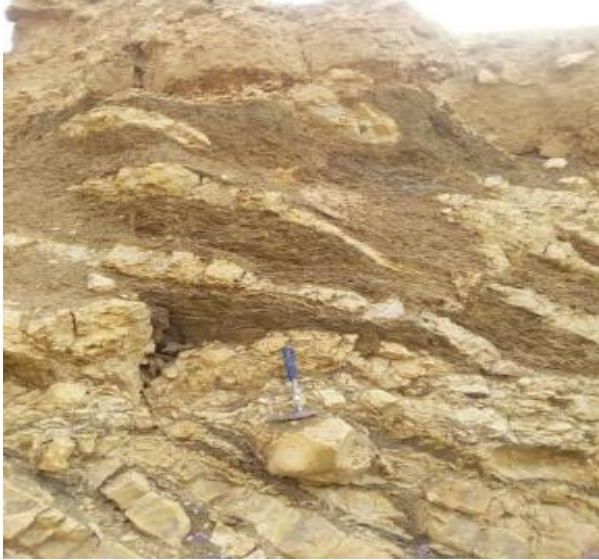
Fig II.5: Marls and marl-limestones of the transition Upper Maastrichtian-Basal Danian.

Fig II.6: Gypsum crystals in a mass of limestone.

Fig II.7: Internal mold of Inoceramus regularus.

Fig II.8: Fossils located in basement layer of the Thanetian unit.

2. Paleocene:

It is represented by fairly thick marine sediments (350 m).

a). Danian: The Danian is lithologically subdivided into two sub-stages: lower and upper.

-Lower Danian It is represented by marly and schistose clays, ranging in color from dark gray to greenish-brown, interspersed with hard and irregular marls. The whole sequence is crossed by gypsum veins. The thickness of the Lower Danian is 30 to 40 m.

-Upper Danian It consists of very fine white hard limestones, often with conchoidal fractures, interspersed with marls, clays, and schists. The thickness varies from a few centimeters to one meter.
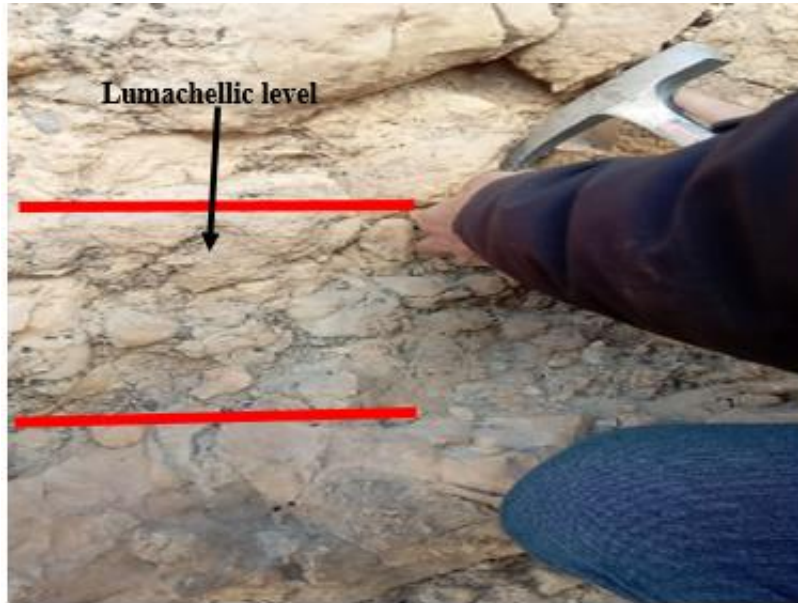
Fig II.9: Lumachellic level intercalated in the Danian facies.

b). Montian: It is represented by detrital limestones to conglomerates with intercalations of marls and dolomite, as well as a small amount of encountered flint. It contains numerous levels of oysters of different colors. The average thickness is 100 m.

c) .Thanetian: This is the horizon bearing the main phosphate mineralization. It is subdivided into two sub-stages.

-Lower Thanetian: is represented by dark gray to black schistose marls. In the lower part, conglomerates and thin phosphate beds are noted, as well as two levels of fauna marls. At the top, phosphate intercalations up to 2m thick appear, overlain by limestones and marls with large gastropods. The thickness varies from 30 to 40 m.

Fig II.10: Schistosose gray marls from the Lower Thanetian
with intercalations of marl-limestone.

-Upper Thanetian: This is the mining layer in the Djebel Onk deposits. It begins with a dolomitic layer with gastropods, and the phosphate layer is on average 30m thick. This layer of Upper Thanetian age is characterized by variations in thickness from one deposit to another in the Djebel Onk basin, noting, for example, in the Djemi-Djema area where the phosphate layer is about 30 m thick, located between a series of laminated black marls on the footwall and a formation of dolomite, then flinty limestone on the hanging wall. In the Djebel Onk Nord area, the phosphate sequence is less. Thick (17 m at most), gradually reducing towards the west until completely disappearing (stratigraphic bevel) (Prian, Cortiel 1993).

Fig II.11: The mining layer in the open pit mine.

3- Eocene:

 a). Ypresian: It directly rests on Thanetian deposits and has a thickness of 32m, noting:

-Lower Ypresian: It is represented by dolomites and dolomitic limestones. Intercalations of highly dolomitic phosphates are well observed, with the presence of numerous black flint debris.

 -Upper Ypresian: It consists of alternating layers of limestones, dolomitic limestones, and marls.

 b). Lutetian: The formations of this stage conformably overlie the Ypresian series. They are widespread in the Djebel-Onk region (270 m thick). Distinguishing from bottom to top:

- Lower Lutetian: It is characterized by a remarkable decrease in limestones, which are replaced by chalky white marls. The presence of quartz geodes and flint nodules is noted, along with characteristic fauna (Hemither Sitea Moracano). Its thickness ranges from 40 to 50 m.

 -Upper Lutetian: These facies are evaporitic; it consists of gypsum and greenish clay, green phosphatic clay, and limestone beds. At the base, green phosphatic clay and limestone beds

with a thickness of 10 m are distinguished. At the top, green clays with intercalated gypsum beds. Its thickness is 65 m. The characteristic fauna is Ostrea Multicostata and Cardia Placunoides.

4.Miocene: It is represented by a complex of terrigenous rocks, conglomerates, clays, sands, and shales. Three lithological formations are distinguished:

 a) . Lower Miocene: It is mainly represented by conglomerates, sands with thin layers of siliceous clay. The color is light, whitish-gray. Its thickness is 200 m.

 b). Middle Miocene: It is mainly clayey, brown in color, sometimes schistose, with intercalations of fine to medium-grained sands. Its thickness reaches 250 m.

 c). Upper Miocene: It is a series of sandy-clayey-conglomeratic deposits. Its thickness reaches 350 m.

5. Quaternary: Quaternary formations cover vast areas in the region. They are mainly represented by scree slopes, sandy deposits, gravels, aeolian, alluvial, and fluvial deposits.
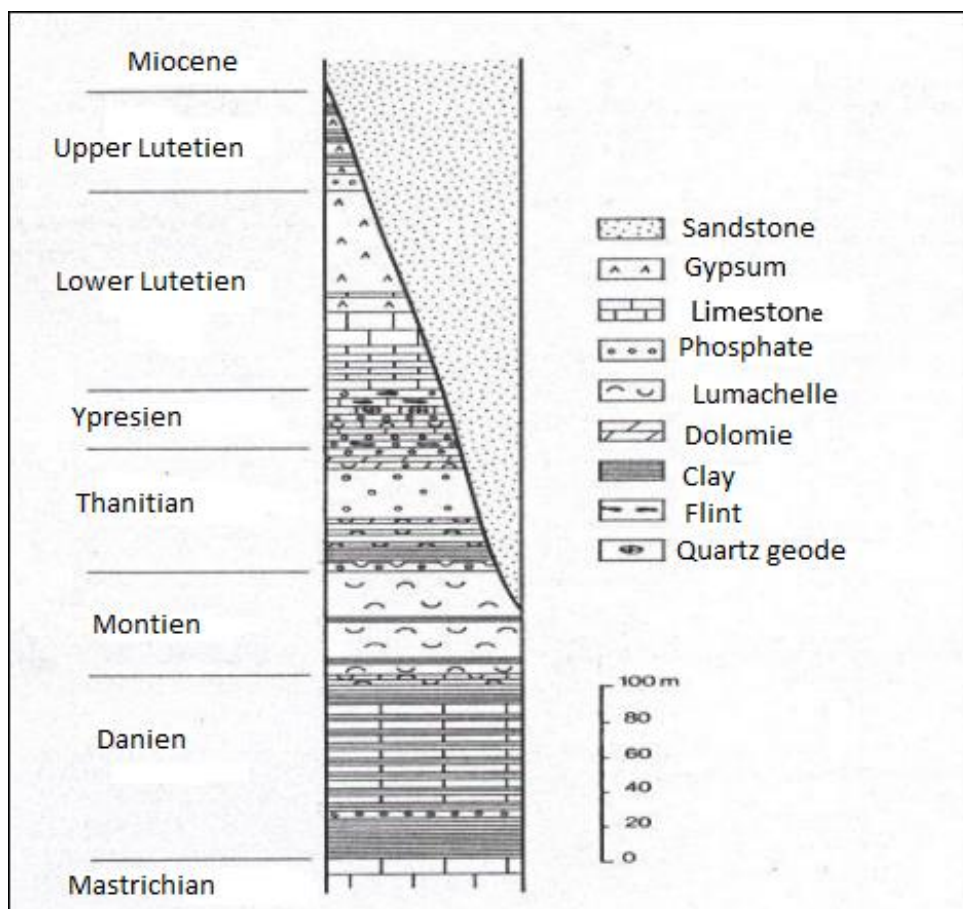
Fig II.12: Schematic stratigraphic section of Djebel Onk (in Chabou-Mostefaï,1987).

II.4.4. Tectonics:

The Djebel Onk region, along with the Tunisian Atlas, constitutes the eastern end of the Saharan Atlas. The Upper Cretaceous to Eocene series of the Djebel Onk-Gafsa-Métlaoui basin is structured into a series of asymmetric anticlines and synclines, often faulted on their SW-NE trending axes and offset by transverse faults-oriented N 120° to N 140° E. The primary structure in the Bir El Ater region is the Djebel Onk anticline, which consists of Upper Cretaceous rocks and extends for about 20 kilometers in length and 3 kilometers in width.

This strongly asymmetric anticline, described by Visse in 1951 as a post-Pliocene anticlinal flexure, features a northern flank with a gentle dip of less than 10 degrees, supporting the Djebel Onk Nord deposit, and a southern flank with a steep dip, occasionally vertical or even overturned (Kechiched, R et al 2018; Abu-Ali, R., & El-Kammar, A.2024).
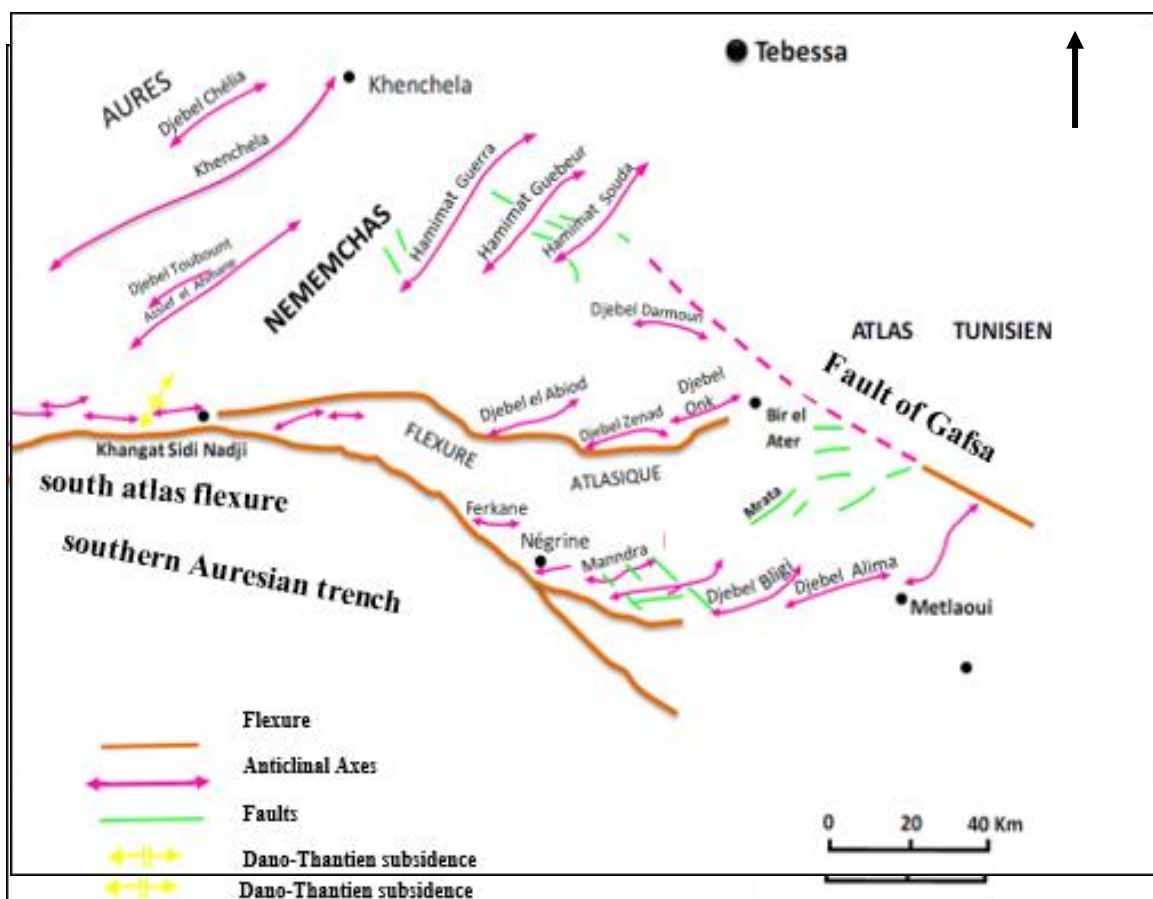
Fig II.13: Tectonic map of Djebel Onk region (Aissaoui, 1984 in Chabou-Mostefaï, 1987).

II.4.5. The hydrogeological conditions:

The hydrogeological conditions in the Djebel Onk region are closely tied to both the climate and the structural characteristics defining it. Various less significant hydrogeological structures contribute to the formation of the following aquifer complexes:

- Quaternary aquifer layers.

-Aquifer complex situated within Miocene deposits.

-Aquifer complex within Eocene limestone formations.

- Aquifer complex within Paleocene layers.

- Maestrichtian aquifer complex located within Upper Cretaceous deposits, with the Eocene limestone aquifer complex being the most hydrogeologically relevant in the region.

   These aquifer complexes are tapped into by multiple wells to supply water to the Djebel Onk mining complex. The chemical composition of this water is diverse, predominantly containing sulfates with mineralization ranging from 1 to 4 g/l (Hamad, A et al. 2018).

II.4.6. Phosphate Morphology:

  From a morphological standpoint, Djebel Onk is characterized by highly varied terrain with significant changes in elevation. The relief features are diverse, showcasing the region's geological complexity. The current morphology of Djebel Onk is influenced by several factors:

-Tectonic movements have played a significant role in shaping the landscape, contributing to the formation of the current geological structures of Djebel Onk.

- Erosion has had a considerable impact, exposed various rock formations and created favorable conditions for different types of erosion processes. This erosion has led to the gradual breakdown and removal of rocks, facilitated by the actions of water.

   These factors collectively contribute to the unique morphology of Djebel Onk, shaping its landscape over geological timescales.

II.4.7. The climatology:

  The climate is subarid, characterized by a continental regime with two distinct seasons: a cold and harsh winter, and a summer where temperatures can exceed 45°C. Precipitation is low, averaging 300 mm/year (semi-arid climate). The regional hydrographic network is diverse, and the mountains and valleys are characterized by a sparse flora. The majority of the population is concentrated in Bir El Ater, while the remaining part consists of nomads (R. RAOUDSEP, 1978). In this region, four stations record weather conditions over long periods:

- Negrine (Weather station code: 063001).

- Saf Saf El Ouessra (Weather station code: 062808).

- Thelidjene (Weather station code: 062503).

- Tebessa (Weather station code: unknown).

1.Temperature:

 The temperature data collected at the Saf Saf El Ouessra station spans from April 1992 to March 2012, offering insights into maximum, minimum, and average monthly temperatures.

  During this period, the region experienced notable temperature extremes:

-Conversely, in August 1993, the mercury soared to a scorching 45.8°C, marking one of the hottest recorded temperatures.

These extreme temperature fluctuations underscore the climatic variability experienced in the area. Such data is essential for understanding local climate patterns and their potential impacts on various sectors, including agriculture, infrastructure, erosion, and stability of mines.

- In February 1996, the temperature plummeted to a frigid -6.2°C.
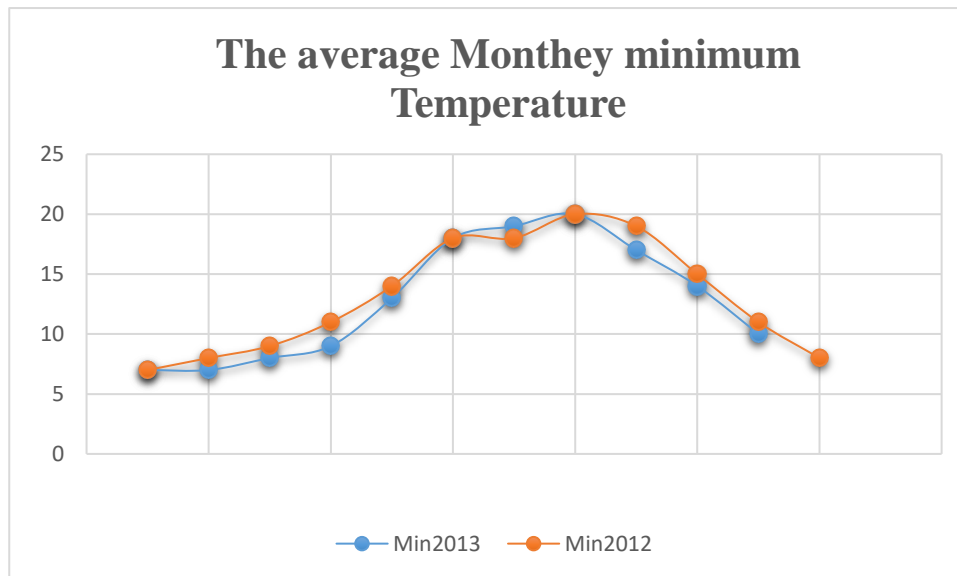
Fig II.14: The average monthly minimum Temperature.
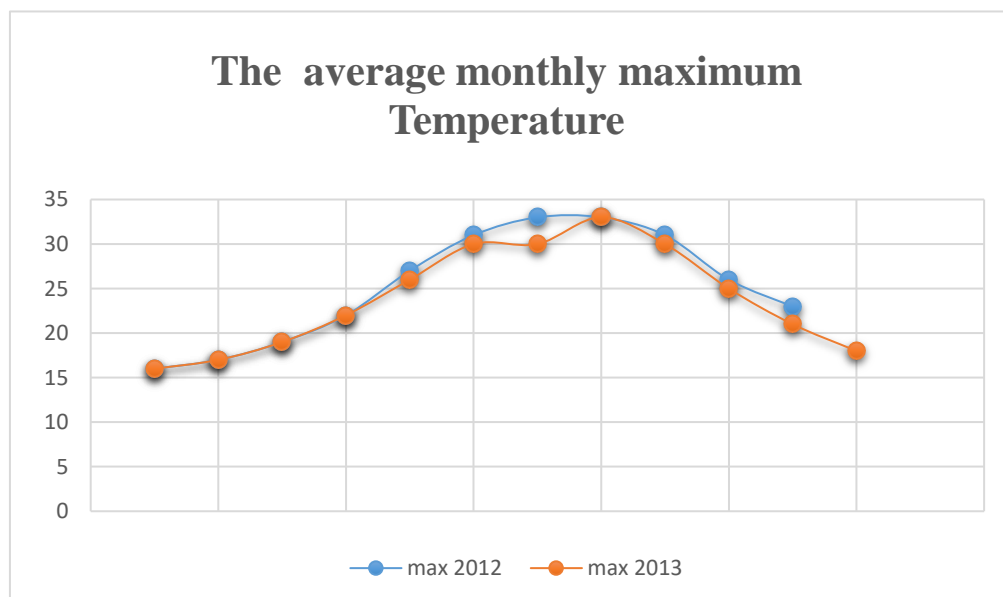
Fig II.15: The average monthly maximum Temperature.

2. Precipitation:

   Annual precipitation totals exhibit significant variability from one year to the next. The monthly precipitation averages depict a distinct peak in September, with an average of 30.1 mm, followed by a gradual decline to 7.5 mm in February. Subsequently, precipitation rates begin to rise again in spring, only to taper off to very minimal levels during July (7.2 mm) and August (11.6 mm).

   The frequent occurrence of thunderstorms during August and September contributes to the precipitation patterns observed during these months. These thunderstorms can lead to localized heavy rainfall, impacting local hydrology and potentially causing flooding in susceptible areas. Understanding these precipitation trends is crucial for water resource management, agriculture, and disaster preparedness planning in the region.
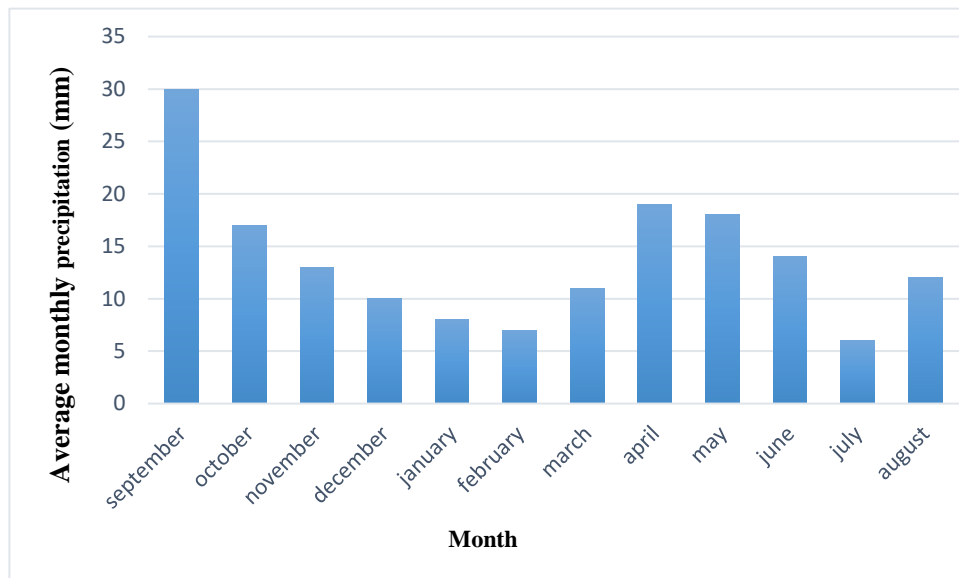
Fig II.16: The monthly precipitation (mm).

3. Humidity:

   Consistently high levels of humidity persist throughout the year, typically fluctuating between 40% and 75%. Winter months tend to experience peak humidity levels, while the summer months exhibit lower humidity levels.
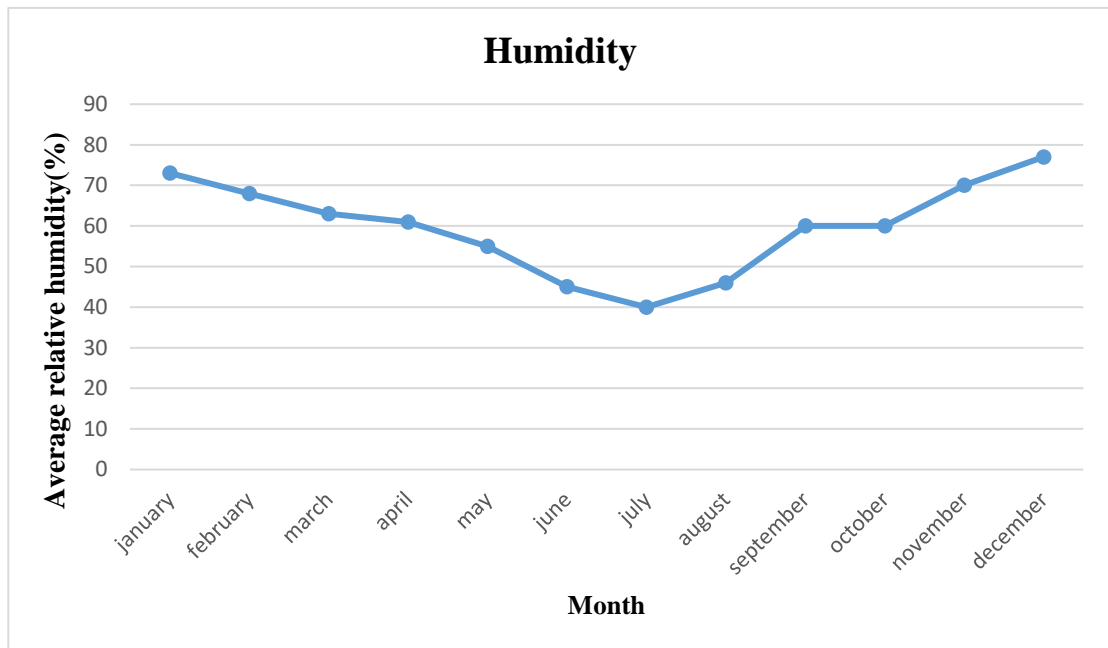
Fig II.17: The average relative humidity (%).

II.5. Impact of Moisture on Mines:

Moisture plays a significant role in mining and extraction operations, affecting the safety and efficiency of operations and the infrastructure of the mine. Here are some key effects of moisture on mines (Pan, Z.et al 2010; A et al 2016; Liu, W et al. 2019):

1-Safety Impact: Moisture can increase the risk of rockfalls and soil collapses inside the mine, posing hazards to workers. It may also lead to increased formation of toxic gases inside the mines, increasing the risk of accidents.

2- Equipment Impact: Moisture can cause corrosion and rusting of equipment and machinery used in mining operations. Maintaining equipment and machinery in good condition requires regular maintenance to avoid unplanned production stoppages.

3-Product Quality Impact: Moisture can have a negative impact on the quality of materials extracted from the mine, such as stones and minerals. Changes in moisture content in materials can lead to changes in their physical and chemical properties.

4- Water Management Impact: Moisture inside the mine can cause water management issues, including water leakage into drill holes and blasts, requiring additional costs for water pumping and management.

To mitigate the impact of moisture on mining operations, appropriate safety measures should be implemented, and suitable technology should be used to maintain equipment and ensure effective productivity in all environmental conditions.

II.6. Geography of Study area:

Located around 750 meters south of the main Djebel-Onk anticline is the smaller Demi Djema anticline, which slopes downward. This anticline displays an axis oriented at 70 degrees east but has limited lateral expansion, resembling either a small branched anticline or a dome-shaped structure (CIGCM 2016).

Fig II.18: Location of Kef Essnoun.

II.7. Local geology of Kef Essnoun:

The geological formation of Kef Essnoun is closely tied to the southern extension of Djebel Onk's antiform flexure, with its primary structural characteristics shaped by tectonic activity after the Miocene epoch. In terms of rock composition, the Kef-Essnoun deposit can be divided into the following layers, from bottom to top (Visse 1952):

-Ypresian series characterized by calcareous-dolomitic rocks with flints.

-Lutetian formations composed of marly limestone.

-Miocene deposits comprising sands.

-Quaternary layers consisting of alluvial deposits.
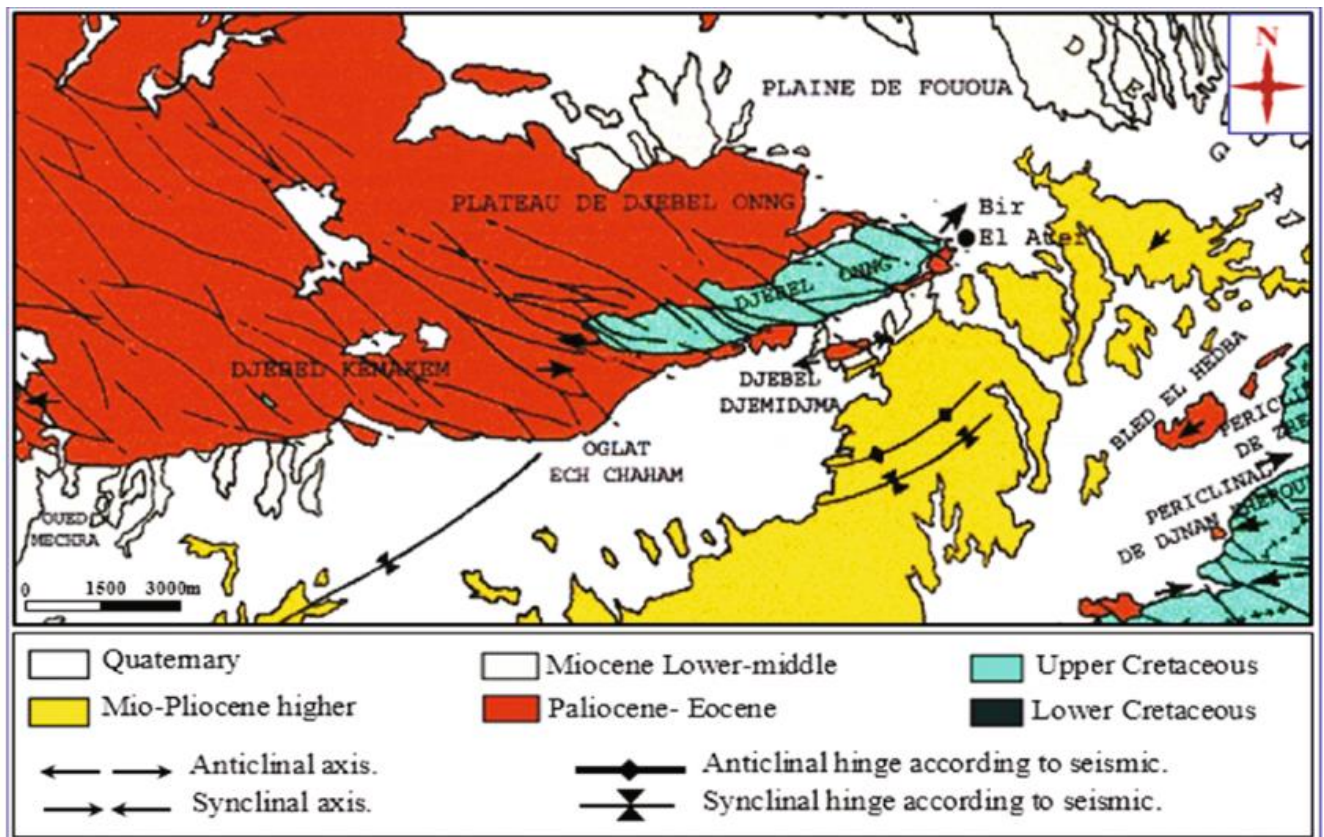
Fig II.19: Geological map of Kef Essnoun.

II.9. Stratigraphy:

The entire lithological succession of Djebel Onk can be observed at Kef Essnoun, but it is notably distinguished by a greater vertical thickness of the phosphate layer, reaching up to 53 meters in some drill cores.

The lithological succession of the Kef Essnoun deposit, from bottom to top, is as follows (Cielensky et al.1985, 1987):

- Lower Thanetian formations (forming the base of the phosphate layer) consist of dark, laminated marls, with two infra-metric thick layers of dolomitic phosphates locally interspersed in the lower part.

- The phosphate layer, belonging to the Upper Thanetian, is composed of a single phosphate layer without any sterile intercalations.

- Above the phosphate layer, there is a calcareous-dolomitic series with flint from the Ypresian, followed locally by Lutetian limestones, then Miocene sands, and finally recent Quaternary deposits mainly consisting of alluvium.

The total thickness of the sterile overburden ranges from 40 meters in the north to 198 meters in the south.

II.10. Tectonics:

The tectonics of Kef Essnoun have been described by several reachers (Cieslinski et al. 1985, 1987; Prian and Cortiel 1993):

The Kef Essnoun deposit is characterized by a simple structure, forming a monocline table with a regular dip angle of 5 to 10° towards the south.

To the south of the table, there is a slope break zone where the dip of the layers reaches 20°. A series of three major faults-oriented NNW-SSE cross the deposit but do not cause significant deformations in the geometry of the phosphate layer.

However, in the Kef Essnoun escarpment zone, which is elongated along N 75° E, both flexible and brittle tectonics have caused a sudden change in the dip of the exposed phosphate layer, where the dip angle is nearly vertical or steeply inclined towards the southeast or northwest. These escarpments, represented by Paleocene formations (Danian, Montian, and Thanetian) and Lower Eocene formations (Ypresian), correspond to the flexure-fault zone on the reverse flank of the Djebel Onk anticline.

To the northeast of the escarpments, the series is overturned, and the phosphate layer dips at an angle of 30° to 60° towards the northwest. In contrast, in the central part of the escarpments, the phosphate layer is in a normal series and dips towards the south.
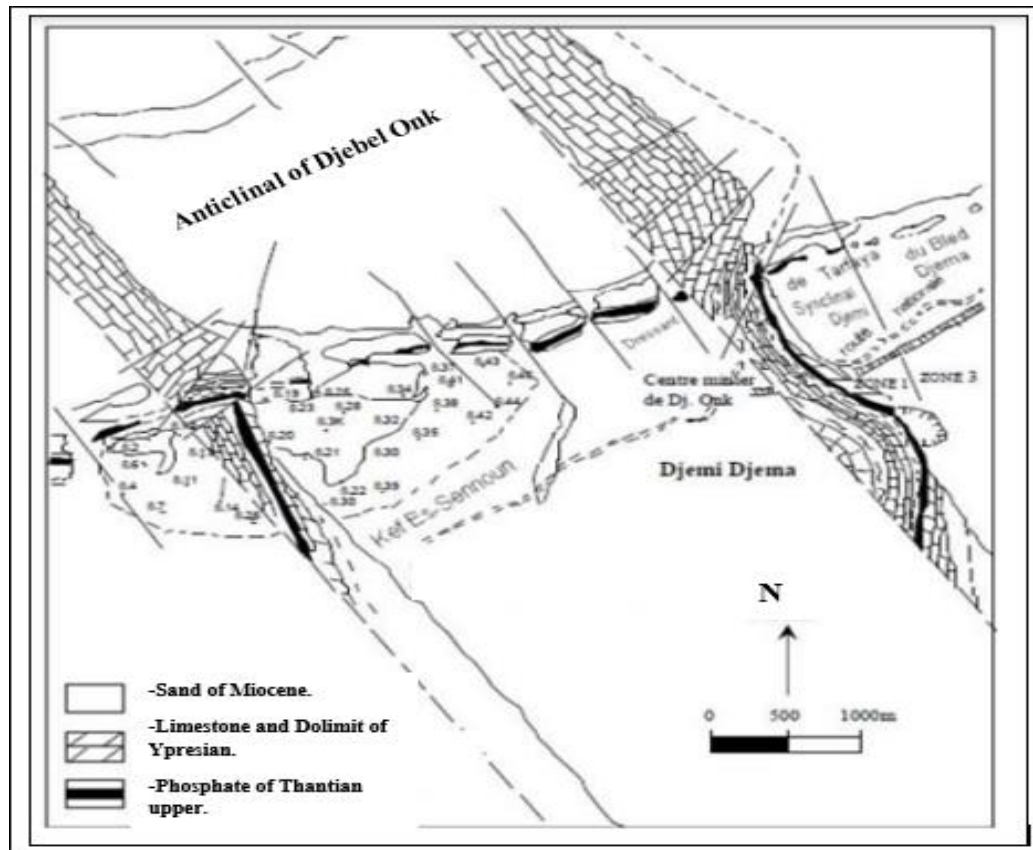
Fig II.20: The tectonics map of Kef Essnoun.

II.11. Hydrogeological Overview:

1. Climatology:

Based on the hydrogeological analysis of the Djebel Onk region, particularly the Kef-Essnoun activity zone conducted by the DED, and the observation of hydrometric data over a period of 22 years (1986-2008), it is noted that the Kef-Essnoun region is characterized by a subarid to arid climate with cold winters and hot, dry summers. The drought period extends throughout the year.

2. Temperature:

Over an average of 5 years, temperatures follow the same pattern. In winter, they fluctuate around 7°C. Temperatures gradually increase from May until reaching very high levels (45°C) in summer, then decrease gradually in autumn.

3. Rainfall:

The average annual rainfall is around 88 mm, with evapotranspiration at approximately 87 mm, representing 100% of precipitation. Rainfall during the summer is extremely rare. Periods without rainfall for more than a month are common. Rainy periods vary between 66 and 107 days per year. Thunderstorms are significant and frequent, especially during the months of August and September. Snow and frost are rare, but temperatures often drop below 0°C in winter.

II.12. Conclusion

Algeria possesses significant reserves of phosphate, primarily found in the deposits of the Djebel Onk region in Tebessa. The phosphate deposits of Kef Essnoun is situated in the extension of the southern slope of the antiform flexure of Djebel Onk, with its major structural formation attributed to post-Miocene tectonics. This deposit is renowned for its high-grade phosphate ores and has been a key contributor to Algeria's phosphate industry.

The stratigraphy of the Djebel Onk region is characterized by a stratigraphic succession ranging from the Upper Cretaceous (Maestrichtian) to the Middle Eocene (Lutetian). These sedimentary layers hold valuable geological information and have been extensively studied for their mineral wealth.

Furthermore, the hydrogeological conditions in the Djebel Onk region are closely related to the climate and structural characteristics that define them. The region experiences around 70 rainy days per year, with frequent thunderstorms during August and September. Although snowfall and frost are rare, temperatures below 0°C are common during winter, affecting the local hydrological systems and groundwater flow.

Chapter III

Geotechnical investigations and data collection

III.1. Introduction:

To understand the causes and modes of slope failure and quantify the stability parameters, a rigorous study is essential. This allows for diagnosing existing problems and designing effective stabilization works. The study includes several key steps:

-Field Investigation: Drilling, sampling, and in-situ tests to quantify rock parameters directly on site.

-Laboratory Research: Analyzing samples to determine the physico-mechanical properties of the rock materials.

-Site Reconnaissance and Identification: Observing and documenting the site's geological, topographical, and hydrological characteristics.

-Analysis of Existing Information: Reviewing previous studies, geological maps, and technical reports.

-Study of Surface Characteristics: Detailed analysis of the topography, slopes, rock structures, and signs of erosion or instability.

For the north-western slope of Kef Essnoun, it is necessary to determine and classify the physico-mechanical properties of the rock mass. Once these properties are characterized and classified, specific interventions can be proposed to stabilize the slope and prevent future failures.

III.2. Physico-mechanical properties:

III.2.1. Context of the Study:

In our case study, the parameters used come from the available database provided by the company. They are derived from previous tests conducted in a laboratory. This allows us to use precise and reliable data to analyze the slope stability, the following tables represent the physico-mechanical properties:

Table III .1 : Results of uniaxial compression tests.

Layer	Sample Type	Uniaxial Compressive Strength (MPa)
Layer 1	Limestone	34.1
Layer 2	Phosphates	10.2
Layer 3	Limestone/Conglomerate	34.1
Layer 4	Marls	21.6

Table III.2: Results of Tensile Strength Tests.

Layer	Sample Type	Tensile Strength (MPa)
Layer 1	Limestone	2.5
Layer 2	Phosphates	1.8
Layer 3	Limestone/Conglomerate	2.5
Layer 4	Marls	2.9

Table III.3: Point Load Index.

Layer	Sample Type	Point Load Index (MPa)
Layer 1	Limestone	2.2
Layer 2	Phosphates	1.0
Layer 3	Limestone/Conglomerate	2.2
Layer 4	Marls	1.6

Table III.4: Results of triaxial compression strength Tests.

Layer	Sample Type	Shear Strength (MPa)
Layer 1	Limestone	64.4
Layer 2	Phosphates	78.3
Layer 3	Limestone/Conglomerate	64.4
Layer 4	Marls	83.6

Table III.5: Young's Modulus values.

Layer	Sample Type	Young's Modulus (MPa)
Layer 1	Limestone	5200
Layer 2	Phosphates	4600
Layer 3	Limestone/Conglomerate	5200
Layer 4	Marls	3600

Table III.6: Internal Friction Angle.

Layer	Sample Type	Internal Friction Angle (φ) (°)
Layer 1	Limestone	23
Layer 2	Phosphates	30
Layer 3	Limestone/Conglomerate	23
Layer 4	Marls	15

Table III.7: Poisson's Ratio.

Layer	Sample Type	Poisson's Ratio
Layer 1	Limestone	0.21
Layer 2	Phosphates	0.24
Layer 3	Limestone/Conglomerate	0.21
Layer 4	Marls	0.14

Table III.8 : Cohesion values.

Layer	Sample Type	Cohesion (C) (MPa)
Layer 1	Limestone	1.4
Layer 2	Phosphates	2.4
Layer 3	Limestone/Conglomerate	1.4
Layer 4	Marls	1.2

Table III.9: Unsaturated Unit Weight (kN/m³).

Layer	Sample Type	Unsaturated Unit Weight (kN/m³)
Layer 1	Limestone	27
Layer 2	Phosphates	21
Layer 3	Limestone/Conglomerate	27
Layer 4	Marls	23

Table III.10: Saturated Unit Weight (kN/m³).

Layer	Sample Type	Saturated Unit Weight (kN/m³)
Layer 1	Limestone	27.46
Layer 2	Phosphates	24.81
Layer 3	Limestone/Conglomerate	27.46
Layer 4	Marls	24

III.2.2. Analysis of Test Results:

-Uniaxial Compressive Strength:

Based on the results:

- Limestone (34.1 MPa) and Marls (21.6 MPa) are classified as having moderate strength.

- Phosphates (10.2 MPa) are classified as having low strength.

-Tensile Strength:

From the results presented in Table III.2:

- Limestone (2.5 MPa), Marls (2.9 MPa), and Phosphates (1.8 MPa) are classified as having moderate strength.

- Triaxial compression strength Tests:

The shear strength results in Table III.4 lead to the following conclusions:

- Limestone (64.4 MPa), Phosphates (78.3 MPa), and Marls (83.6 MPa) are all classified as strong.

-Point Load Index:

- Limestone (2.2 MPa): Classified as low strength based on the point load index.

- Phosphates (1.0 MPa): Classified as low strength.

- Limestone/Conglomerate (2.2 MPa): Classified as low strength.

- Marls (1.6 MPa): Classified as low strength.

-Interpretation of Cohesion values:

- Limestone (1.4 MPa): Moderate cohesion.

- Phosphates (2.4 MPa): High cohesion.

- Limestone/Conglomerate (1.4 MPa): Moderate cohesion.

- Marls (1.2 MPa): Moderate cohesion.

-Interpretation of Internal Friction Angle values:

- Limestone (23°): Moderate internal friction angle, indicating moderate shear resistance.
- Phosphates (30°): High internal friction angle, indicating high shear resistance.
- Limestone/Conglomerate (23°): Moderate internal friction angle, similar to pure limestone.
- Marls (15°): Low internal friction angle, indicating lower shear resistance.

-Interpretation of Young's Modulus values:

- Limestone (5200 MPa): Indicates a high stiffness, implying the material is relatively rigid and deforms less under stress.

- Phosphates (4600 MPa): Also indicates good stiffness, though slightly less than limestone.

- Limestone/Conglomerate (5200 MPa): Similar to pure limestone, indicating high stiffness.

- Marls (3600 MPa): Lower stiffness compared to the other materials, indicating more deformation under stress.

III.3. Geomechanical rock classification of the site:

The classification of rock formations is highly significant during the feasibility analysis and initial sizing process.

Classification systems take into account several factors affecting the stability of rock masses. These factors are particularly related to the strength of the rock matrix, the presence of water, and the description of discontinuities (number of families, spacing, roughness, weathering of joints, filling material...) (Laubscher, D. H. 1990; Palmstrom, A., & Broch, E.2006).

III.3.1. The determination of RQD (Rock Quality Designation):

The RQD index is determined during geotechnical core logging. The RQD index (Rock Quality Designation index) is a (core-related) value for the degree of natural internal fragmentation of the rock mass. This factor is quoted as a value between 0 and 100 (Deere, D. 1988; Deere, D. U., & Deere, D. W 1989).

It has been calculated:

- From field measurements (NS):

Fig III.1 Field measurements of RQD.

- From the core sample:

Fig III.2: Core drilling photo.

- Results and discussion:

- From field measurements:

Table III .11 : RQD value of different facies.

Rock Type	RQD (%)	Rock Quality
Limestone (Danian-Montian)	85	Good
Ypresian Limestone	72	Fair

- From the core sample:

Table III.12 : RQD value of different facies (according to SOMIFOS).

Rock Type	RQD (%)	Rock Quality
Limestone (Danian-Montian)	84	Good
Marl	45	Poor
Phosphate	73	Fair
Ypresian Limestone	70	Fair

According to the results obtained from the application of the RQD method on the conditions of the Kef-Essnoun mine, it is observed that this rock mass consists of facies of: good quality (Danian-Montian Limestone), medium quality (Phosphate, Ypresian Limestone), and poor quality (Marl) with an RQD score ranging between 45 and 84.

III.3.2. The Rock Mass Rating (RMR) classification:

The Rock Mass Rating (RMR) classification of the Kef-Essnoun rock mass utilizes Bieniawski's index (1989) to assess the stability of the rock formation. This method was chosen for open-pit mining due to its simplicity, cost-effectiveness, and suitability for the geological conditions. In the case of Castellans, the RMR index was determined for each structural domain defined by the mining fronts, considering parameters such as RQD, uniaxial compressive strength, spacing, aperture, persistence, roughness, filling, and weathering of discontinuities, as well as the presence of water and its effect relative to the excavation axis (ROMANA, M. R. 1993).

Table III.13: RMR Values for Ypresian Limestone Facies.

		Value	Note
Parameters	**Facies**	Ypresian Limestone	/
	Rc (MPa)	27	4
	RQD (%)	70	13
	Joint Nature	Slightly rough surface, thickness > 1m	25
	Joint Spacing (m)	0.6 - 0.2	10
	Hydrogeology	Completely dry	15
	Base RMR	-	67

Table III.14: RMR values for Phosphate facies.

		Value	Note
Parameters	**Facies**	Phosphate	/
	Rc (MPa)	6	1
	RQD (%)	73	13
	Joint Nature	Slightly rough surface, thickness > 1m	25
	Joint Spacing (m)	0.6 - 0.2	10
	Hydrogeology	Completely dry	15
	Base RMR	-	64

Table III.15: RMR values for Marl facies.

		Value	Note
Parameters	**Facies**	Marl	/
	Rc (MPa)	6.78	1
	RQD (%)	45	8
	Joint Nature	Discontinuities: Smooth or filling < 5 mm thick or joints open 1 - 5 mm and continuous.	10
	Joint Spacing (m)	<0.06	5
	Hydrogeology	Completely dry	15
	Base RMR	-	39

Table III.16 : RMR values for Danian-Montian limestone facies.

		Value	Note
Parameters	**Facies**	Danian-Montian limestone	/
	Rc (MPa)	26.8	4
	RQD (%)	84	17
	Joint Nature	Slightly rough surface, thickness > 1m	25
	Joint Spacing (m)	<0.06	10
	Hydrogeology	Completely dry	15
	Base RMR	-	71

Based on the results of the base RMR, it can be inferred that the Ypresian limestone and Danian-Montian limestone phosphate facies have good quality and are better resistance. However, the marl facies are of poor quality.

III.3.3. SMR Classification of the Kef Essnoun Rock Mass:

The SMR classification established based on in-situ observations indicates that the quality of the rock mass varies depending on the different facies (Romana, M. 1991).

Table III.17: Joint and slope orientation.

Facies	Joint Dip Direction (α_j) (°)	Joint Dip (β_j) (°)	Slope Dip Direction (α_s) (°)	Slope Dip (β_s) (°)
Ypresian Limestone	170	23	270	75
Phosphate	180	10	270	75
Marl	40	28	270	75
Danian-Montian Limestone	68	52	270	75

Table III.18: SMR value of different geological formations.

	Ypresian Limestone	Phosphate	Marl	Danian-Montian Limestone
RMR base	67	64	39	71
F1	0.15	0.15	0.15	0.15
F2	0.4	0.15	0.4	1
F3	-60	-60	-60	-60
F4	-8	-8	0	0
SMR	55.4	54.56	35.4	62
Class	III	III	VI	II
Description	Medium	Medium	Bad	Good

According to the SMR classification results we see that the marly interface constitutes the probable cause of instability of the massif.

III.3.4. GSI Classification of the Kef Essnoun Rock Mass:

The GSI index is used to estimate the reduction in rock mass strength under different geological conditions. This system provides an estimated GSI value based on the structure of the massif and the surface conditions of the discontinuities. this value is directly applied to estimate the parameters of the Hoek-Brown strength criterion for rock masses (Hoek, E et al 1998; Marinos, P., & Hoek, E. 2000)

Through field measurements, the GSI value ranges from 70 to 80.
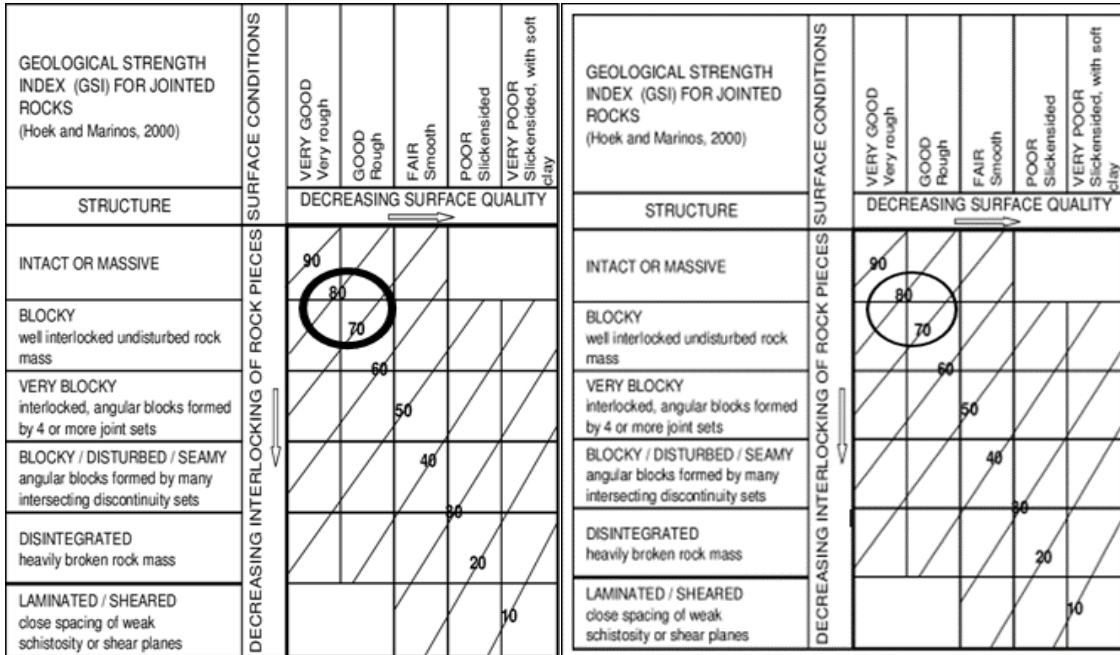
Fig. Station N°=1.

Fig. Station N°=2.
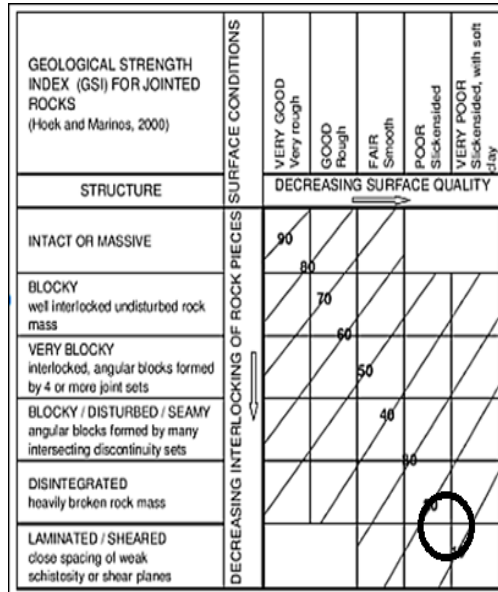
Fig. Station N°=3.

Fig III.3: The GSI value of Kef Essnoun region.

III.4. Conclusion

Understanding slope stability and preventing failure requires a comprehensive approach involving field investigations, laboratory research, and detailed site analysis. The study of the north-western slope of Kef Essnoun involves determining the physico-mechanical properties of the rock mass, which are crucial for designing effective stabilization measures. Laboratory tests reveal varying strengths among different rock layers, with limestone (34.1 MPa) and marls (21.6 MPa) showing moderate uniaxial compressive strength, while phosphates exhibit low strength (10.2 MPa). Shear strength results show that marls (83.6 MPa) have the highest shear strength, followed by phosphates (78.3 MPa), and limestone (64.4 MPa).

Geomechanical classifications such as RQD, RMR, SMR, and GSI provide insights into the quality and stability of the rock mass. RQD values indicate good quality for Danian-Montian Limestone (84-85%) and fair quality for Ypresian Limestone (70-72%) and phosphates (73%), while marls are of poor quality (45%). RMR values show good quality for Danian-Montian Limestone (71) and Ypresian Limestone (67), medium quality for phosphates (64), and poor quality for marls (39). SMR classification results highlight the marly interface as a probable cause of instability, with marls receiving the lowest score (35.4). The GSI index ranges from 70 to 80, suggesting a reduction in rock mass strength under different geological conditions.

The findings emphasize the importance of detailed geomechanical analysis for predicting rock behavior and ensuring safe mining operations, indicating that specific interventions are needed to stabilize the slope and prevent future failures.

Chapter IV

Geological, geotechnical modeling and safety analysis

IV.1. Geological modeling:

Geological modeling involves creating a digital representation of subsurface geological features based on data from various sources like boreholes, seismic surveys, and surface mapping. The goal is to understand and predict the spatial distribution of rock types, structural features, and fluid properties within the Earth (Jarna, A et al.2015).

IV.1.1. Rock mass classification in the northwest flank of the Kef Essnoun mine:
IV.1.1.1. Evaluation of discontinuities:

At the Kef Essnoun mine, we've opted for Dips 7.0 software by Rocsience for analyzing the kinematics of slope stability. Dips is specifically tailored for interactively analyzing geological data, focusing on the orientation of various discontinuities such as joints, fissures, and faults…

-Measurements stations:

Table IV.1: Station N°=1.

Station	Kef Essnoun
UTM Coordinates	X=404614
	Y=3840846
	Z=806
Lithology	Limestone
Age	Maastrichtian
Weathering(I-VI)	III
Bedding	massive
Strength(R0-06)	R 05

Table IV.2: Station N°=2.

Station	Kef Essnoun
UTM Coordinates	X=404908
	Y=3844093
	Z=767
Lithology	Phosphate
Age	Thanetian
Weathering(I-VI)	IV
Bedding	regular
Strength(R0-06)	R 02

Table IV.3: Station N°=3.

Station	Kef Essnoun
UTM Coordinates	X=404995
	Y=38407
	Z=784
Lithology	Marl
Age	Danian
Weathering (I-VI)	I
Bedding	massive
Strength (R0-06)	R0

-Morphology of deformations:

In these stations, deformation is very complicated, two surface of discontinuity observable:

-Discontinuity surface of sedimentary origin mineralized by stratification joints.

-Discontinuity surface of tectonic origin: joints, faults.

-Treatment of data (projection stereography):

   1/ In the first step, we establish a file containing structural data in the form of dip/dip direction table:

Table IV.4: Station N°=1.

Bedding		Joints	
Dip	**Dip direction**	**Dip**	**Dip direction**
40	70	75	90
50	70	80	110
65	75	50	90
65	75	65	160
50	65	80	170
80	60	80	165
55	70	35	170
50	70	80	135
40	80	80	130
40	80	70	135

Table IV.5: Station N°=2.

Bedding		Joints	
Dip	**Dip direction**	**Dip**	**Dip direction**
60	60	55	180
75	70	80	140
75	75	80	170
90	75	90	120
60	75	85	150
75	45	55	170
50	70	80	170
65	65	30	110
40	70	75	165
80	90	75	150

Table IV. 6: Station N°=3.

Bedding		Joints	
Dip	**Dip direction**	**Dip**	**Dip direction**
60	160	30	108
56	162	40	110
65	165	35	70
60	158	50	80
65	160	56	82
		60	215
		50	216
		40	218
		45	225
		52	220

2/ The Dips software automatically generates the stereographic projections and representation of the outputs data as shown in the **Fig IV.1**
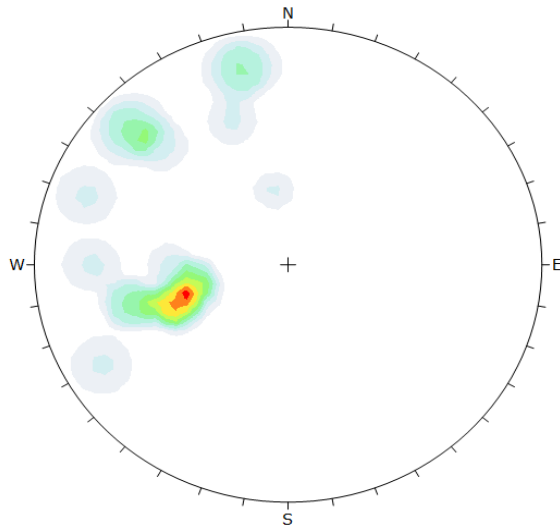
Equal Frequency Contour Diagram of Poles to Slots.
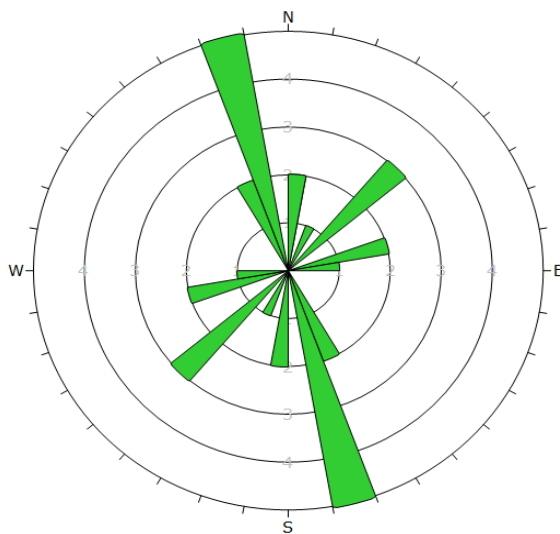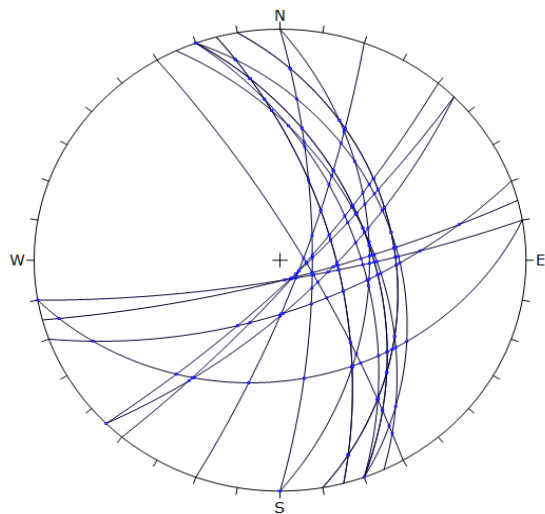
Rosette plot.

Major plans plot.

Fig IV.1: Limestone station.
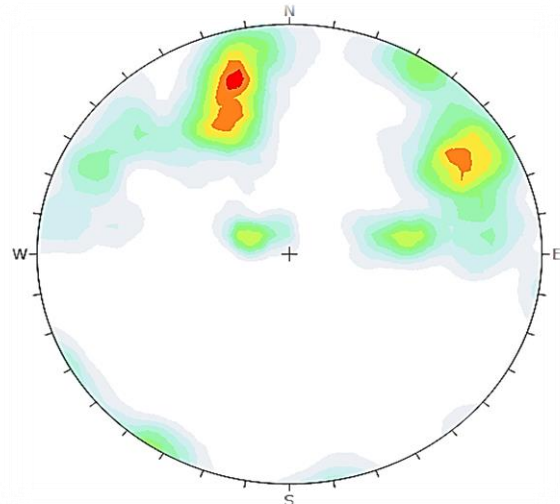
Equal Frequency Contour Diagram of Poles to Slots.
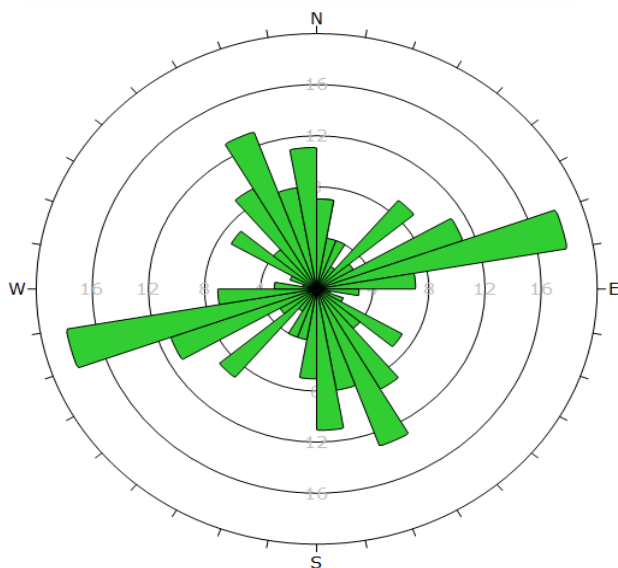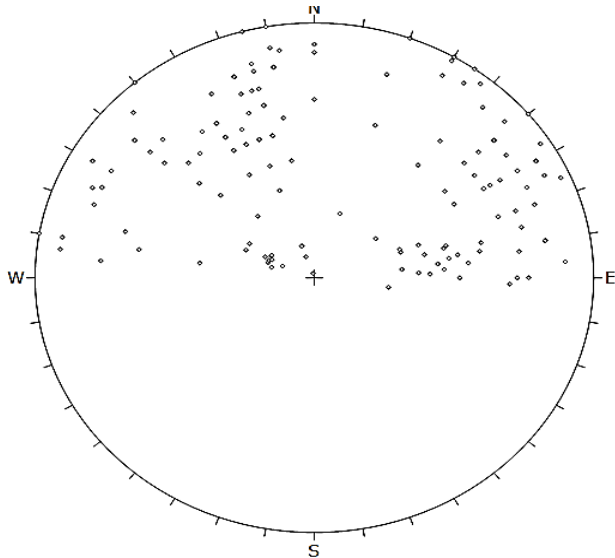
Rosette plot.

Squatter point of plotting pole.

Fig IV.2: Phosphate station .
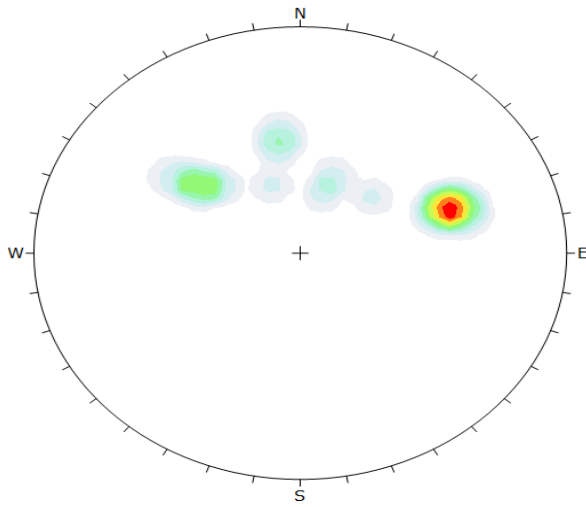
Equal Frequency Contour Diagram of
Poles to Slots.
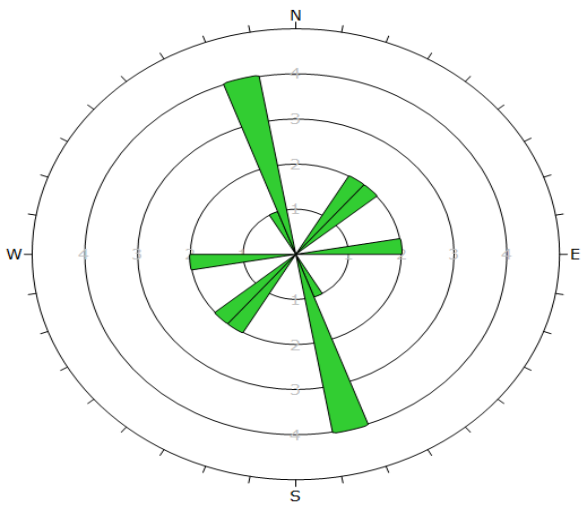
Rosette plot.
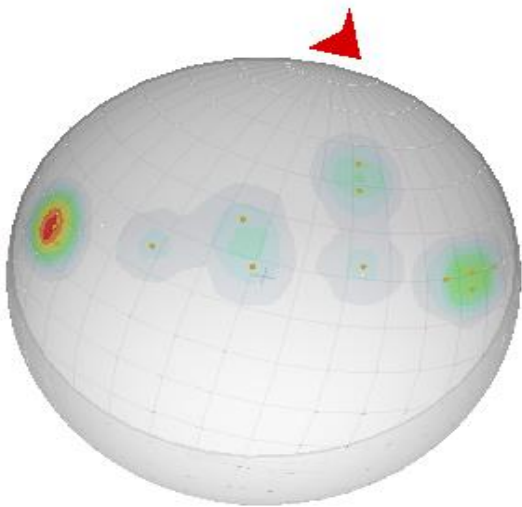
Hemispherical projection in 3D view.

Fig IV.3: Marl station.

IV.1.2. Rock mass description of the kef Essnoun mine:

Through field measurements collected, they have been compiled in a table Dis 7.0 (dip/dip direction) The following results were obtained:

In **Fig IV. 4** we have the families of discontinuities with their Respective orientations (Dip/Dip Direction) and which have been processed with the Dips software, depending on the concentration of poles there are two families of discontinuities as shown in the figure:
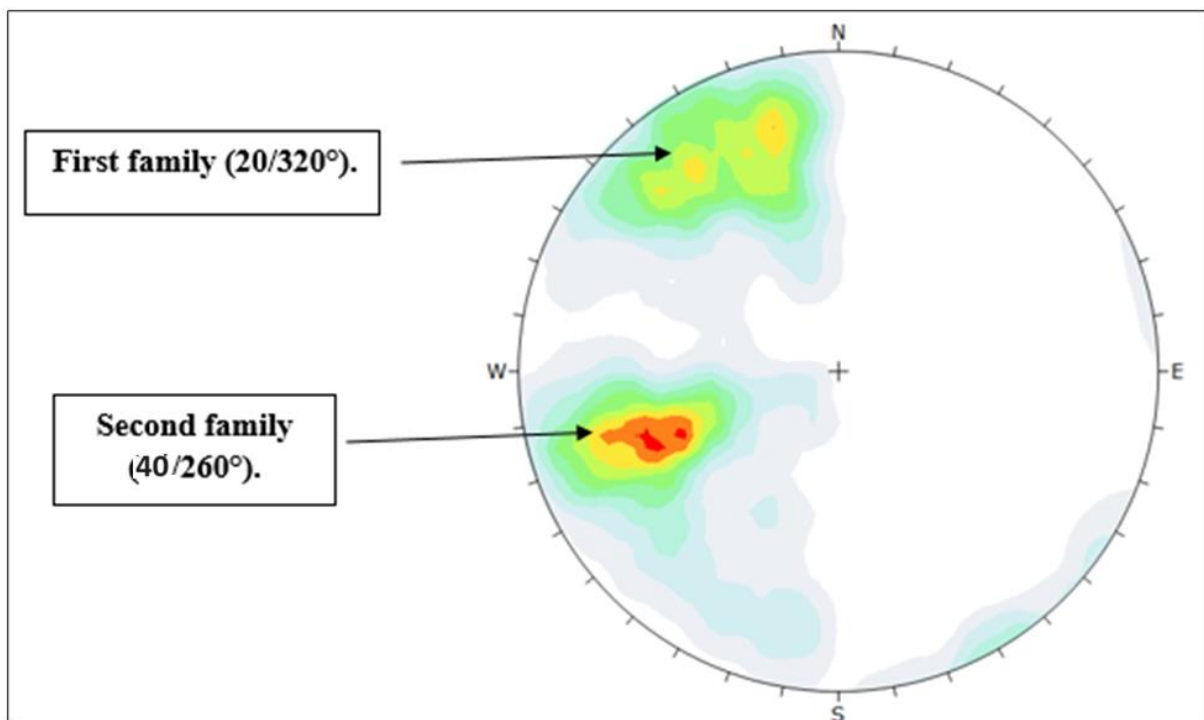
Fig IV. 4: Equal Frequency Contour Diagram of Poles to Slots.

IV.2.1. Different failure modes:

a).Planar sliding:

As shown in the figure the percentage of planar sliding is equal to 4.11% this movement cannot occur.

Color	Density Concentrations	
	0.00	-	0.70
	0.70	-	1.40
	1.40	-	2.10
	2.10	-	2.80
	2.80	-	3.50
	3.50	-	4.20
	4.20	-	4.90
	4.90	-	5.60
	5.60	-	6.30
	6.30	-	7.00

Contour Data	Pole Vectors
Maximum Density	6.49%
Contour Distribution	Fisher
Counting Circle Size	1.0%

Kinematic Analysis	Planar Sliding
Slope Dip	63
Slope Dip Direction	106
Friction Angle	30°
Lateral Limits	20°

	Critical	Total	%
Planar Sliding (All)	29	705	4.11%
Planar Sliding (Set 1: 1)	2	215	0.93%
Planar Sliding (Set 2: 2)	10	216	4.63%

Plot Mode	Pole Vectors
Vector Count	705 (705 Entries)
Hemisphere	Lower
Projection	Equal Angle

Fig IV.5: Kinematic analysis represent planar slide.

- **Results interpretations:**

Critical Intersections: The red-highlighted and shaded region on the stereonet indicates where the orientations of geological features meet the criteria for planar sliding failure under the given slope and friction conditions.

Density Concentrations: Areas with high-density pole vectors suggest significant concentrations of planar features that could contribute to potential failure zones.

Failure Probability: The data shows that 4.11% of the features analyzed meet the criteria for potential planar sliding failure, with specific subsets (0.93% and 4.63%) indicating the contribution from different sets of planes.

This stereonet analysis highlights the potential for planar sliding failure within the slope. The critical areas identified suggest that the slope stability could be compromised if these planar features align unfavorably. The relatively lower percentage of potential planar sliding failures compared to previous analyses indicates a moderate risk that must be addressed through proper slope stabilization measures and monitoring.

b). Planar slide (no limits):

As show in the table the percentage of planar sliding (no limits) is equal to 20.14% From these results, we expect the possibility the occurrence of this failure type.

Color	Density Concentrations	
	0.00	-	0.70
	0.70	-	1.40
	1.40	-	2.10
	2.10	-	2.80
	2.80	-	3.50
	3.50	-	4.20
	4.20	-	4.90
	4.90	-	5.60
	5.60	-	6.30
	6.30	-	7.00

Contour Data	Pole Vectors
Maximum Density	6.49%
Contour Distribution	Fisher
Counting Circle Size	1.0%

Kinematic Analysis	Planar Sliding
Slope Dip	63
Slope Dip Direction	106
Friction Angle	30°

	Critical	Total	%
Planar Sliding (All)	142	705	20.14%
Planar Sliding (Set 1: 1)	14	215	6.51%
Planar Sliding (Set 2: 2)	78	216	36.11%

Plot Mode	Pole Vectors
Vector Count	705 (705 Entries)
Hemisphere	Lower
Projection	Equal Angle

Fig IV.6: Kinematic analysis represent planar slide (no limits).

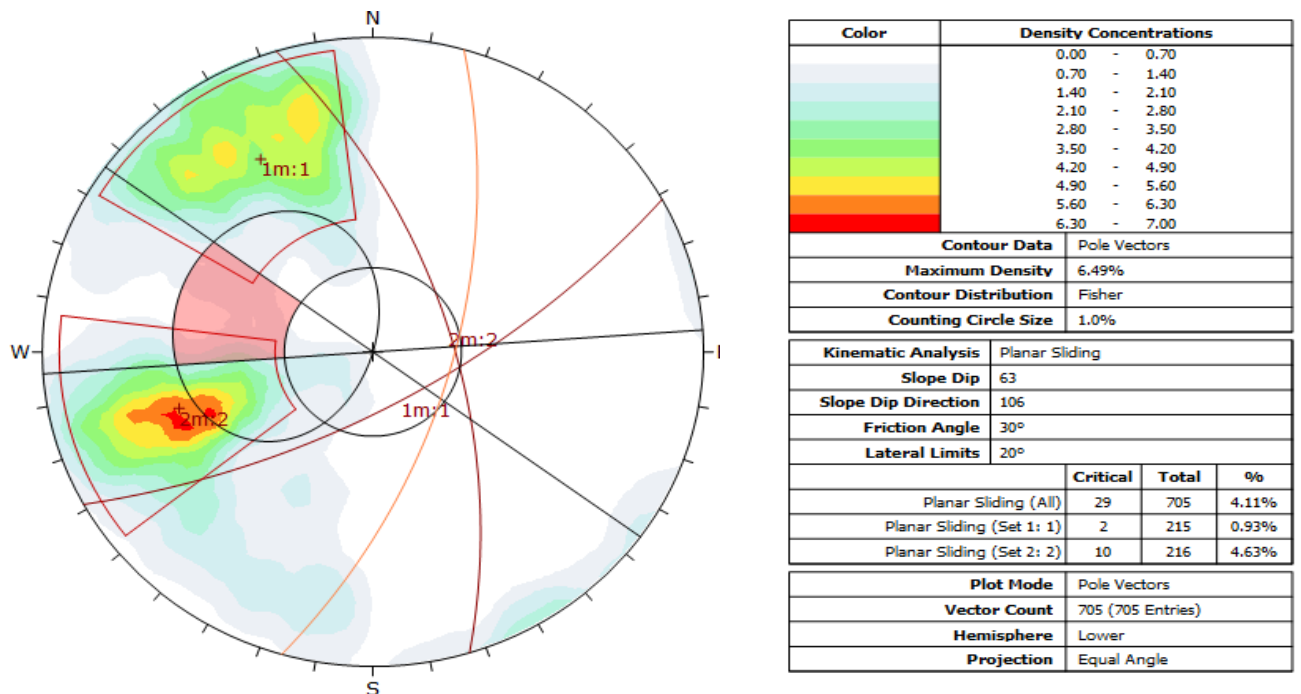- **Results interpretations:**

Critical Intersections: The red-highlighted and shaded region on the stereonet indicates where the orientations of geological features meet the criteria for planar sliding failure under the given slope and friction conditions.

Density Concentrations: Areas with high-density pole vectors suggest significant concentrations of planar features that could contribute to potential failure zones.

Failure Probability: The data shows that 20.14% of the features analyzed meet the criteria for potential planar sliding failure, with specific subsets (6.51% and 36.11%) indicating the contribution from different sets of planes.

This stereonet analysis highlights the potential for planar sliding failure within the slope. The critical areas identified suggest that the slope stability could be compromised if these planar features align unfavorably. The relatively high percentage of potential planar sliding failures indicates a significant risk that must be addressed through proper slope stabilization measures and monitoring.

c). Wedge sliding:

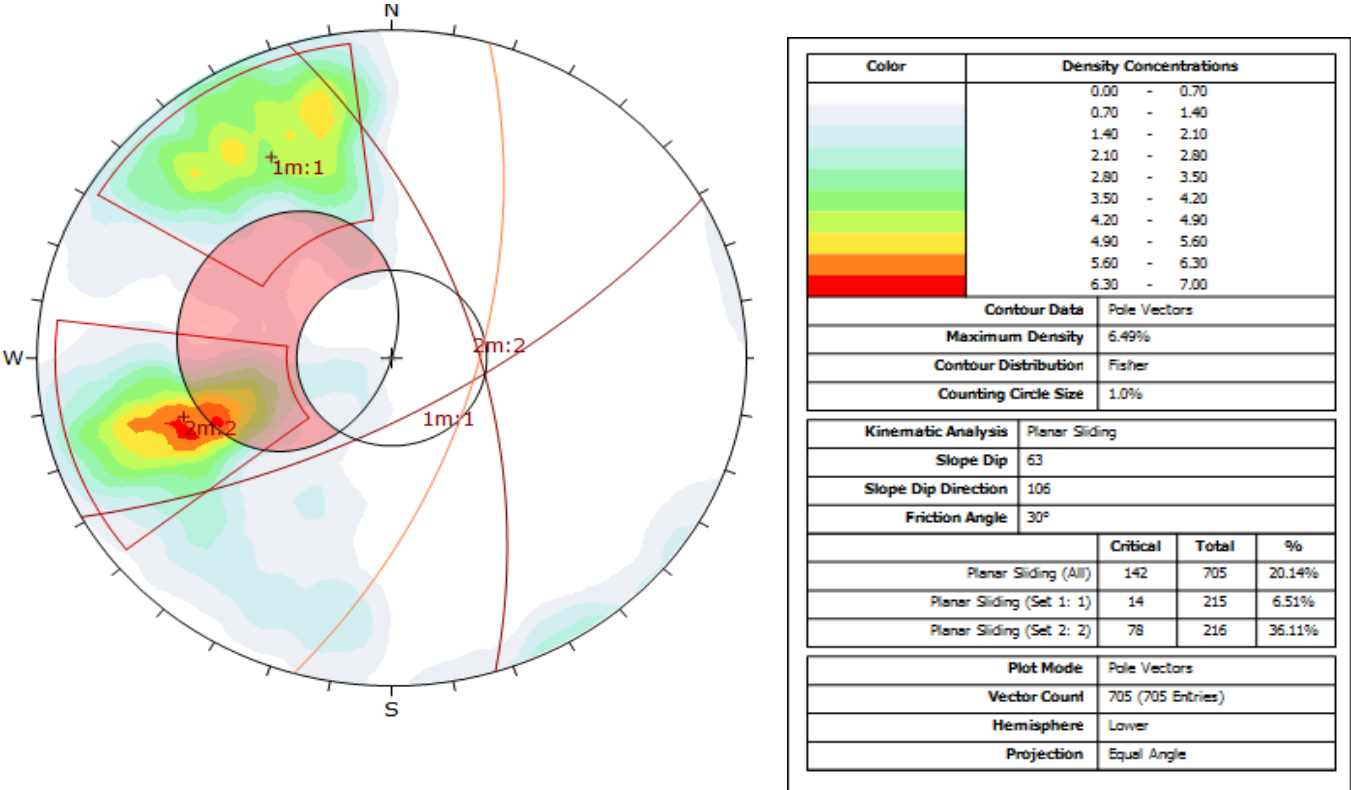As show in the table the percentage of wedge sliding is equal to 34.18%.

Fig IV.7: Kinematic analysis represent wedge sliding.

- **Results interpretations:**

Critical Intersections: The red-highlighted and shaded zone on the stereonet indicates areas where the orientation of geological features makes the slope susceptible to wedge sliding failure under the given slope and friction conditions.

Density Concentrations: Areas of high-density pole vectors suggest a concentration of planar features that could contribute to potential failure zones.

Failure Probability: 34.18% of the analyzed data meets the criteria for potential wedge sliding failure, which is a significant proportion indicating a high risk.

This stereonet analysis provides a detailed understanding of the potential for wedge sliding failure in the slope, given the specified geological and geometrical parameters. The highlighted critical areas suggest where attention should be focused to mitigate the risk of slope instability. The high percentage of potential wedge sliding failure indicates that this mode of failure is a significant concern and should be addressed in slope stability assessments and mitigation plans

d).Flexural toppling:

As show in the table the percentage of Flexural Toppling is equal to 1.28% this movement cannot occur.
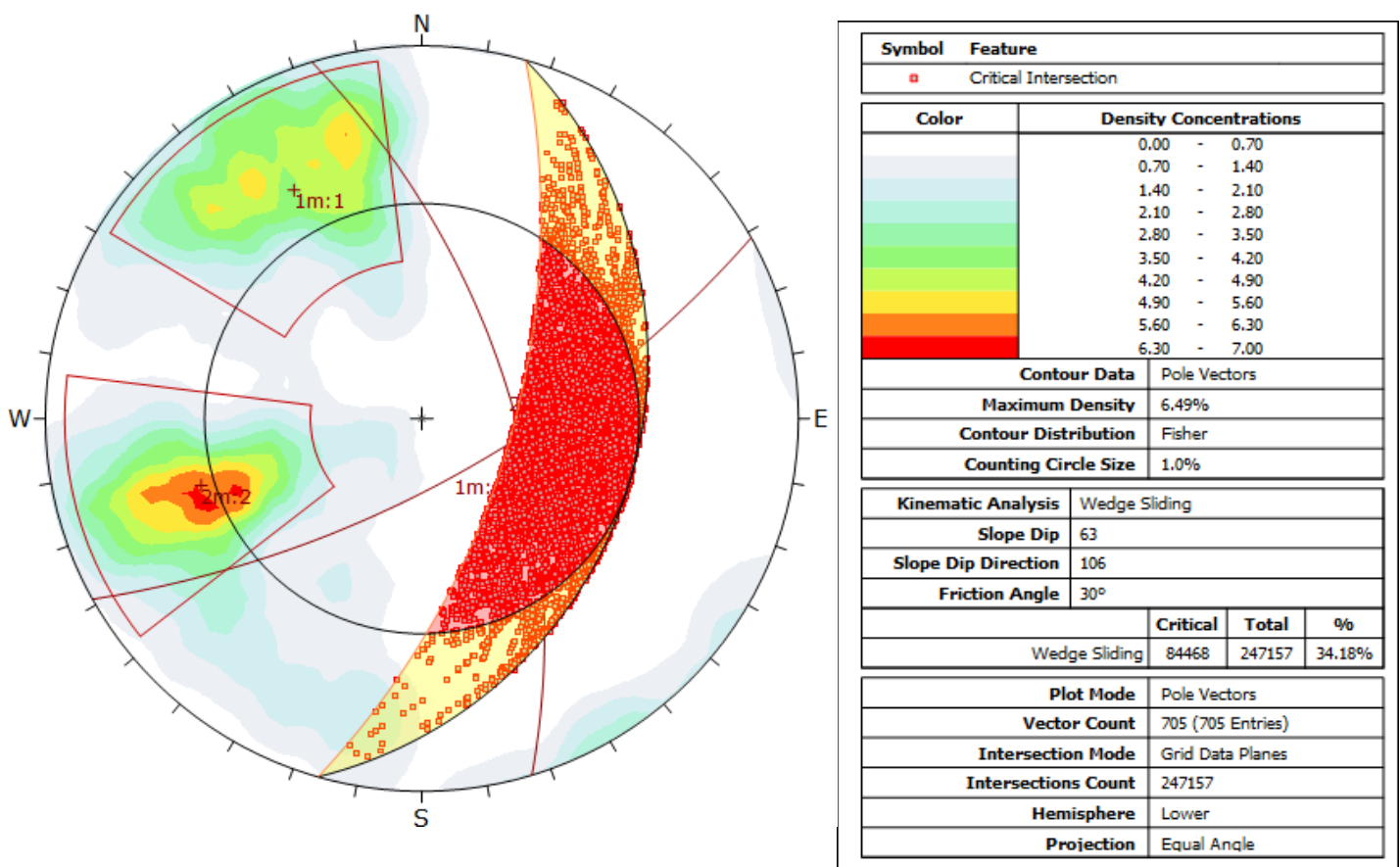

Fig IV.8: Kinematic analysis represent flexural toppling.

- **Results interpretations:**

Critical Intersections: The red-highlighted and shaded zone on the stereonet indicates areas where the orientation of geological features makes the slope susceptible to flexural toppling failure under the given slope and friction conditions.
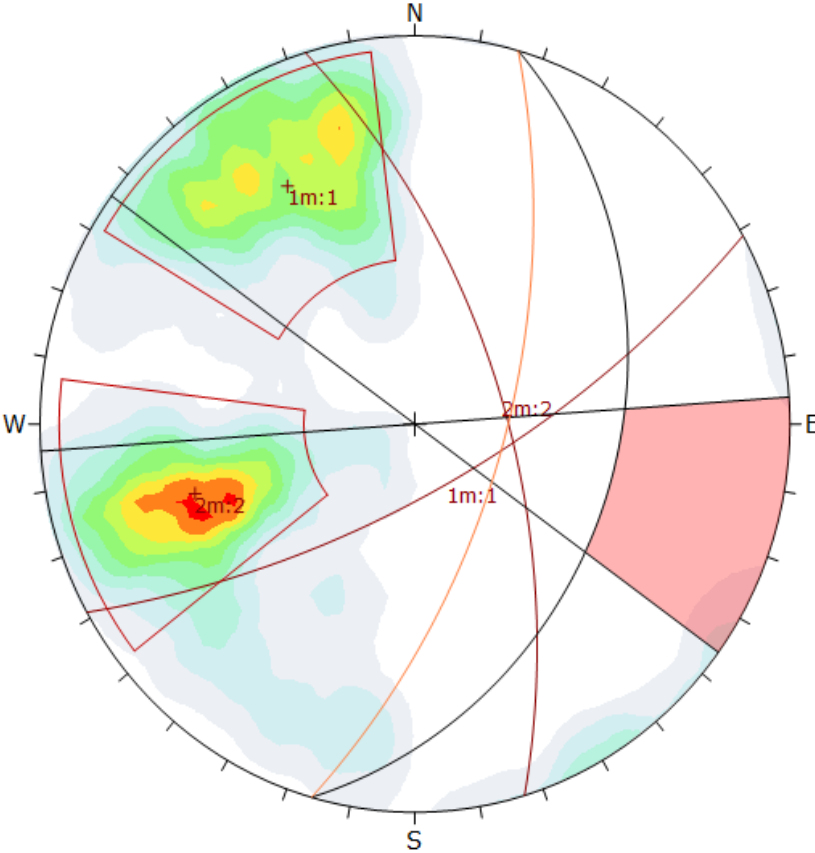
Density Concentrations: Areas of high-density pole vectors suggest a concentration of planar features that could contribute to potential failure zones.

Failure Probability: 1.28% of the analyzed data meets the criteria for potential flexural toppling failure, which is a relatively low proportion indicating a lower risk compared to other failure modes.

This stereonet analysis provides a detailed understanding of the potential for flexural toppling failure in the slope, given the specified geological and geometrical parameters. The highlighted critical areas suggest where attention should be focused to mitigate the risk of slope instability. The low percentage of potential flexural toppling failure indicates that this mode of failure is not a significant concern but should still be considered in comprehensive slope stability assessments and mitigation plans.

e).Direct toppling:

As show in the table the percentage of Flexural Toppling is equal to 10.64%.

Symbol	Feature
▫	Critical Intersection

Color	Density Concentrations	
	0.00	-	0.70
	0.70	-	1.40
	1.40	-	2.10
	2.10	-	2.80
	2.80	-	3.50
	3.50	-	4.20
	4.20	-	4.90
	4.90	-	5.60
	5.60	-	6.30
	6.30	-	7.00

Contour Data	Pole Vectors
Maximum Density	6.49%
Contour Distribution	Fisher
Counting Circle Size	1.0%

Kinematic Analysis	Direct Toppling
Slope Dip	63
Slope Dip Direction	106
Friction Angle	30°
Lateral Limits	20°

	Critical	Total	%
Direct Toppling (Intersection)	387	247157	0.16%
Oblique Toppling (Intersection)	6306	247157	2.55%
Base Plane (All)	75	705	10.64%
Base Plane (Set 1: 1)	2	215	0.93%
Base Plane (Set 2: 2)	10	216	4.63%

Plot Mode	Pole Vectors
Vector Count	705 (705 Entries)
Intersection Mode	Grid Data Planes
Intersections Count	247157
Hemisphere	Lower
Projection	Equal Angle

Fig IV.9: Kinematic analysis represent direct toppling.

- **Results interpretations:**

Critical Intersections: The red-highlighted zones on the stereonet indicate areas where the orientation of geological features makes the slope susceptible to direct toppling failure under the given slope and friction conditions.

Density Concentrations: The high-density areas of pole vectors suggest a concentration of planar features that could contribute to potential failure zones.

Failure Probability: The percentage values indicate the proportion of the analyzed data that meets the criteria for potential failure. For direct toppling, 0.16% of the analyzed intersections are critical, while 2.55% are critical for oblique toppling.

This stereonet analysis provides a detailed understanding of the potential for flexural toppling failure in the slope, given the specified geological and geometrical parameters. The highlighted critical areas suggest where the risk of slope instability is higher, which can be crucial for designing mitigation measures.

IV.3. Kef Essnoun area mapping:

ArcGIS is a versatile tool that allows for detailed analysis and interpretation of various types of geographical and geological data. Following the next underlines steps the used software allows to elaborate the different maps (Geological Slope, Hill shade, and Watershed, … etc.

IV.3.1. Data collection, preparation and treatment:

The data collect is from USGS (the United States Geological Survey), for the treatment of data It is limited to transforming coordinates from Lambert to UTM coordinates system .and Nord_Sahara_1959_UTM_Zone_32N for projection coordinates.
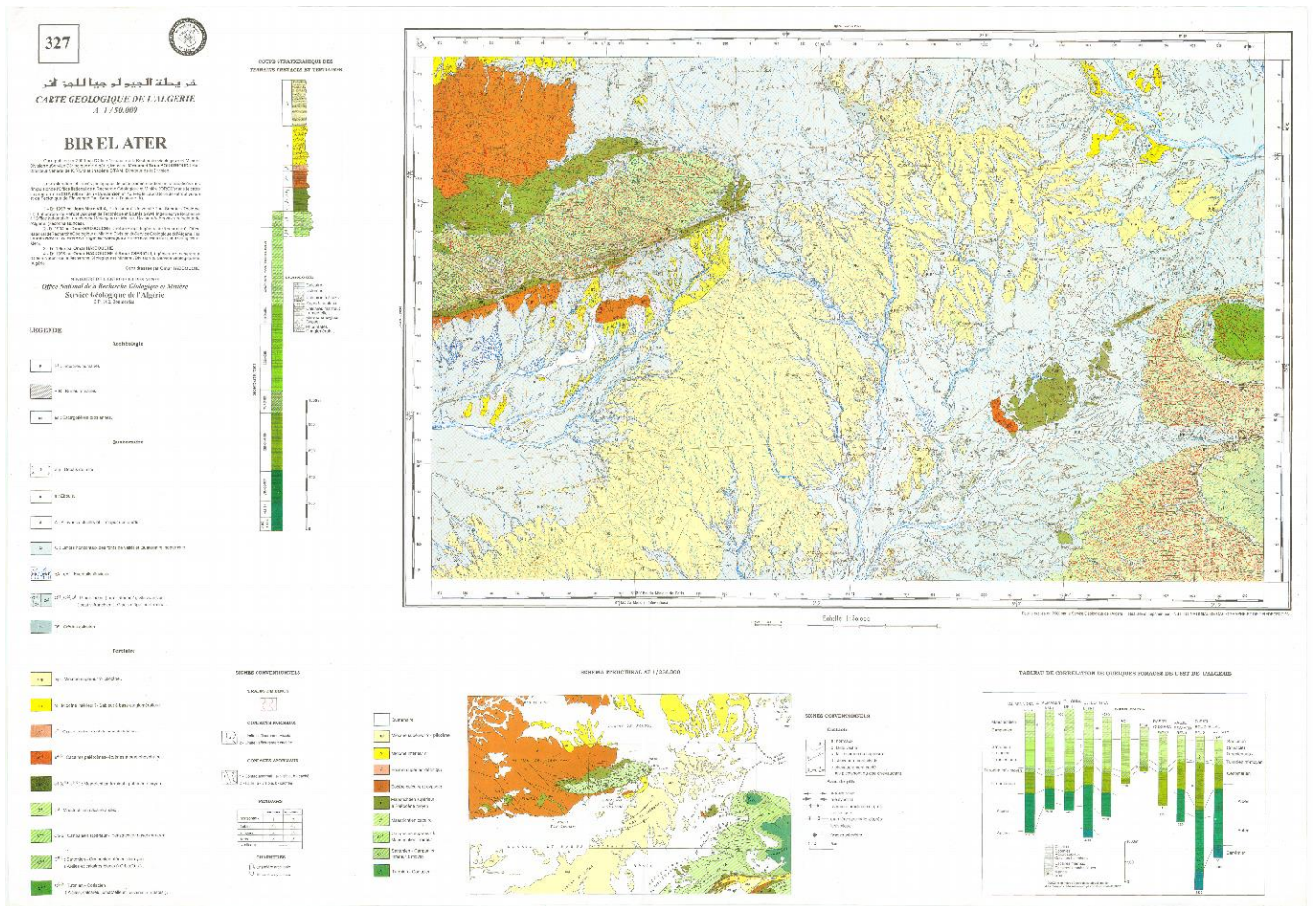
Fig IV.10: Geological map of BIR ELATER city.

Table IV.7 : X Y coordinates .

Points	X	Y
1	401838	3849956
2	434276	3847774
3	400578	3829664
4	432942	3827646
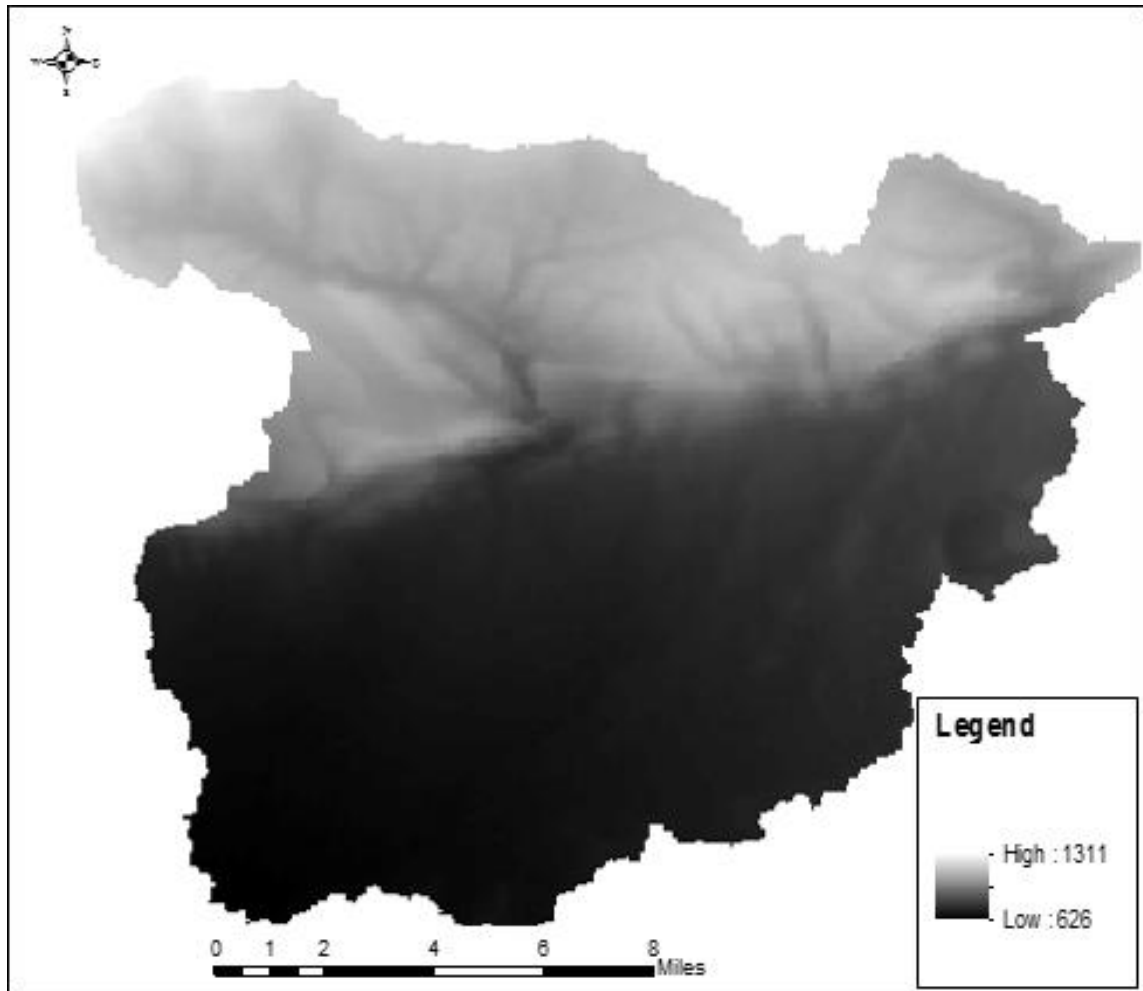
Fig IV.11: DEM of Kef Essnoun area.

IV.3.1. Creation of geological maps:

1.Contour map:

A contour map is a type of topographic map that uses contour lines to represent the three-dimensional shape of the terrain on a two-dimensional surface. To create a contour map in ArcGIS, A contour map extracted from the DEM data downloaded from USGS (**Fig IV.11**) Contour maps provide valuable information about the topography of an area, including the elevation and slope of the land (**Fig IV.12).** The way contour lines are arranged on a map can influence the drainage network in several ways:

1. Identification of Drainage Patterns: Contour maps help identify various drainage patterns such as dendritic (tree-like), radial, parallel, and rectangular. **Drainage patterns** are largely dictated by the underlying topography, including slope and elevation changes, which are depicted on contour maps.

2. Determining Watershed Boundaries: Contour lines that form closed loops on a map **delineate watersheds or drainage basins.** Watershed boundaries are crucial for understanding how

water flows across the landscape. High points in the landscape, indicated by concentric contour lines, mark the divide between watersheds, determining where water will flow and how it will be distributed.

3. Gradient and Flow Direction : Contour lines closer together indicate steeper slopes, while contour lines spaced farther apart represent gentler slopes. Water tends to flow perpendicular to contour lines, from higher elevations to lower elevations. By examining contour maps, you can infer the direction of water flow and identify potential drainage paths.

4. Accumulation Areas : Low-lying areas surrounded by higher elevations, often depicted by closely spaced contour lines forming concentric circles, indicate potential locations for water accumulation, such as ponds, lakes, or wetlands. These areas can act as natural points of water storage and contribute to the overall drainage network by collecting runoff from surrounding areas.

5. Channel Formation : Contour maps help identify potential locations for stream channels based on the convergence of contour lines and the presence of valleys or depressions in the landscape. Streams and rivers typically follow paths of least resistance, flowing along valleys and low-lying areas depicted by contour maps.

In summary, contour maps provide essential information about the topography of an area, which directly influences the formation and characteristics of the drainage network. Understanding the relationship between contour lines and drainage patterns is crucial for various applications, including land development, flood management, and environmental conservation.
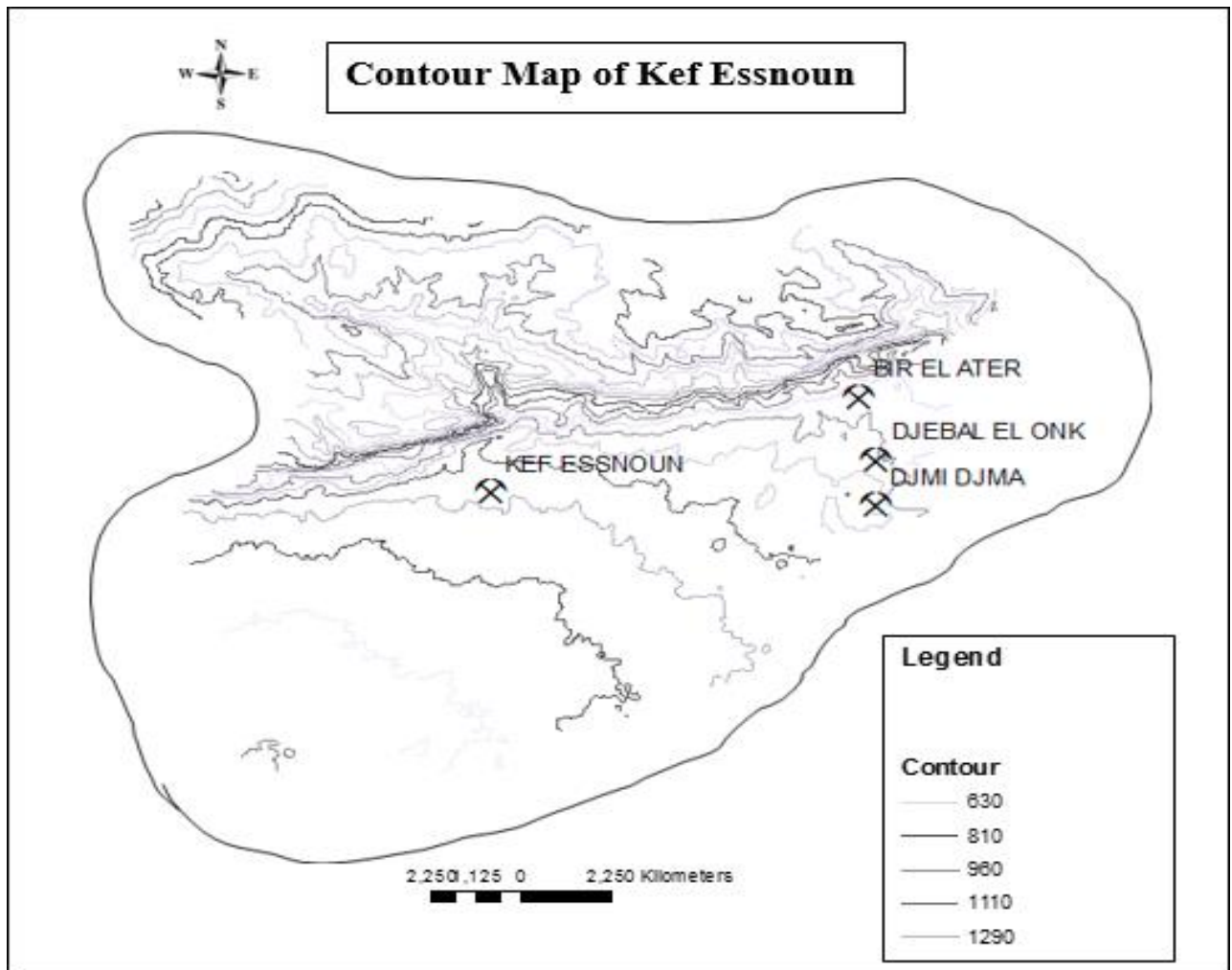
Fig IV.12: Contour map of Kef Essnoun.

2. Local geological map drawing:

The geological map of Kef Essnoun provides detailed information on the different geological formations and lithologies present in the region (**Fig IV.13).**

Interpreting a geological map involves understanding the distribution, nature, and relationships of different rock types, geological structures, and other features present in a particular area. Here are some key steps and considerations for interpreting a geological map:

The legend of the geological map provides information about the different rock units, geological structures (such as faults and folds), and other features.

The geological maps often display the relative positions of rock strata. the arrangement of rock units in sub-vertical succession, which provides information about the geological history of the area, including deposition, erosion, and deformation events. Thus, the structural features

depicted on the map, such as faults, folds, joints, and cleavage planes. Note the orientation, displacement, and relationships between different structural elements, which can provide insights into the tectonic history and deformation processes that have affected the area. The geological maps can help assess the susceptibility of different locations to natural hazards and inform land-use planning and risk management strategies.
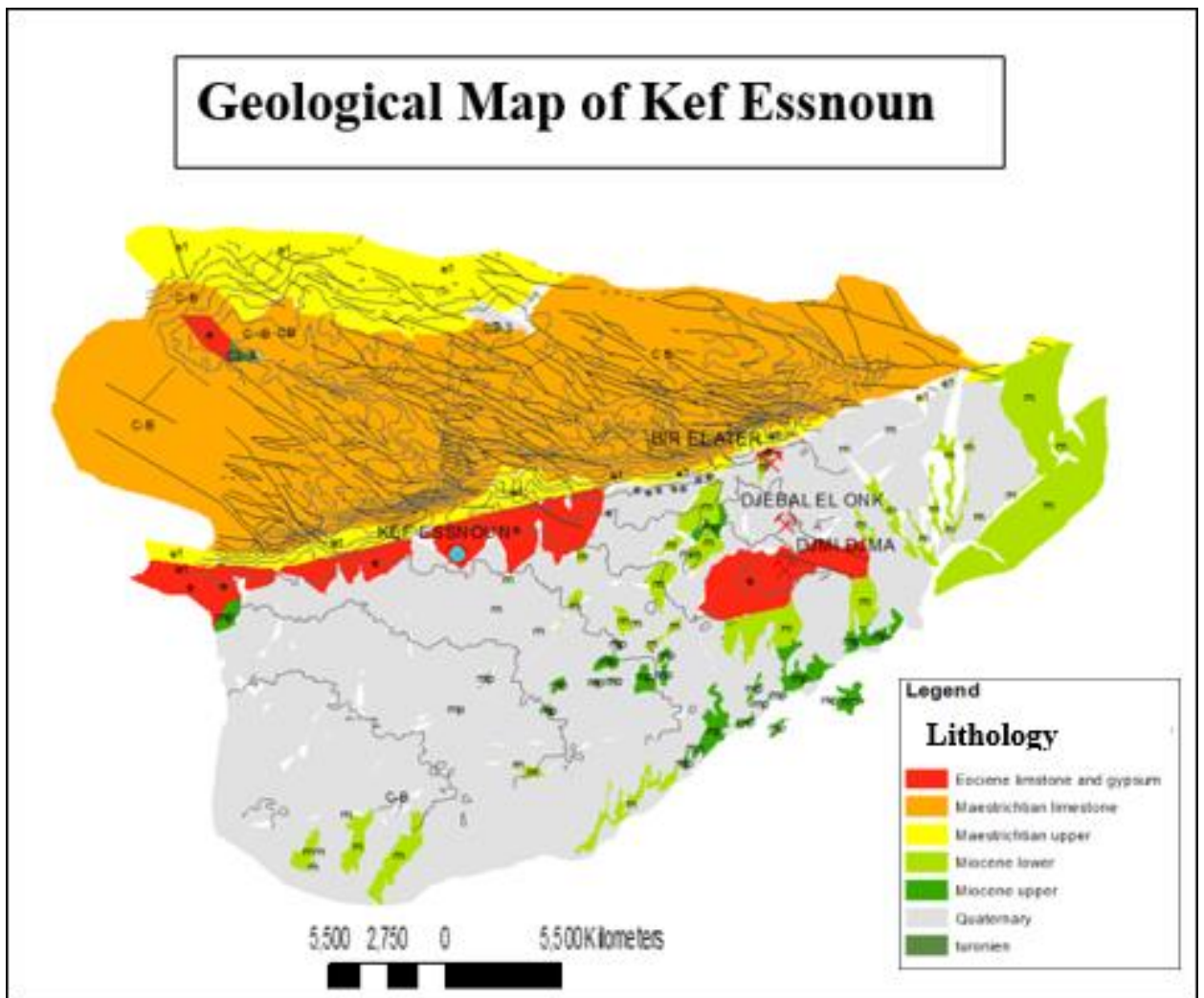
Fig IV.13: Local geological map of Kef Essnoun.

3. Slope Map of the study area:

The slope map displays the steepness or incline of the terrain, derived from a digital elevation model (DEM). It uses color gradients to represent different slope angles, this slope map can be used for land planning, identify suitable areas for construction, agriculture, and other developments. it is also useful for hazard assessment, pinpointing areas at higher risk of landslides and erosion, thereby informing mitigation strategies.
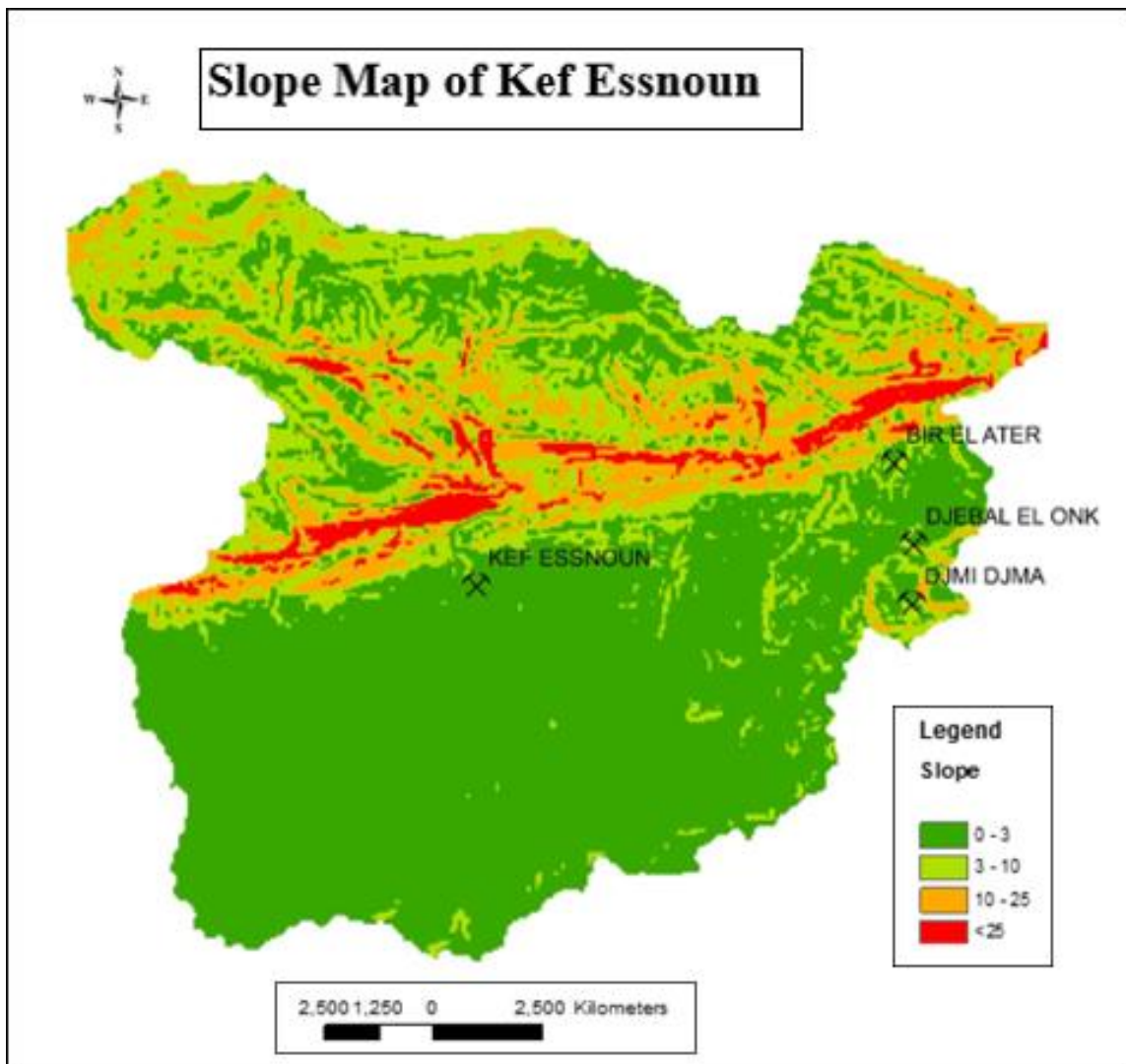
Fig IV.14: Slope Map of Kef Essnoun.

-Color Gradient Interpretation:

- **Green (0-3%)**: These areas represent gentle slopes, indicating relatively flat terrain. They are generally more stable and suitable for construction and agriculture.
- **Yellow to Orange (3-25%)**: These colors indicate moderate slopes. Areas with these slope percentages are prone to some erosion and may require careful management for construction and land use.
- **Red (<25%)**: The red areas indicate steep slopes. These regions are highly prone to erosion, landslides, and instability. They are less suitable for construction without significant stabilization measures.

4.Hill shade Map:

The Hill Shade map uses simulated light and shadows to provide a three-dimensional appearance to the terrain, enhancing the visualization of topographic features.
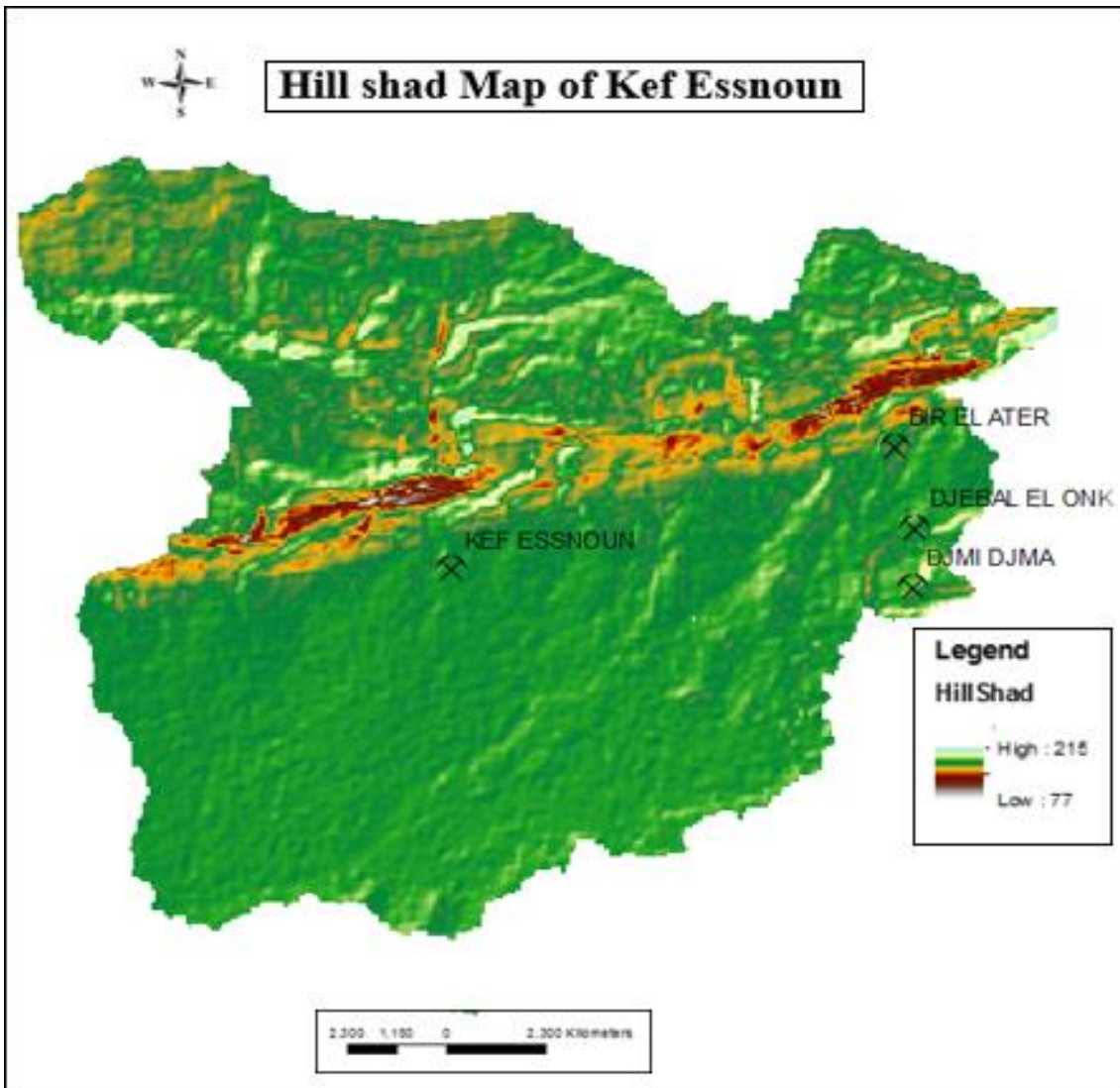
Fig IV.15: Hill shad of Kef Essnoun.

-Interpreting Slope and Hill Shade maps:

Involves understanding the terrain characteristics and landforms represented by these cartographic products. Here's a breakdown of how to interpret each type of map.

Color or Shading: Slope maps often use color gradients or shading to represent different slope categories, with darker shades indicating steeper slopes and lighter shades representing gentler slopes. Interpretation involves identifying areas with varying degrees of slope, which can influence land use, terrain stability, and drainage patterns. Steep slopes may indicate areas prone to erosion, landslides, or limited accessibility for development.

Interpreting both Slope and Hill Shade maps often involves integrating information from other sources, such as aerial imagery, geological maps, and field observations, to gain a comprehensive understanding of the terrain characteristics, landforms, and potential implications for various applications:

Slope and Hill Shade maps can inform land use planning decisions by identifying suitable areas for development, agriculture, forestry, or conservation based on terrain characteristics and stability.

Understanding slope and hill shade can help assess the suitability of terrain for various natural resource management activities, such as watershed management, habitat conservation, and mineral exploration.

Hillshade maps are valuable for terrain visualization and navigation purposes, aiding outdoor activities such as hiking, mountaineering, and surveying by providing a realistic representation of the landscape's relief and topographic features.

In summary, interpreting slope and hillshade maps involves analyzing terrain characteristics, landforms, and their implications for land use, natural resource management, and terrain navigation. Integrating these maps with other geospatial data can enhance understanding and decision-making in various fields.

a. 5.Hydrological map:

-The watershed map:

The watershed map of Kef Essnoun illustrates the drainage patterns and boundaries of the watershed areas.

Interpreting watersheds involves understanding the boundaries, drainage patterns, and hydrological characteristics of areas where surface water drains into a common outlet. Key aspects include:

. Watershed Delineation:
- **Boundary Identification:** Defined by ridgelines and drainage divides.
- **Hierarchy:** Watersheds can be nested, with smaller watersheds within larger ones.

. Drainage Patterns:
- **Stream Network:** Analyzing patterns such as dendritic, radial, parallel, or rectangular.
- **Stream Order:** Classification indicating the position within the stream hierarchy.

. Topographic Characteristics:

- **Elevation Variation:** High points form divides, low points are outlets.
- **Slope and Aspect:** Influences water movement and vegetation distribution.

. Hydrological Processes:

- **Water Flow:** Governs precipitation, runoff, infiltration, and groundwater recharge.
- **Water Quality:** Affected by sediment load, nutrient concentrations, and pollutants.

Summary:

Effective watershed interpretation involves integrating geospatial data, hydrological models, and field observations to support sustainable water resource management and informed decision-making.
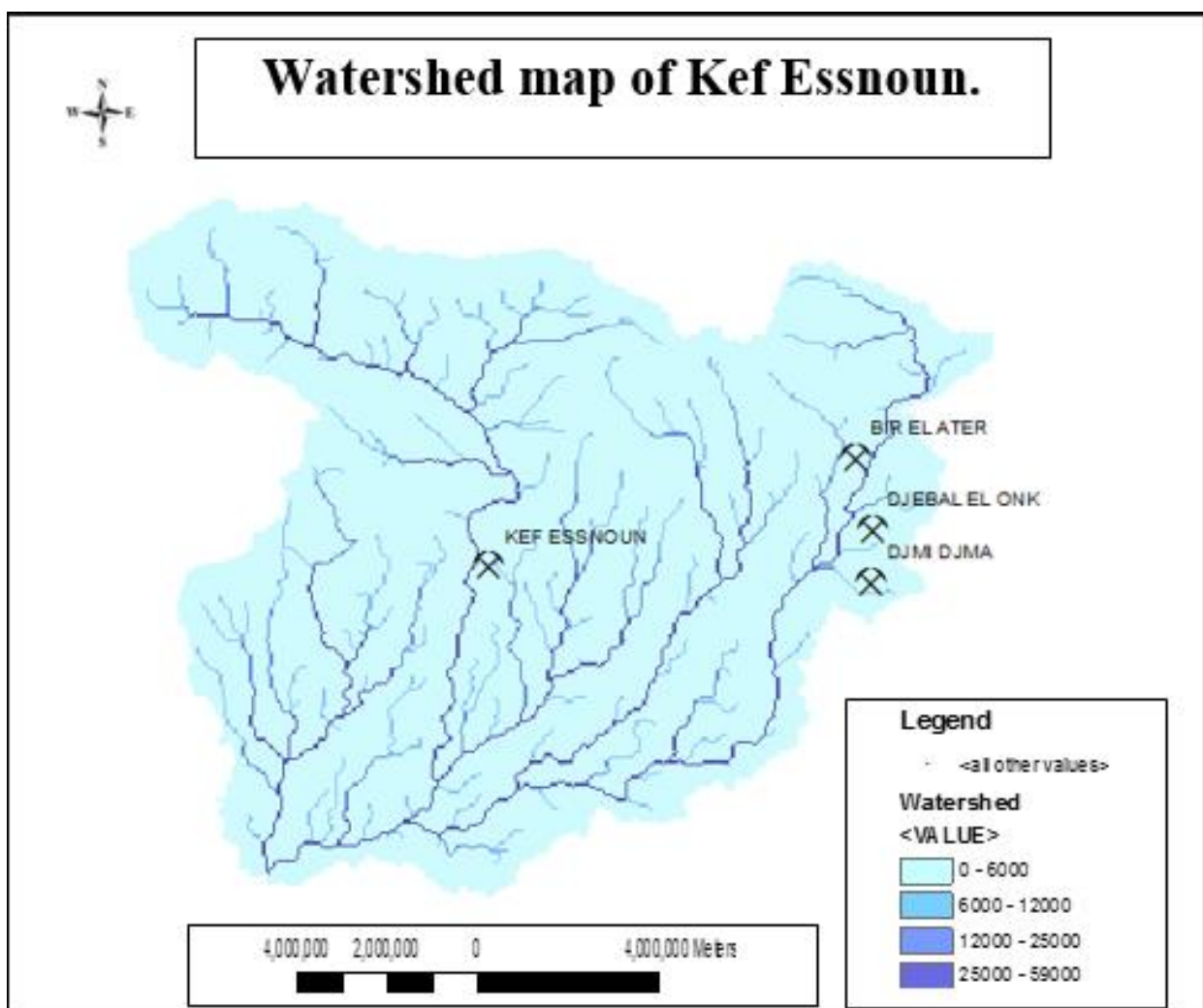

Fig IV.16: Watershed map of Kef Essnoun.

According to the watershed map it is concluded that various stream crossing the Kef Essnoun study area, this allow rainoff to percolate over permeability formation.

Interpretations:

The deep cartographic study over the geological, geomorphological, and hydrological maps, shows that the lineaments of the major fractured limestone layers are concomitant with the drainage network. the waterflow paths from higher elevations, oriented northwest to southeast and, in the lower areas where the runoff water percolate into the underground is oriented northeast to southwest.

The Major streams and tributaries in the pattern of watersheds and drainage lines suggests the influence of the topography. The hydrogeological investigation indicates the highly fractured geological units allowing infiltration of the runoff, spatially in the rainfall period. In this case it is important to indicate the significant frequency of heavy rain in the region.

IV.4. Conclusion

The local geological study for structures features and tectonics at the Kef Essnoun mine, utilizing Dips 7.0 software for the stereographical projection, uncovered critical structural features across varying lithologies like limestone, phosphate, and marl. This analysis revealed notable discontinuities, including sedimentary stratification joints and tectonic faults, indicating potential instability zones affecting slope stability.

Kinematic analysis identified different risk levels for various slope failure types. Planar sliding exhibited a moderate risk of 4.11%, increasing to 20.14% without specific limits. Wedge sliding posed the highest risk at 34.18%, necessitating immediate mitigation efforts. Flexural toppling showed minimal risk at 1.28%, while direct toppling indicated a notable risk of 10.64%, requiring targeted interventions.

ArcGIS mapping provided detailed visualizations of geological and topographical features. Geological maps delineated lithologies and structural elements, while slope maps highlighted erosion-prone areas. Hill Shade maps offered a 3D terrain perspective, and watershed maps detailed drainage patterns, essential for understanding hydrological impacts on slope stability.

The hydrological analysis identified significant interactions between geological structures and water flow, indicating potential runoff and percolation issues. Various streams and drainage patterns emphasized the importance of considering hydrological factors in slope stabilization measures.

In summary, the integration of geological, geotechnical, and hydrological data offers a comprehensive understanding of slope stability at the Kef Essnoun mine. Continuous monitoring and targeted risk mitigation measures are crucial to ensuring safety and operational sustainability

IV.5. Geological modeling and design of Kef Essnoun mine:

lithological modeling is an essential aspect of the mining industry for the evaluation of slope stability. The purpose of lithological modeling is to give illustration through 3D modeling.

IV. 5.1. Methodology:
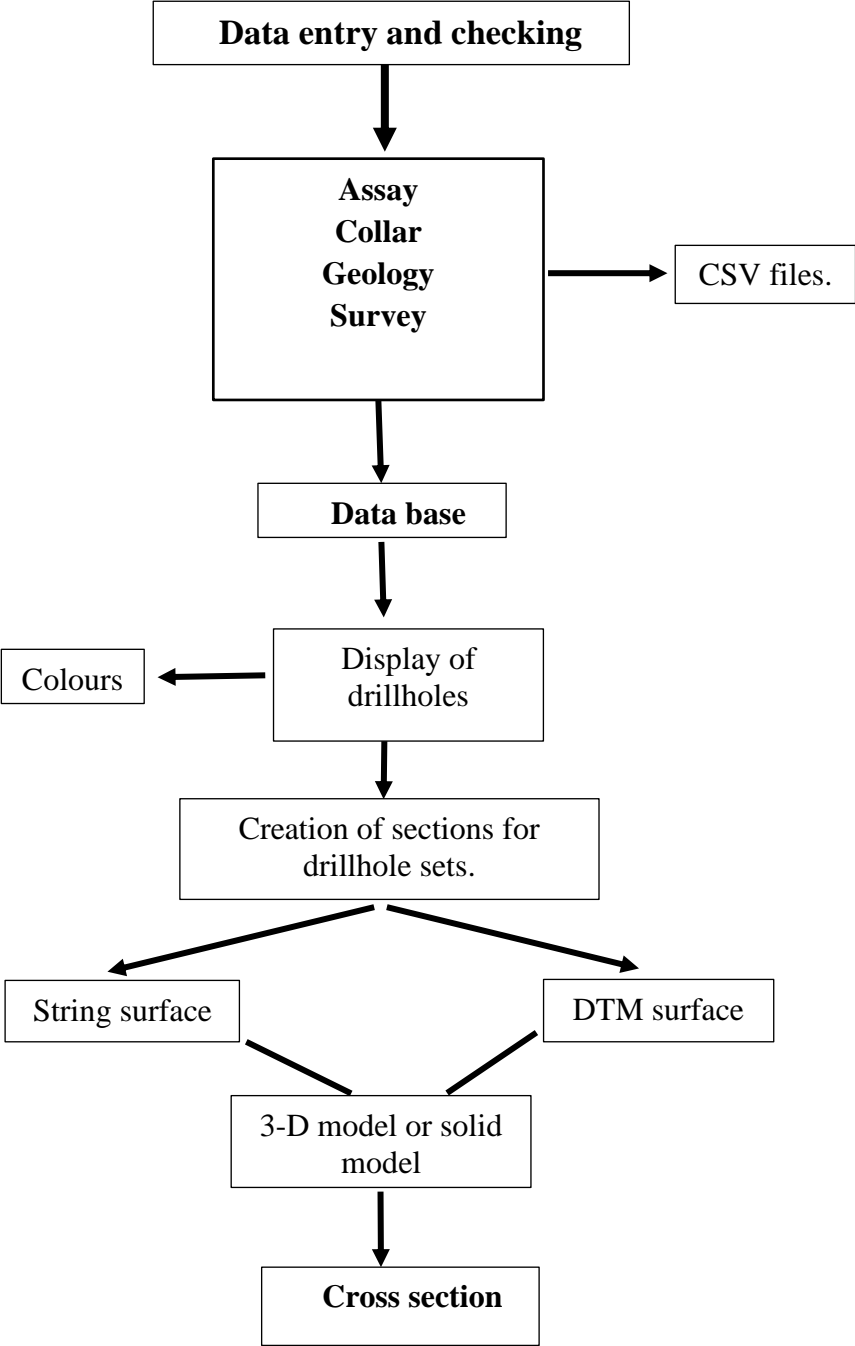
Fig IV.17: Methodology of creation in Surpac software.

IV.5.2. Data input and checking:

Input Data for this modeling phases requires different drilling information including the following CSV files: assay, collar, survey, and geology.

Table IV.8: Collection database.

Collar:	Survey:	Geology:	Assay:
-Hole_id. -X -Y -Z -Max_depth. -Hole_path.	-Hole_id. -Azimuth. -Dip. -Depth.	-Hole_id. -Depth_from. -Depth_to. -Lithology. -Description.	-Hole_id. -Simple_id. -Depth_to. - Depth_from. -P2O5. -CaO. -MgO.

N.B: To read boreholes information in surpac software, we use the software **"Microsoft access database".**

IV.5.3. Display of boreholes:
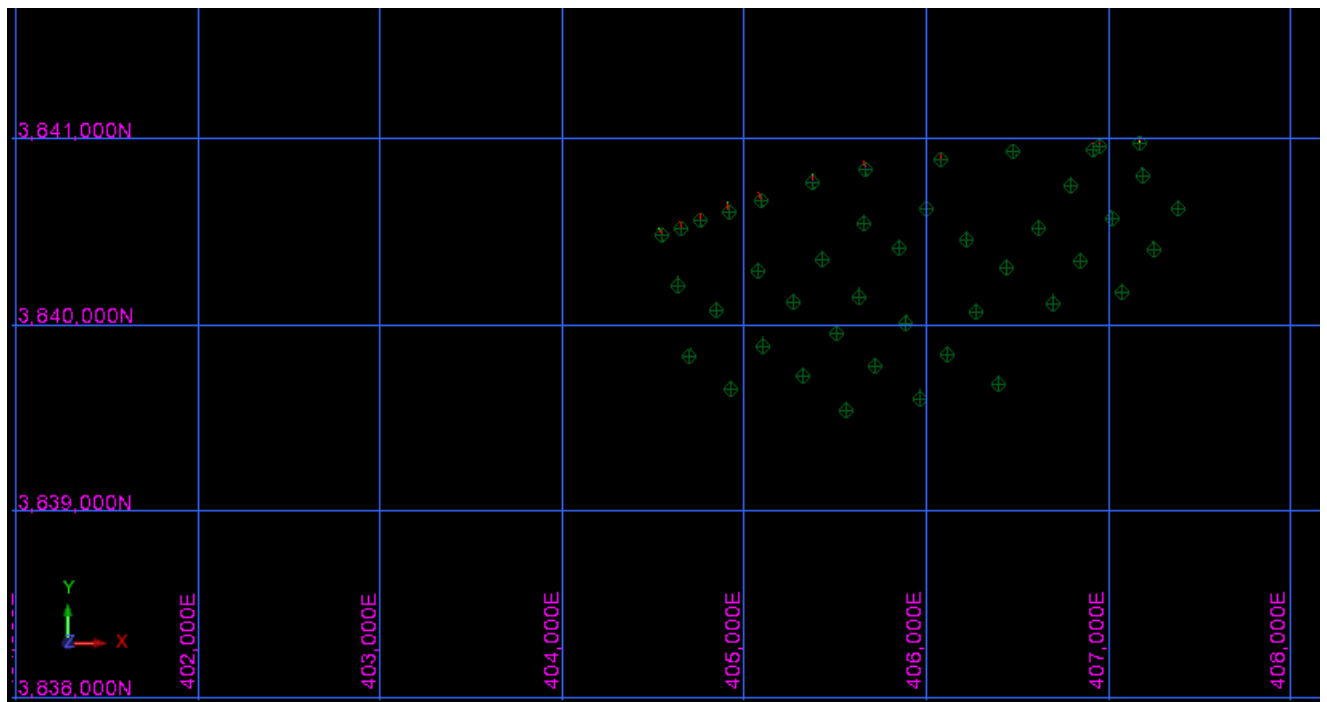
Fig IV.18: Boreholes are displayed in view of the "X" and "Y" axes.
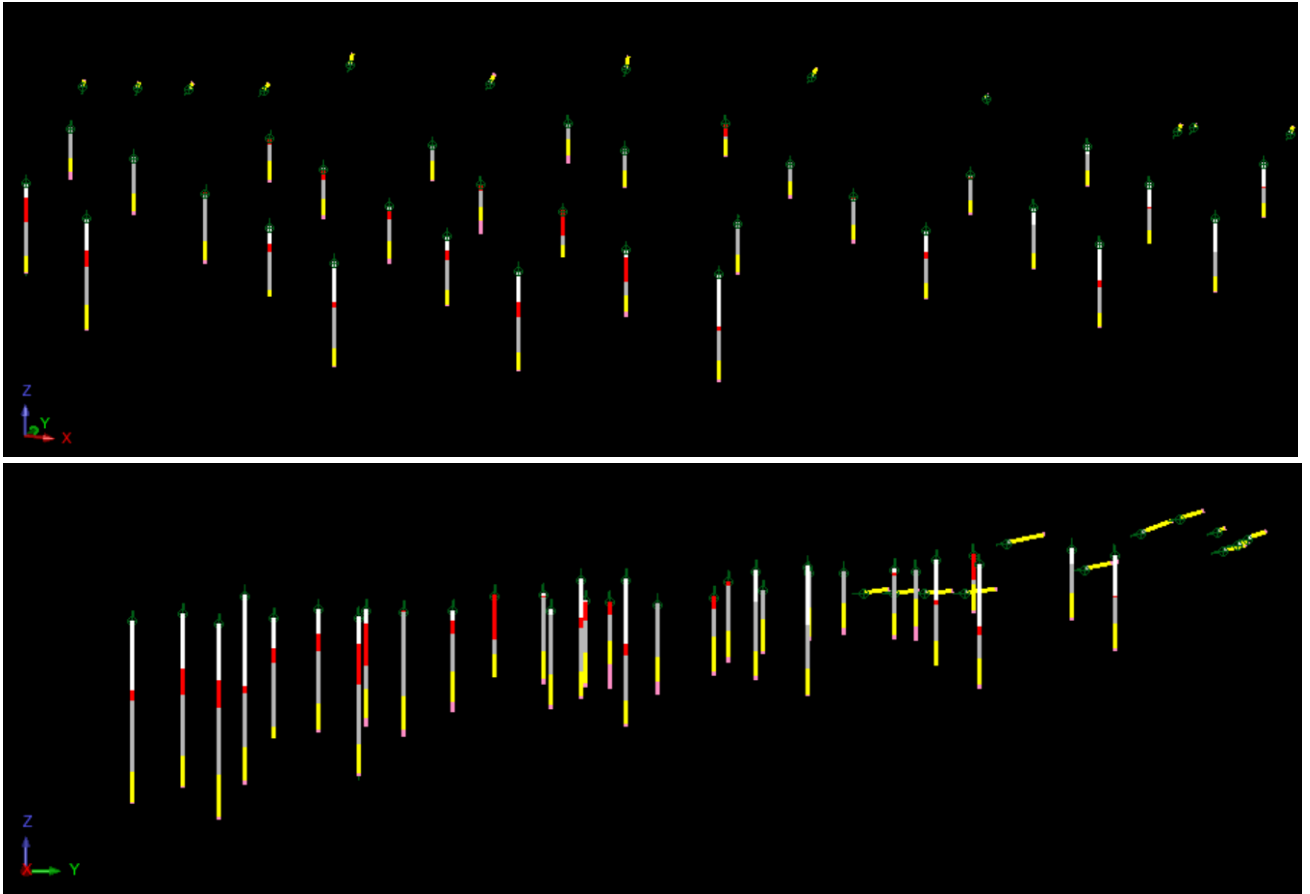
Fig IV.19: The boreholes are displayed in 3D view on the axes: "X", "Y" and "Z".
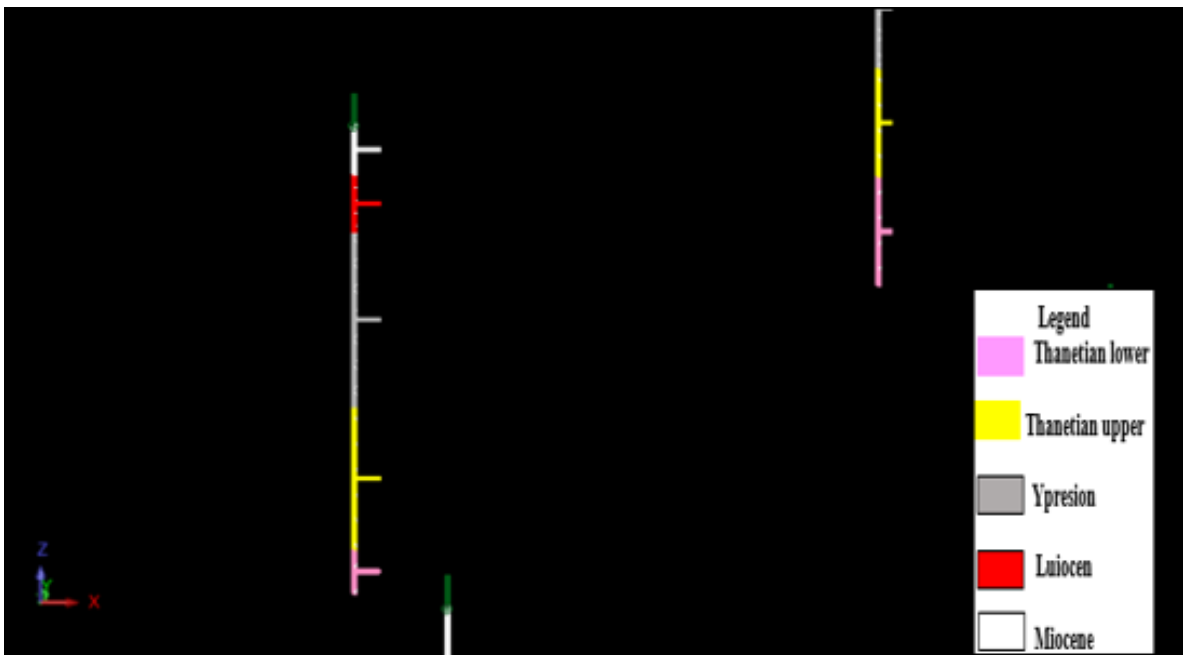
Fig IV.20: The different layers of according to the display of the boreholes.

IV.5.4. Creating the strings:

At this step correlated lines between all the borholes plan points have been drawn .
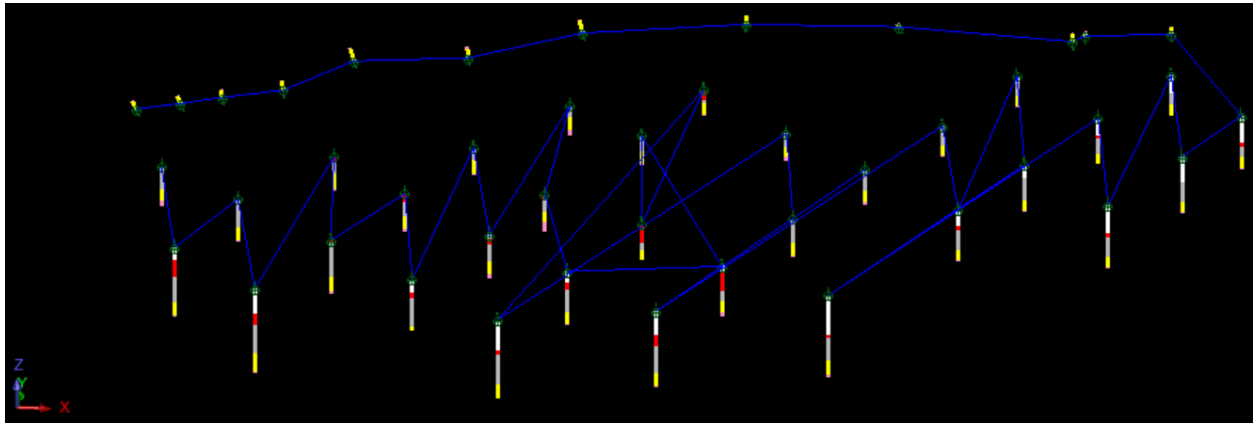
Fig IV.21: Sections for borehole sets in 2D,3D.

IV.5.5. Geological and Topographic Modeling:

Geological and topographic modeling is a fundamental aspect of understanding and representing the subsurface and surface characteristics of Kef Essnoun mine.
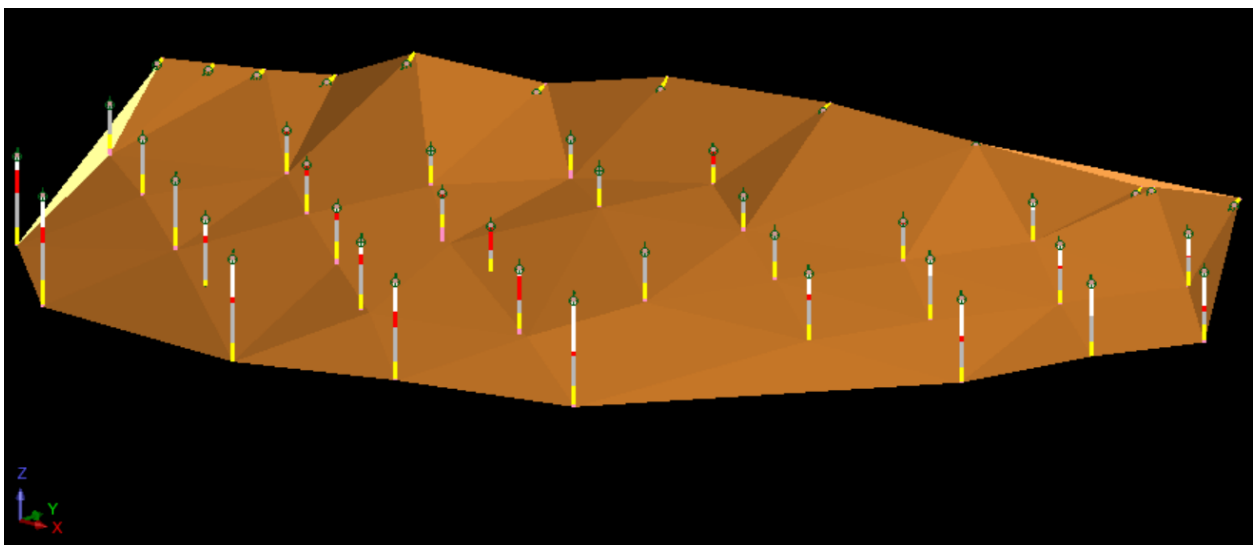
Fig IV.22: Topographic Model.

IV.5.6. Creation of the surface:

 The surface creation on the top string called " natural terrain bottom ", at the same time, it presents the roof of the first geological layer which is the Miocene layer.
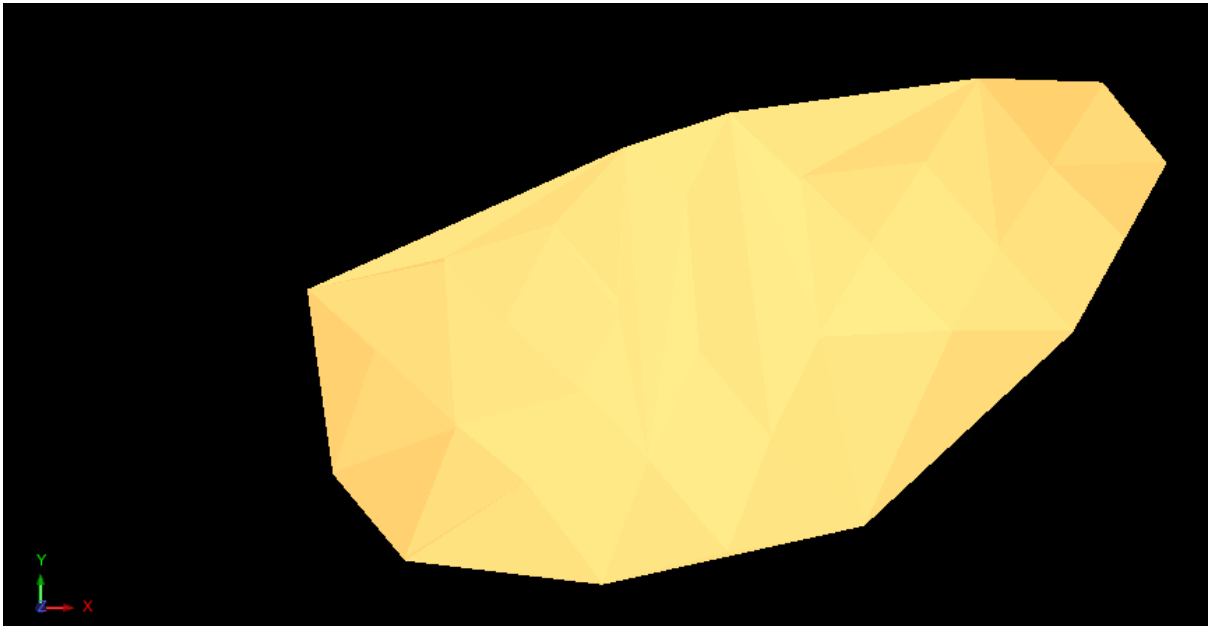
Fig IV.23: Natural terrain bottom.

Using the same method, correlated surfaces were created between the entire roof and the entire Ripe, with each layer from top to bottom represented in different colors .
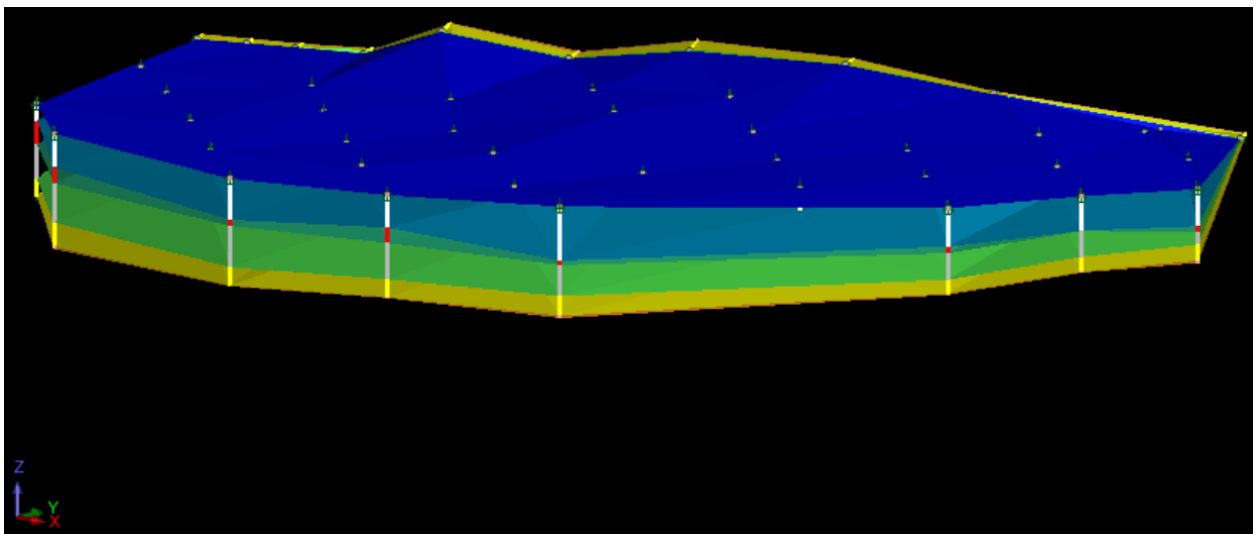
Fig IV.24: the surface of all geological layers.

IV.5.7. Creation of solid:

After creating the surfaces we create a solid between the roof surface and the surface first layer.
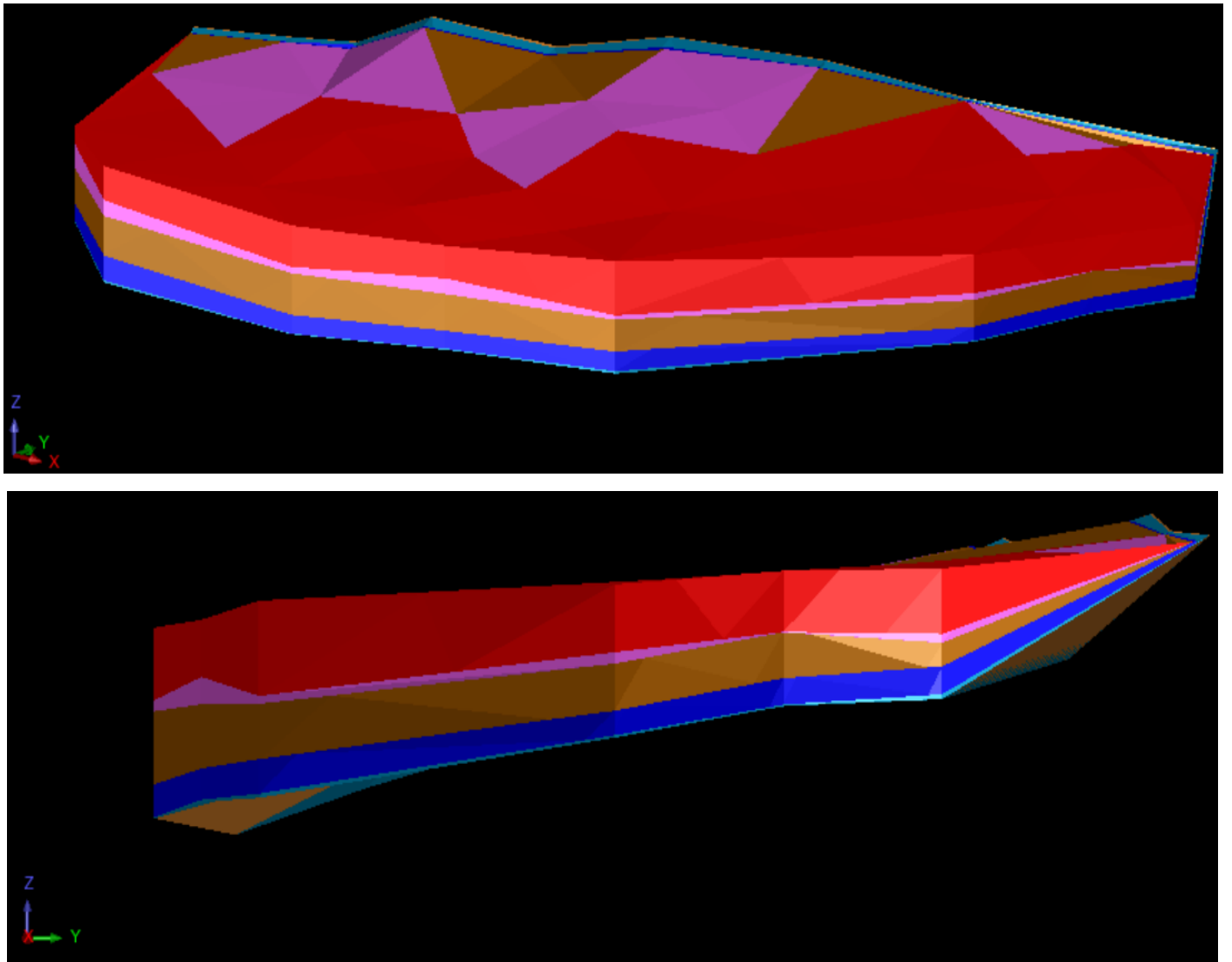
Fig IV.25: Solids from all geological layers

✓ **Interpretation:**

After collecting, treating and simulating the data obtained from phosphate company SOMIPHOS, the main resultats are the following:

-The total number of boreholes is 32 extended along the discovered mineral body.

-Boreholes labeled S-2 to S-46 were placed along prospecting profiles in a northwest-southeast direction, with a grid spacing of 250 x 300 meters. The deepest drill hole, S-7, reaches 250 meters and is located to the southwest of the deposit. The shortest, S-25, is 76.1 meters deep and is situated near the outcrop band of the Kef Essnoun escarpment. All the drillholes penetrated the phosphatic layer down to the base, except for S-14, which only reached 13.5 meters due to a technical issue during drilling. Additionally, EREM conducted 22 trenches in

the escarpment area, labeled Tr22 to Tr44, with depths ranging from 1.0 to 2.0 meters, a width of 1.0 meter, and lengths varying based on the thickness of the exposed phosphate layer.

-The drillholes core are mostly shown generally four layers: Limestone, Marl, Phosphate and Sand.
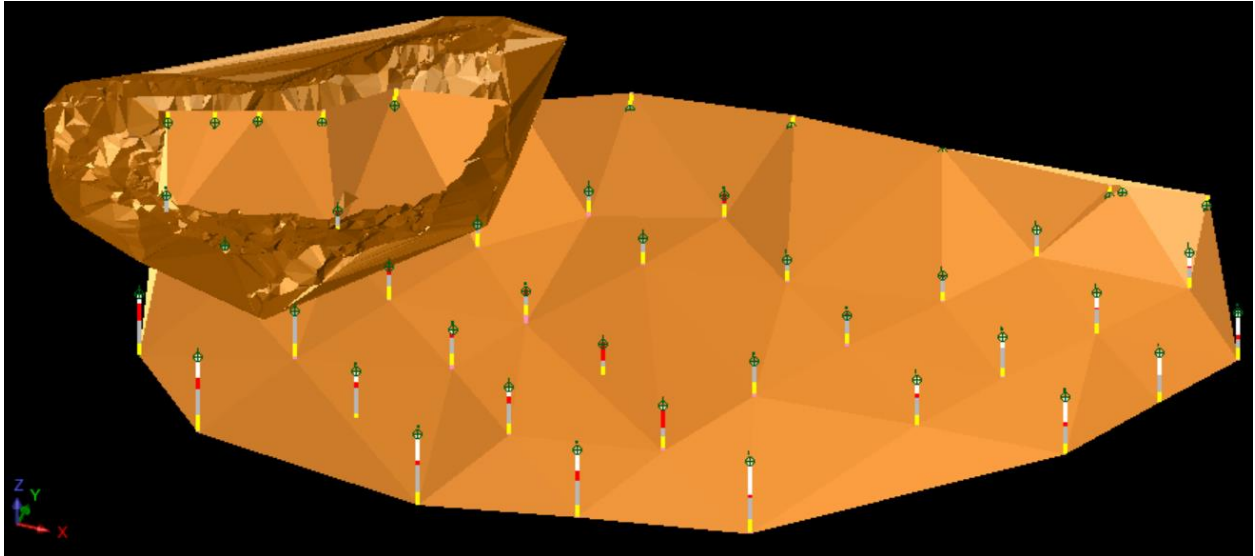
Fig IV.26: Solid topographic map showing the limit of boreholes situation in relation to the mine of Kef Essnoun ''NW ''.

IV.5.8. Cross section creation:

To create cross sections in Surpac, first load the data, define the section line, and create a plane. Then create and display the cross-section, then add interpretations and explanations. Finally, save and export a design, ensuring that the data is validated and saved on a regular basis.
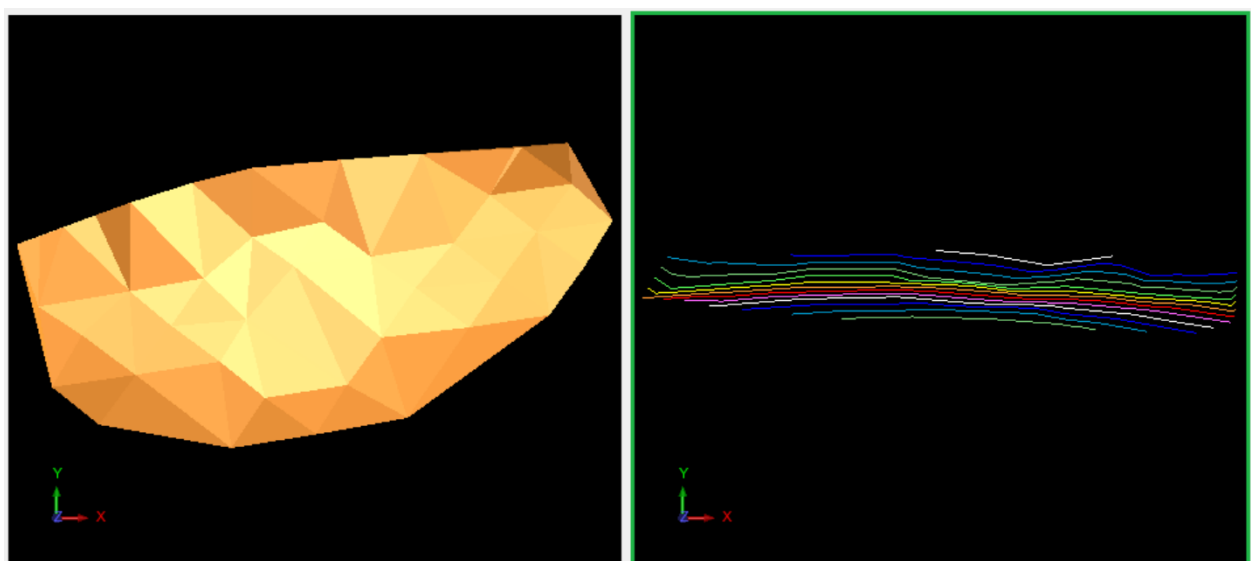
Fig IV.27: Cross section creation.

✓ **Cross section before mining:**
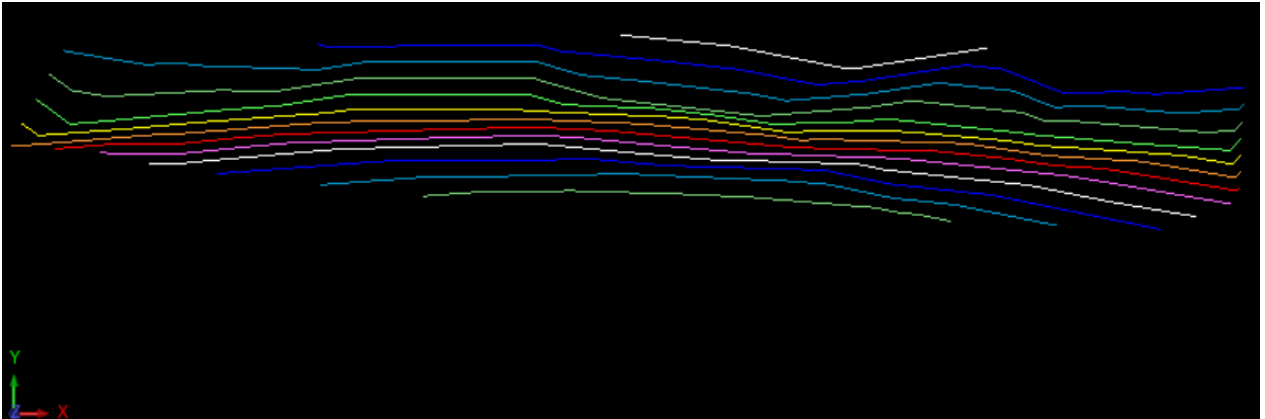
Fig IV.28: Cross section befor mining.

✓ **Cross section after mining:**
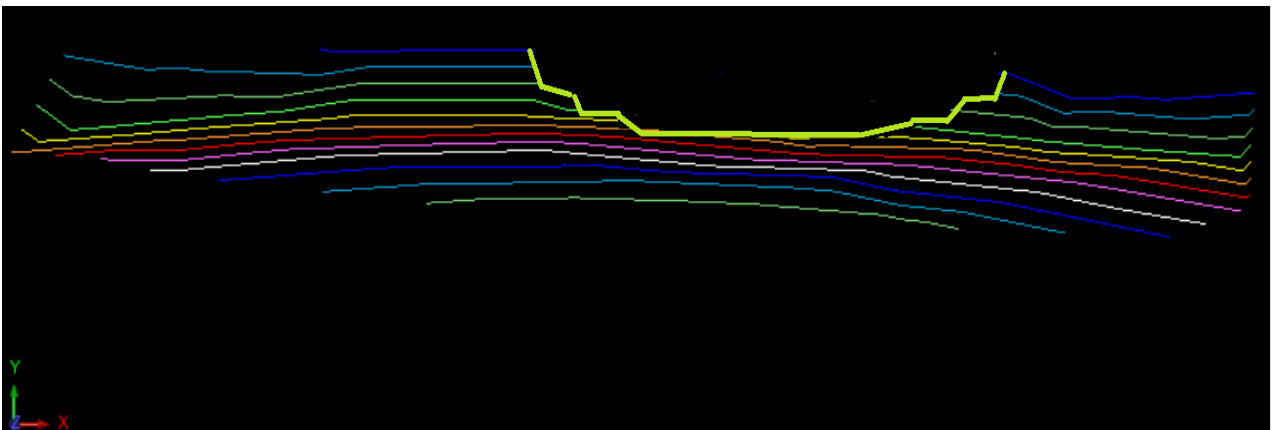
Fig IV.29: Cross section after mining.

IV.5.9. Geometrical model of the open pit used to the stability assessment step:
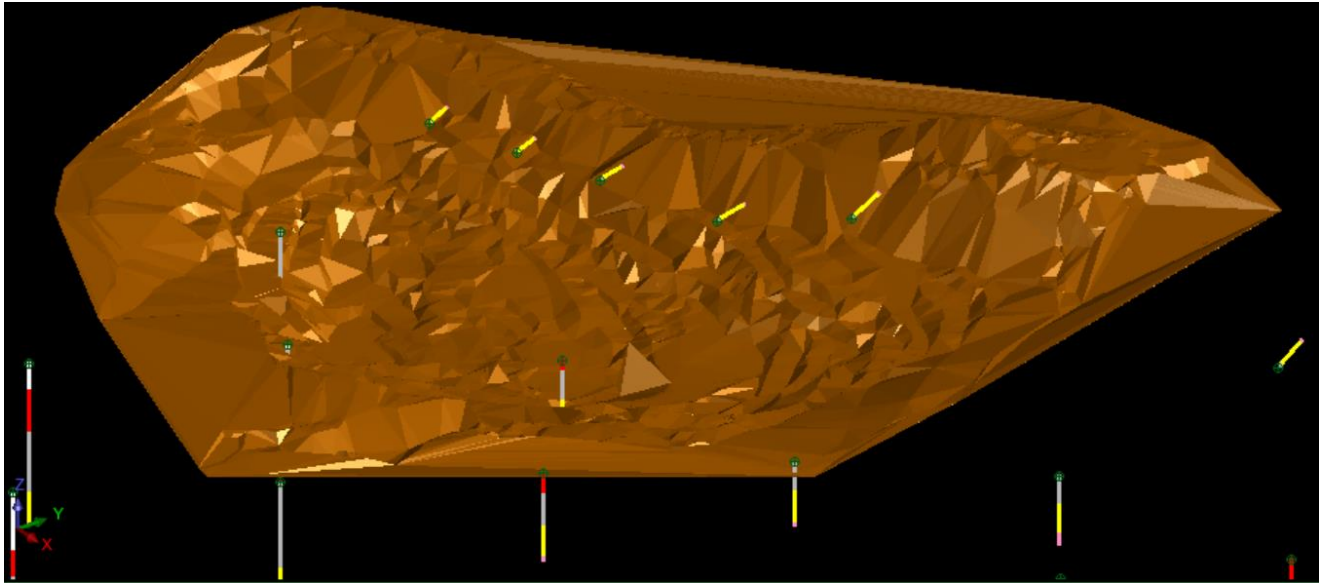
Fig IV.30: 3D creation.

The lithological modeling conducted at the Kef Essnoun mine using Surpac software has provided valuable insights into slope stability evaluation. By employing a methodology illustrated in Figure IV.17, the study encompassed data input and checking, borehole display in 2D and 3D views (Figures IV.18, IV.19), creation of correlated strings, and geological and topographic modeling (Figure IV.22).

Through the creation of surfaces and solids representing different geological layers (Figures IV.23, IV.24, IV.25), the study revealed crucial findings. It identified 32 boreholes distributed along the mineral body, providing insights into the composition and depth of the deposits. The boreholes penetrated various layers, including limestone, marl, phosphate, and sand, offering comprehensive information for further analysis.

The creation of cross-sections before and after mining (Figures IV.28, IV.29) enabled the visualization of potential changes in the geological structure post-mining, aiding in the assessment of stability. Additionally, the geometric model of the open pit (Figure IV.30) provided a three-dimensional representation essential for evaluating stability.

Overall, the lithological modeling and design at the Kef Essnoun mine have yielded significant insights into slope stability assessment. The comprehensive analysis of geological layers, borehole data, and cross-sections lays the foundation for informed decision-making regarding mining operations and slope management strategies.

IV.6. Geotechnical modeling:

Geotechnical modeling involves using analytical, numerical, and empirical methods to understand and predict the behavior of soil and rock masses under various conditions. The primary goal is to ensure the safety and stability of civil engineering structures like buildings, bridges, slopes, tunnels, and dams (Miranda, T., Correia,et al.2011).

A). Define the Geometry:

- ▪ **Input:** Limestone layer:
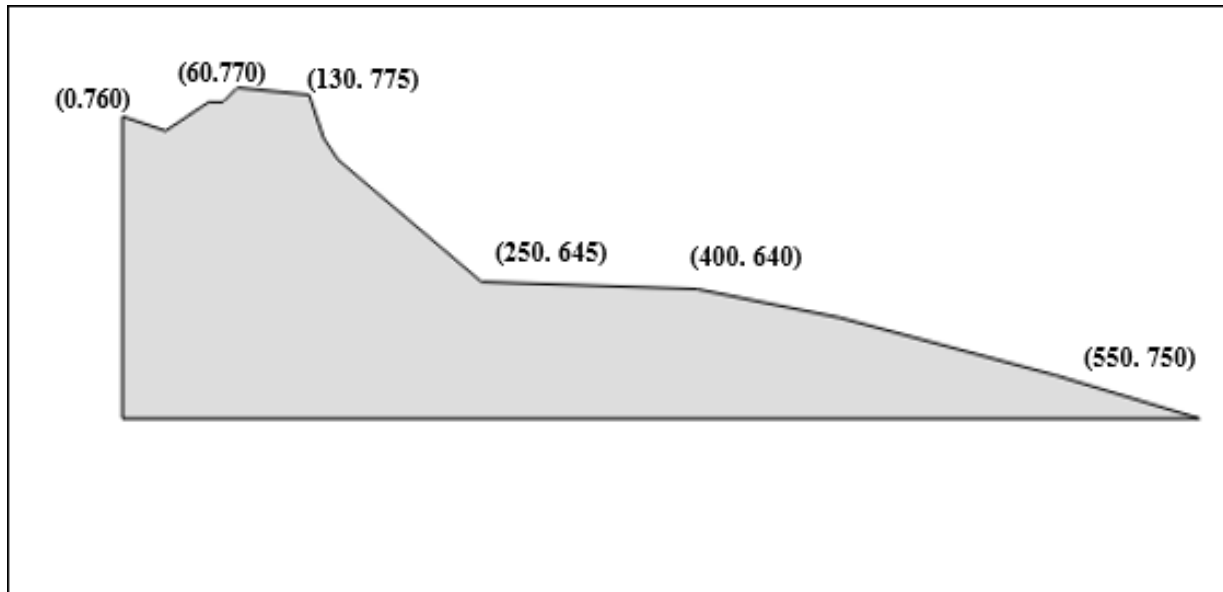
Fig IV.31: The Geometry limestone layer.

Marl layer:
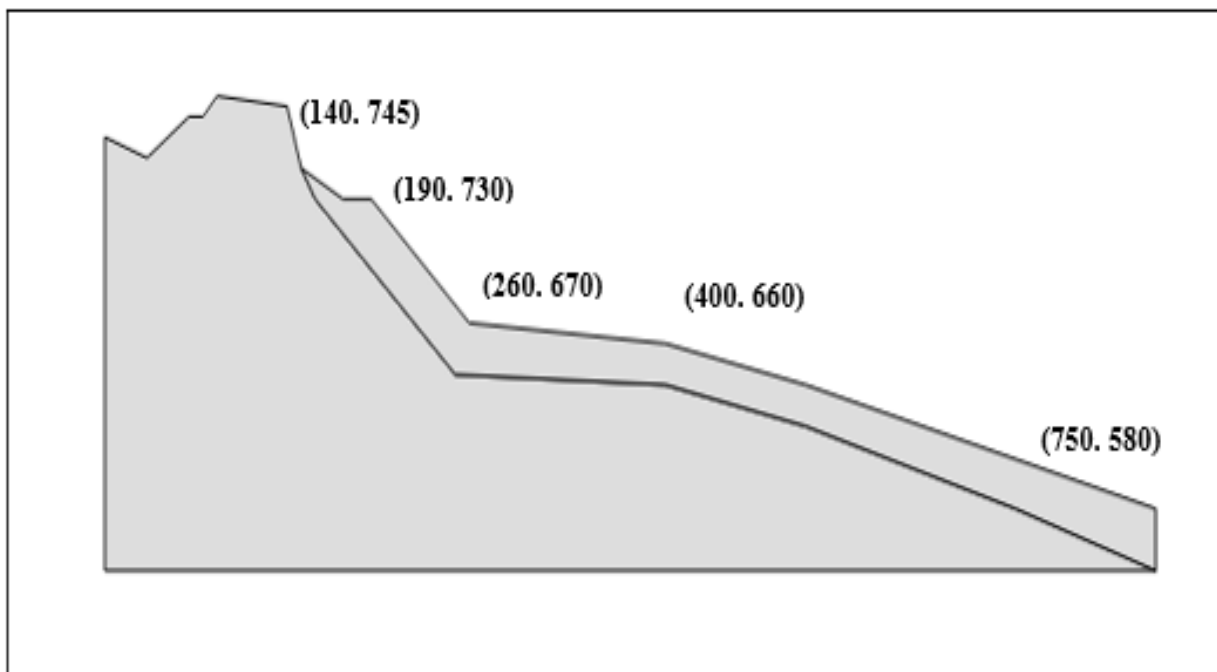
Fig IV.32: The Geometry marl layer.

Phosphate layer:
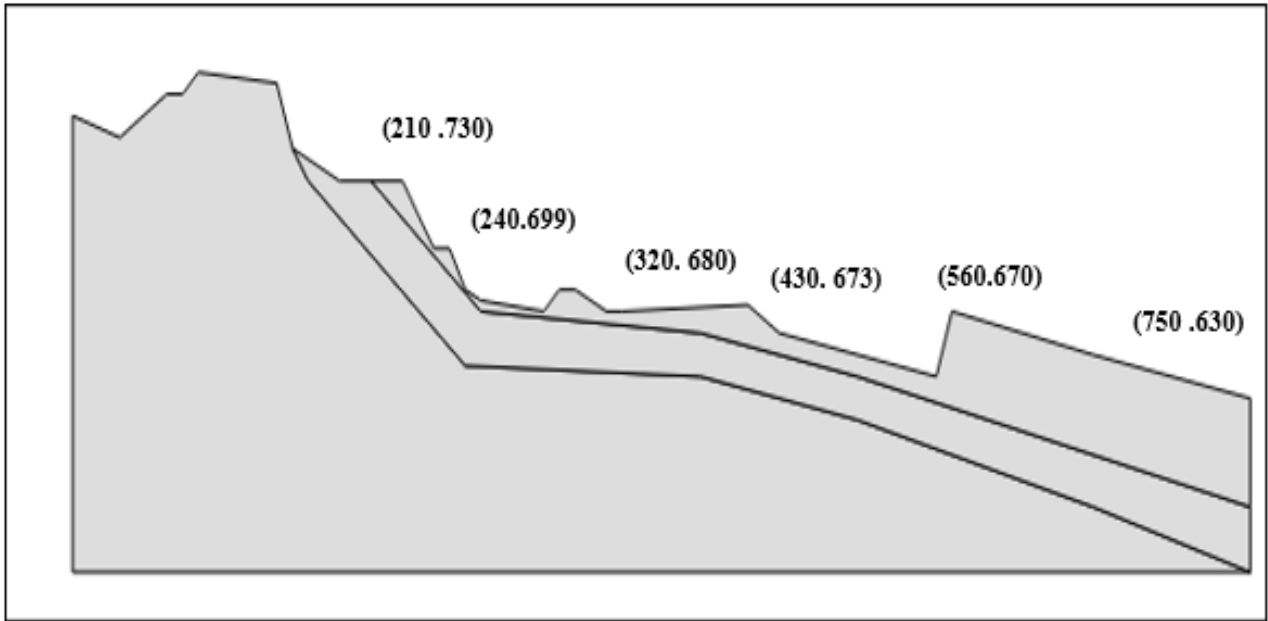
Fig IV.33. Geometry of the phosphate layer.

Danio -limestone layer:
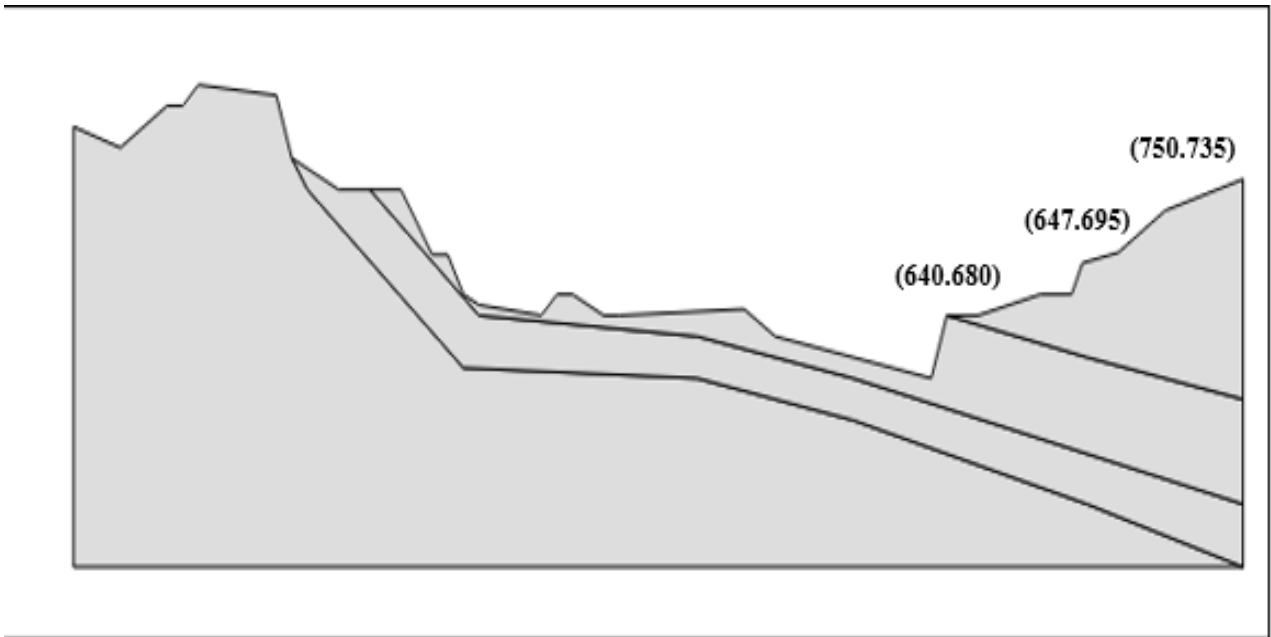
Fig IV.34: The Geometry Danio -limestone layer.

Materials properties (Tables below used in 2D , 3D modeling):
Layers properties are given in Tables.

TableIV.9 : Limestone layer properties.

Parameter	Name	Value	Unit
Material model	Model	Jointed Rock	-
Type of material behaviour	Type	Drained	-
Saturated Unit weight	γsat	27.46	kN/m³
Unsaturated Unit weight	$\gamma unsat$	27	kN/m³
Young's modulus	E'	5.600E6	kN/m²
Poisson's ratio	ν	0.21	-
Permeability	Kx, Ky	10	m/day

TableIV.10: Danio-limestone layer properties.

Parameter	Name	Value	Unit
Material model	Model	Jointed Rock	-
Type of material behavior	Type	Drained	-
Saturated Unit weight	γsat	27.46	kN/m³
Unsaturated Unit weight	$\gamma unsat$	27	kN/m³
Young's modulus	E'	5.600E6	kN/m²
Poisson's ratio	ν	0.21	-
Permeability	Kx, Ky	10	m/day

Table IV.11 : Marl layer properties.

Parameter	Name	Value	Unit
Material model	Model	Jointed Rock	-
Type of material behaviour	Type	Drained	-
Saturated Unit weight	γsat	24	kN/m³
Unsaturated Unit weight	$\gamma unsat$	23	kN/m³
Young's modulus	E'	3.600E6	kN/m²
Poisson's ratio	ν	0.14	-
Permeability	Kx, Ky	1	m/day

Table IV.12: Phosphate layer properties.

Parameter	Name	Value	Unit
Material model	Model	Jointed Rock	-
Type of material behaviour	Type	Non porous	-
Saturated Unit weight	γsat	24.81	kN/m³
Young's modulus	E'	4.600E6	kN/m²
Poisson's ratio	ν	0.24	-

TableIV.13: Plans properties.

Parameters	Name	Plan 1	Plan 2	Unites
Cohesion	C ref	100	100	kN/m²
Angle of internal friction	ϕ	30	30	Degrees
Dip (*-180≤ α1≤ 180*)	α1	25	170	Degrees

C). Input Material:
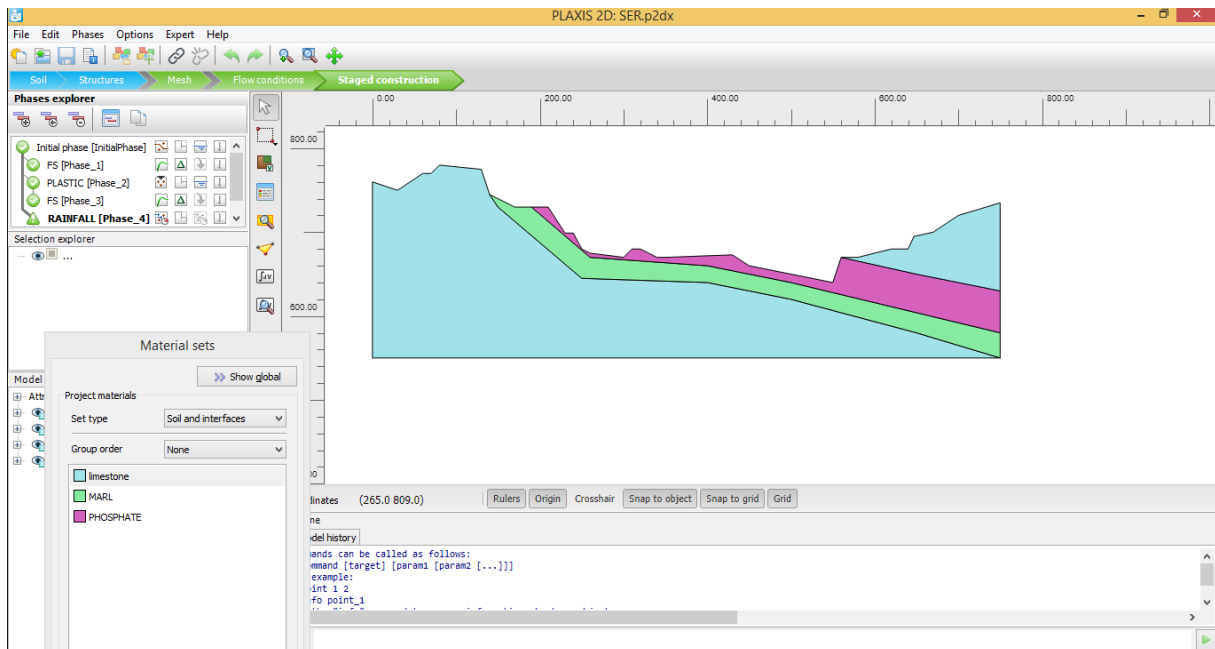
Fig IV.35: Input Material.

D). Boundaries conditions:
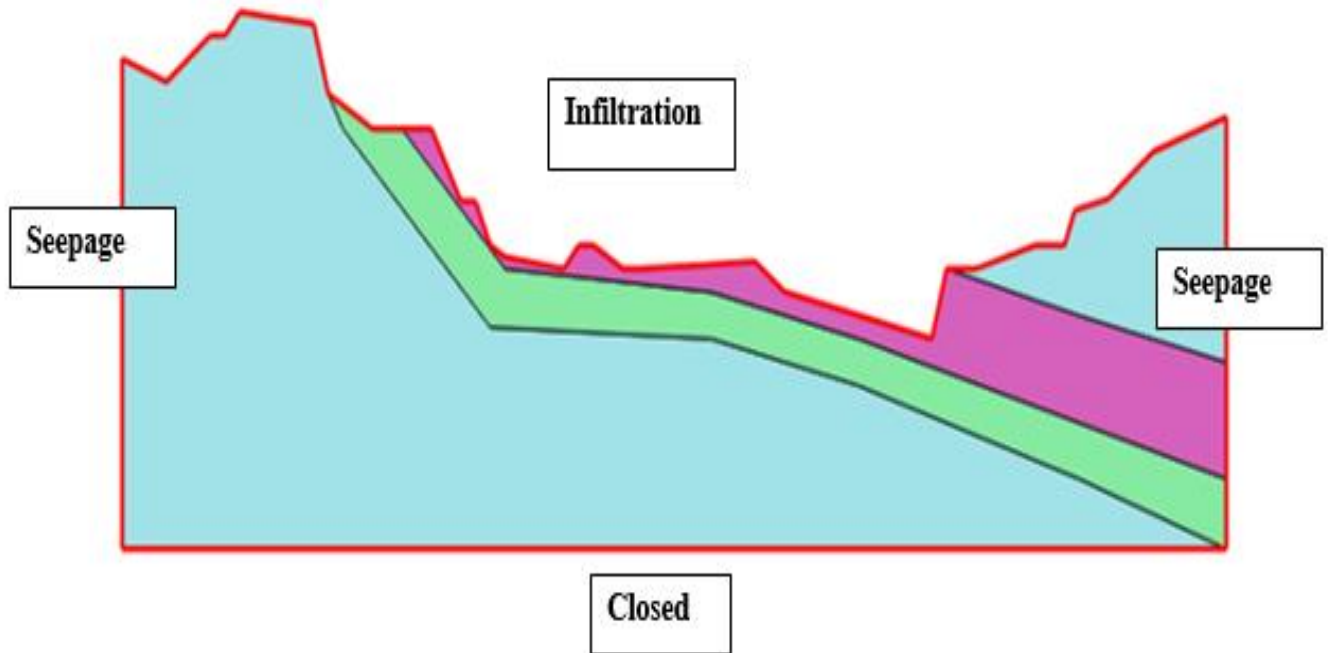
Fig IV.36: Boundaries conditions.

E). Mesh generating:
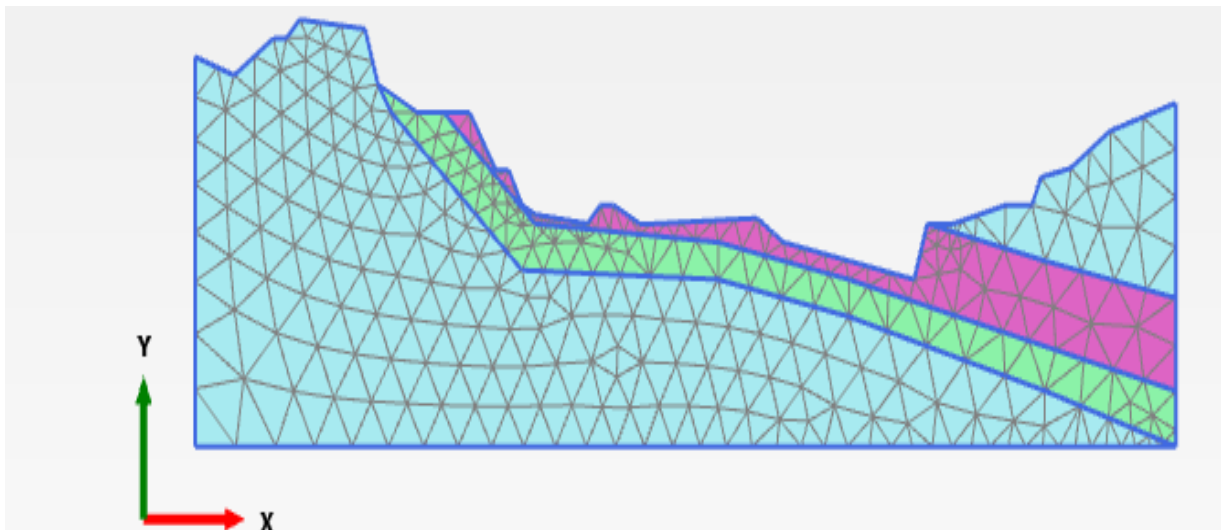
Fig IV.37: Generate mesh.

F). Flow conditions (Initial Conditions):

According to hydrogeological study mentioned before the water table there is not considered in the Kef Essnoun mine but we do take into consideration the flow generated from to the infiltration of the rainfall period, it is important to indicate that heavy rain have been registered during the month September.

G). Staged Construction (Calculations):

has been effectuated in five phases of calculation.

 - Initial phase: using Gravity loading calculation type.

 - First phase: the safety factor of the first phase.

 - Second phase: plastic phase calculation type.

 - Third phase: the safety factor of the second phase.

 - Fourth phase: the Rainfall phase (0.12m/day): fully coupled flow-deformation calculation type.

 -Fifth phase: the safety factor of the fourth phase.

- Results and discussion:

At this stage of simulation, the output phase generates results as follows:

a). Initial phase: Gravity loading calculation type.
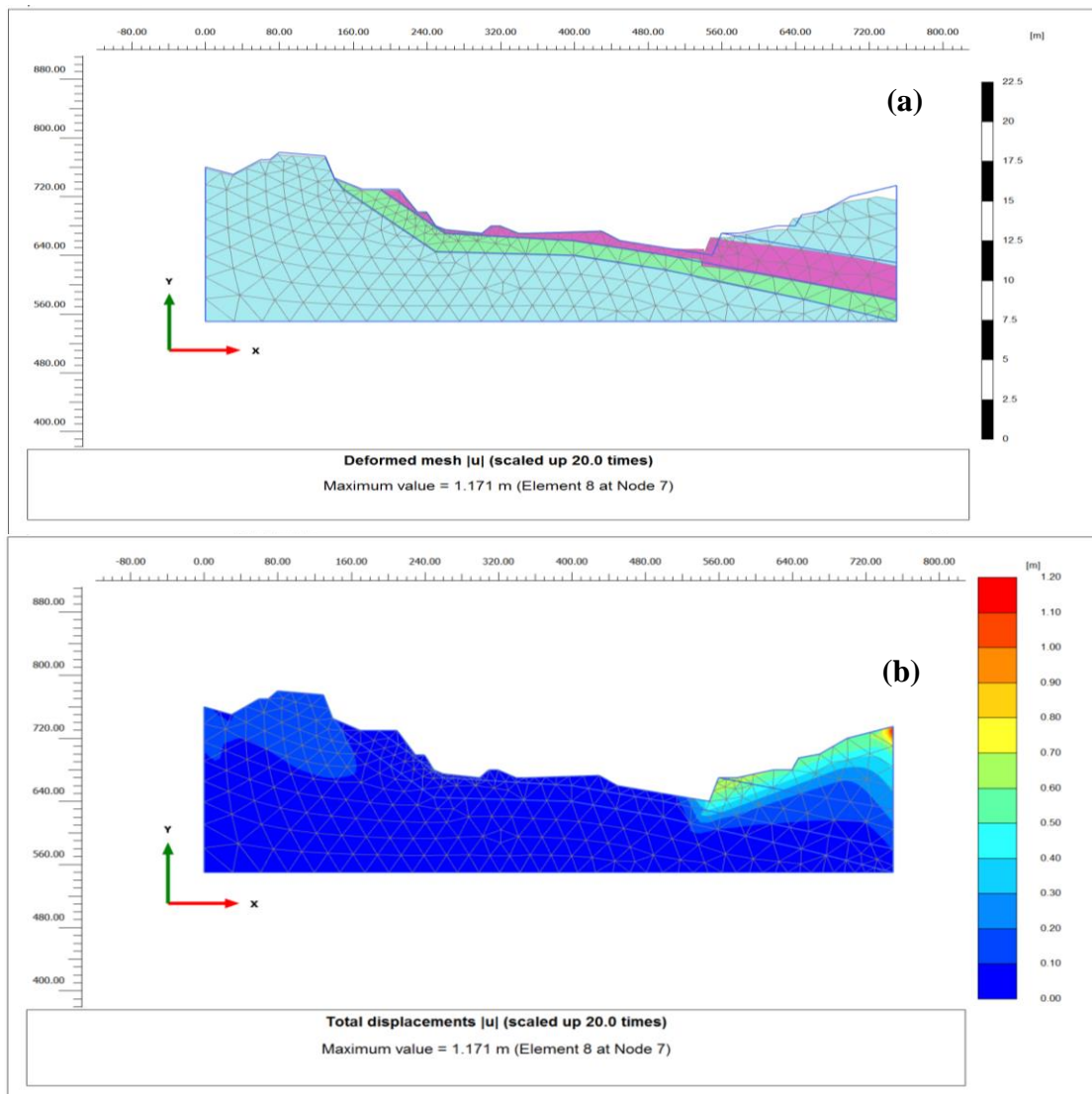
Fig IV.38: (a): Deformed mesh **(b):** Total displacement.

b). Phase 1: the safety factor of the first phase.

Deformed mesh |u| (scaled up 50.0 times)
Maximum value = 0.5179 m (Element 8 at Node 7)

Total displacements |u| (scaled up 50.0 times)
Maximum value = 0.5179 m (Element 8 at Node 7)
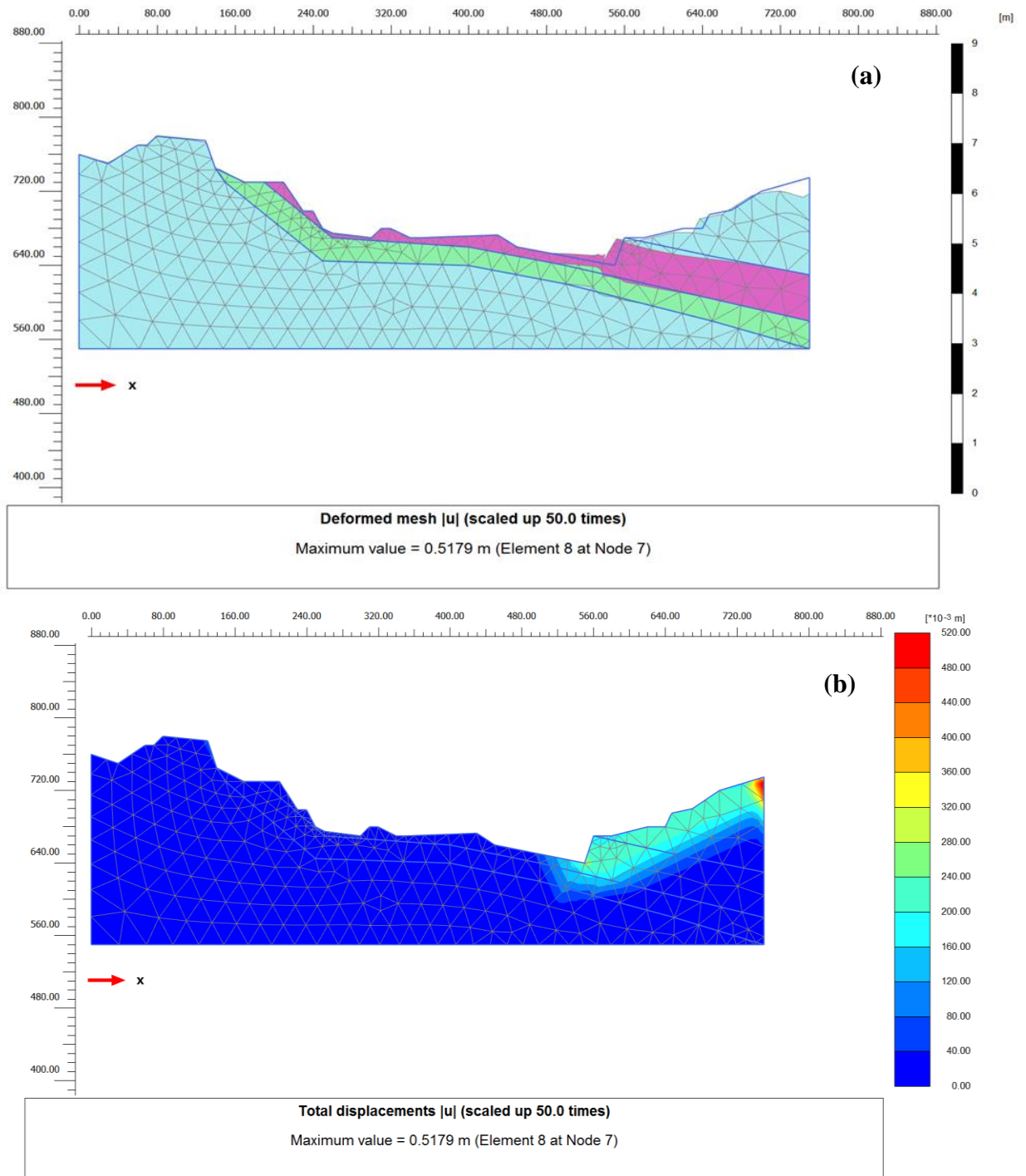
Fig IV.39: (a): Deformed mesh **(b):** Total displacement.

c). Phase 2: plastic phase calculation type.

Deformed mesh |u| (scaled up 500*10³ times)

Maximum value = 0.06401*10⁻³ m (Element 8 at Node 2)

Total displacements |u| (scaled up 500*10³ times)

Maximum value = 0.06401*10⁻³ m (Element 8 at Node 2)
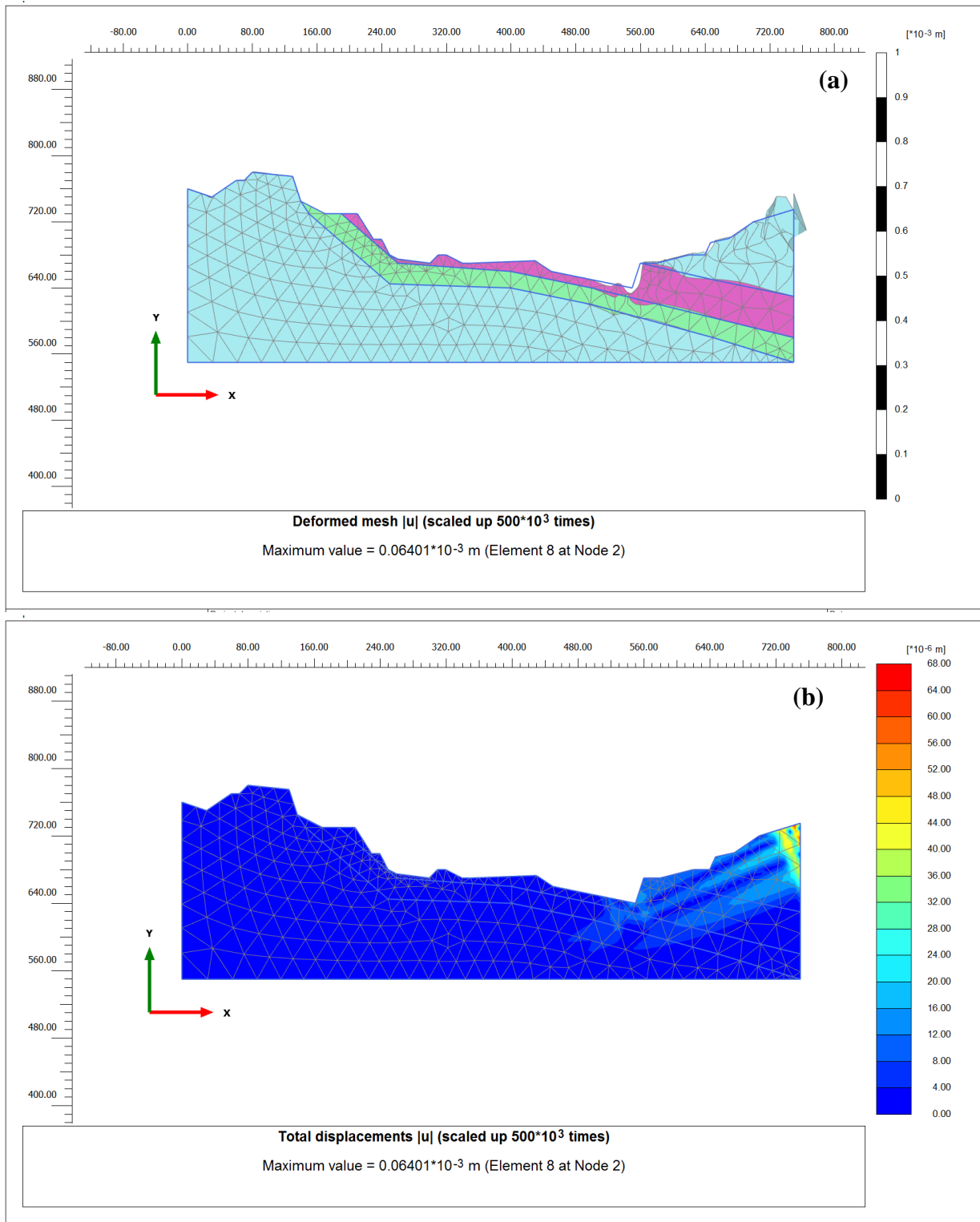
Fig IV.40: (a): Deformed mesh **(b):** Total displacement.

d). Phase 3: the safety factor of the second phase.
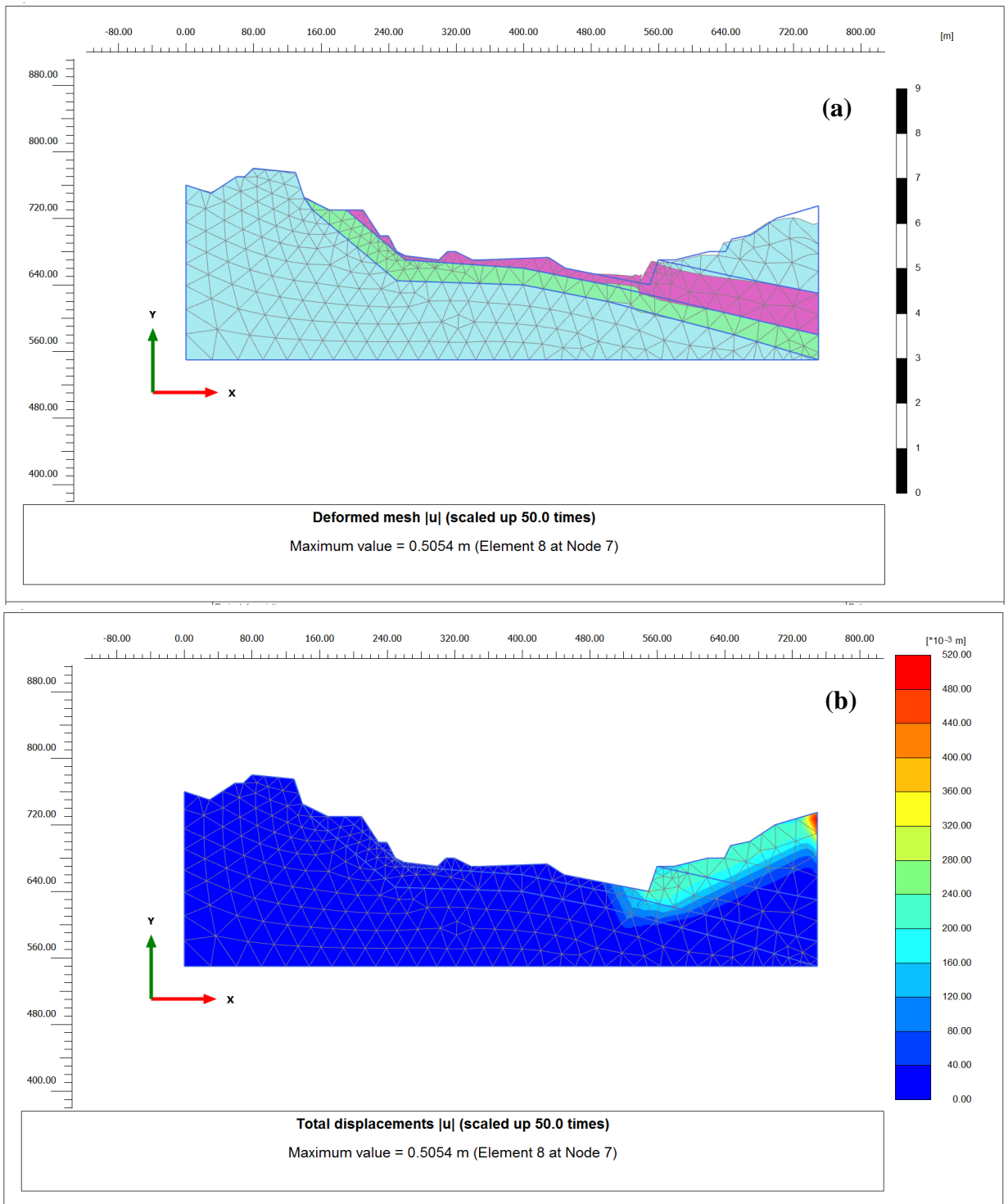
Fig IV.41: (a): Deformed mesh (b): Total displacement.

e. Phase 4: the Rainfall phase (0.12m/day): fully coupled flow-deformation calculation type.

Deformed mesh |u| (scaled up 500 times) (Time 1.000 day)

Maximum value = 0.04954 m (Element 8 at Node 7)

Total displacements |u| (scaled up 500 times) (Time 1.000 day)

Maximum value = 0.04954 m (Element 8 at Node 7)
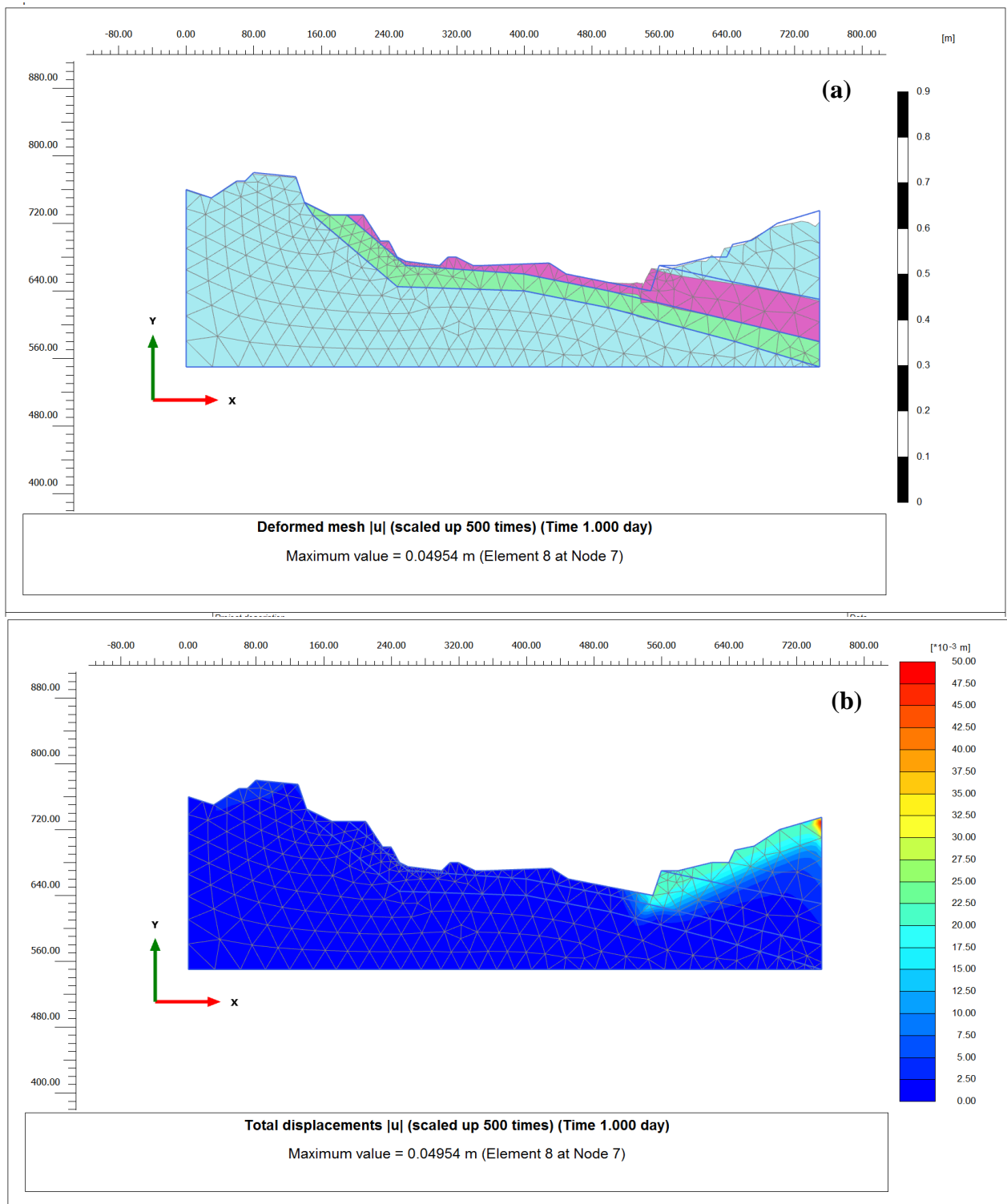
Fig IV.42: (a): Deformed mesh **(b):** Total displacement.

f). Phase 5: the safety factor of the fourth phase.
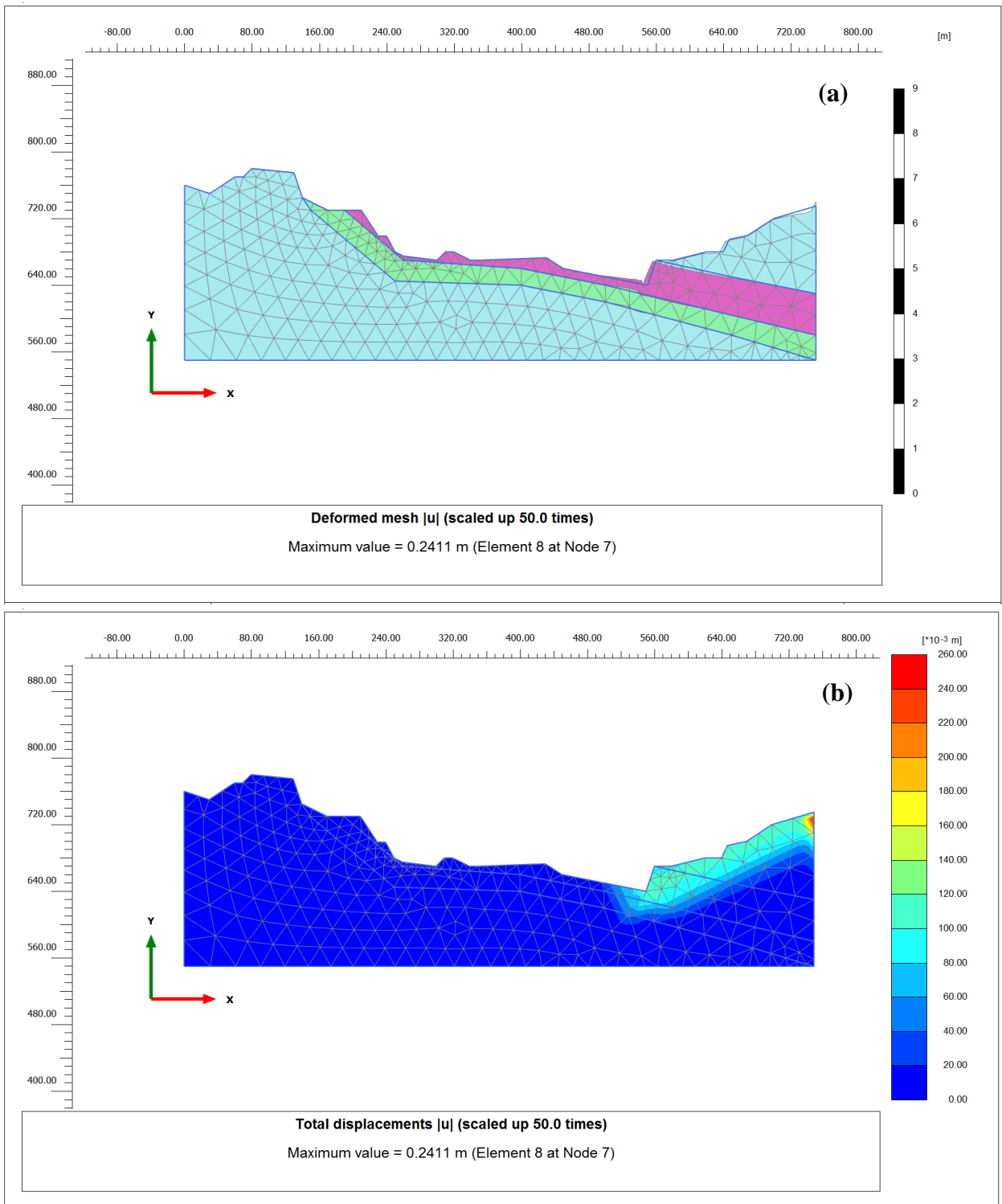
Fig IV.43: (a): Deformed mesh **(b):** Total displacement.

K). Curves:
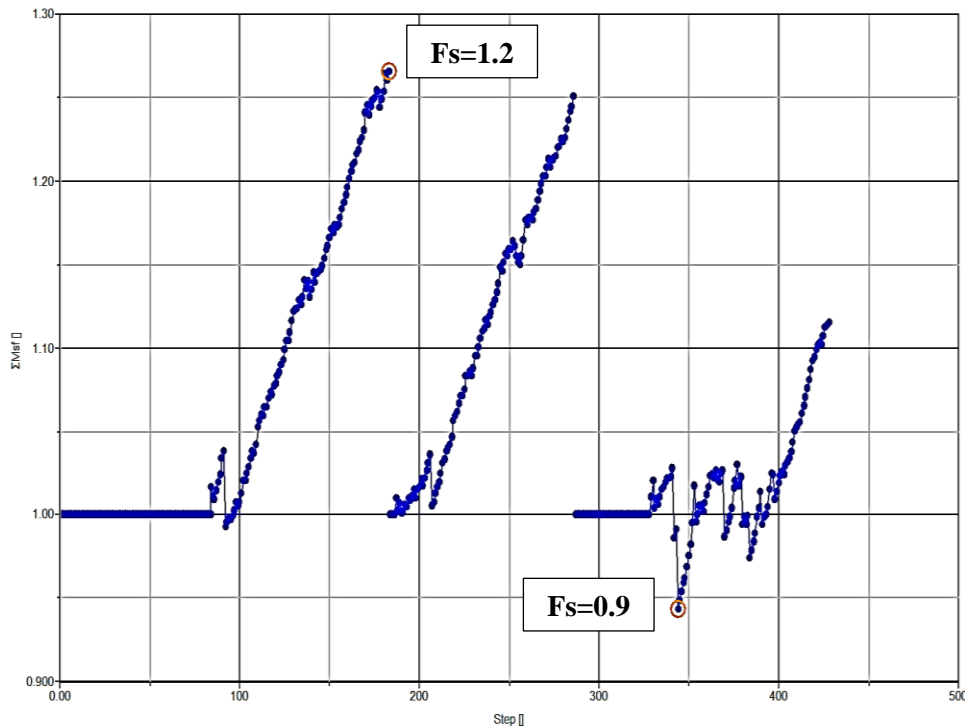
Fig IV.44: Curve represent the change of Fs.

The curve is a plot of factor of safety (Fs) versus step number, which is commonly used in numerical simulations to monitor the stability of a slope or other geotechnical structure over time or different loading conditions.

K).1. Key Points of the Curve:

- **Initial Stability (Fs ≈ 1.0):**

-At the beginning (Step 0), the factor of safety is approximately 1.0, indicating a marginally stable condition.

-This is typically the baseline condition of the slope or structure under consideration.

- **Increase in Factor of Safety (Fs = 1.2):**

-Around Step 100 to Step 200, there is a sharp increase in the factor of safety, reaching a peak of Fs = 1.2.

-This indicates an improvement in stability, possibly due to a reduction in applied loads, reinforcement measures, or other stabilizing interventions.

- **Stabilization Period:**

-Following the peak at Fs = 1.2, the factor of safety returns to around 1.0, indicating a period of stabilized conditions with no significant change in stability.

-This plateau could represent a phase where the slope or structure is under consistent loading or conditions.

- **Decrease in Factor of Safety (Fs = 0.9):**

-Around Step 300, there is a noticeable drop in the factor of safety to Fs = 0.9.

-This decrease signifies a reduction in stability, potentially due to increased loading, changes in environmental conditions, or degradation of structural components.

-A factor of safety below 1.0 indicates an unstable condition where failure is likely.

- **Fluctuating Stability:**

-Beyond Step 300, the factor of safety shows significant fluctuations.

-These variations could be due to dynamic changes in loading, environmental conditions, or progressive failure mechanisms.

K).2. Analysis and Interpretation:

- **Stable Phases:** The periods where Fs is consistently around 1.0 suggest that the system is in a marginally stable state under constant conditions.

- **Stabilization Measures:** The increase in Fs to 1.2 suggests that some stabilization measures were effective, temporarily increasing the safety margin.

- **Unstable Phase:** The drop to Fs = 0.9 indicates a phase of instability, highlighting the need for immediate attention to prevent failure.

- **Dynamic Conditions:** The fluctuations in Fs beyond Step 300 indicate that the system is experiencing varying conditions, which could be due to cyclic loading, environmental changes, or progressive damage.
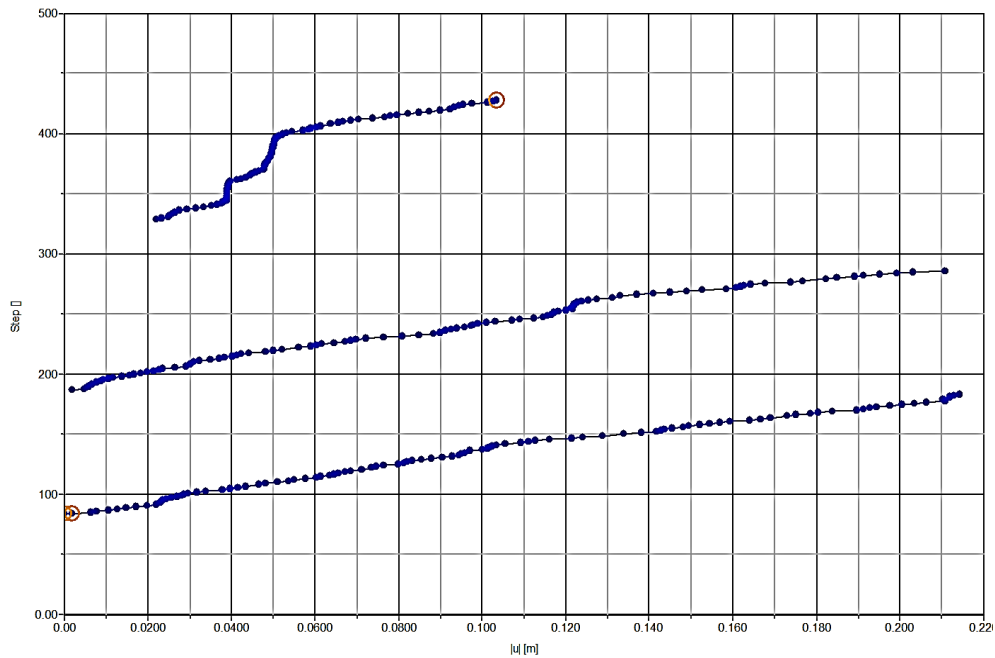
Fig IV.45: Curve represent the change of total displacement (node 125).

The plot is a displacement-time (or step) graph often used in geotechnical modeling to show the progression of displacements over time or steps.

K).3. Key Points of the Curve:

-Axes Interpretation:

-X-Axis (|u| [m]): Represents the magnitude of displacement in meters.

-Y-Axis (Step [i]): Represents the simulation steps or time steps.

K).4. Analysis and Interpretation:

-Initial Phase (Steps 0-100):

-All three curves start from the origin, indicating no initial displacement.

-Gradual increase in displacement, suggesting initial loading or changes in conditions.

-Middle Phase (Steps 100-300):

-Displacements increase steadily, with different rates for each curve.

-This phase indicates a period of continuous deformation under steady conditions.

-Late Phase (Steps 300-500):

-Further increase in displacement with noticeable steps or jumps, especially in the upper curve.

-The jumps suggest sudden changes in conditions, possibly due to failure mechanisms or changes in loading conditions.

-The upper curve shows a more pronounced increase in displacement, indicating a higher rate of deformation or instability compared to the other two curves.

K).5. Interpretation:

-Gradual Displacements: The gradual increase in displacements in the initial and middle phases suggests stable deformation under steady conditions.

Sudden Jumps: The sudden jumps in displacement in the later steps indicate potential failure events or significant changes in loading or boundary conditions.

-Different Rates of Displacement: The varying rates of displacement among the three curves indicate different response behaviors, possibly due to varying properties or conditions within the model.
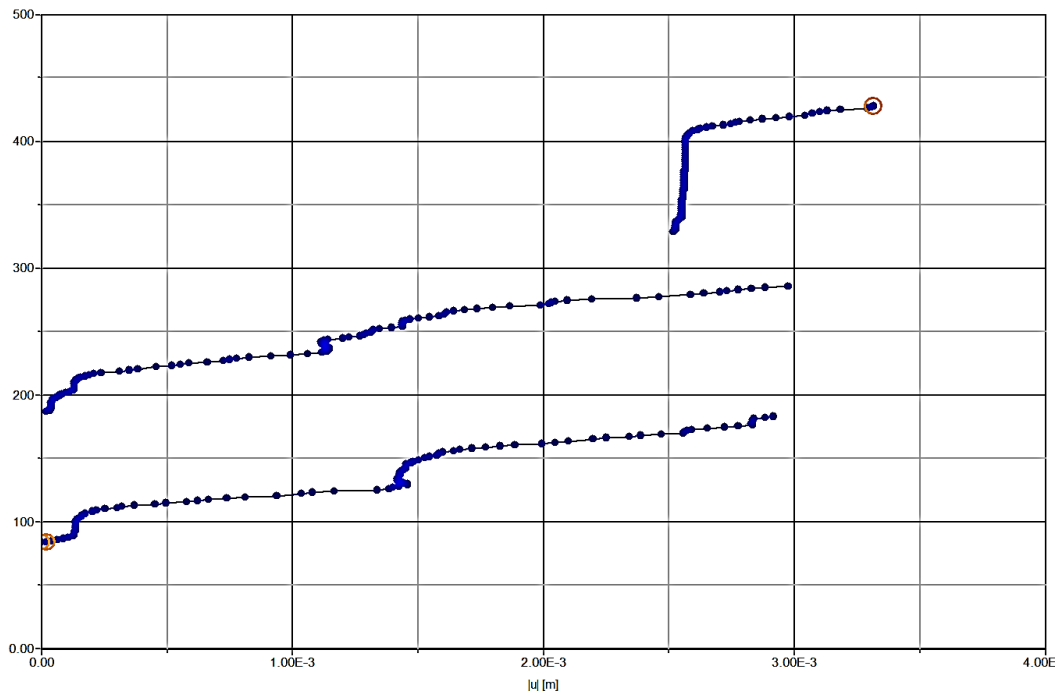
Fig IV.46: Curve represent the change of total displacement (node 4502).

K).6. Interpretation of the Figure:

The figure represents a graph plotting some form of experimental or simulation data. The x-axis shows |u| in meters, which suggests it could be representing a physical displacement, deformation, or a similar quantity. The y-axis is unlabelled, but it likely represents a dependent variable such as force, pressure, or another relevant measurement.

The data points are represented by three distinct sets of blue dots, each displaying a step-like pattern with increments at certain points, creating a staircase effect.

-K).7. Analysis:

-Axes and Units:

-The x-axis, labeled |u| (in meters), indicates a measure of absolute displacement or a related

physical quantity.

-The y-axis is not labeled, but it is critical to identify this variable to fully understand the data being represented.

-Data Points and Trends:

-Three sets of data points are plotted, each showing a step-like increase at specific intervals.

-These increments suggest the presence of a threshold effect or phase transition, where the variable on the y-axis changes significantly at certain values of |u|.

-Potential Interpretation:

-If this is a stress-strain plot, the steps could correspond to yield points or regions where a material undergoes plastic deformation.

-The three lines may represent different experimental conditions or samples, each exhibiting similar behavior but starting from different initial conditions.

IV.7. 3D geotechnical modeling:

3D geotechnical modeling involves creating a comprehensive three-dimensional representation of the subsurface geological and geotechnical features of an area.

-Define the Geometry:
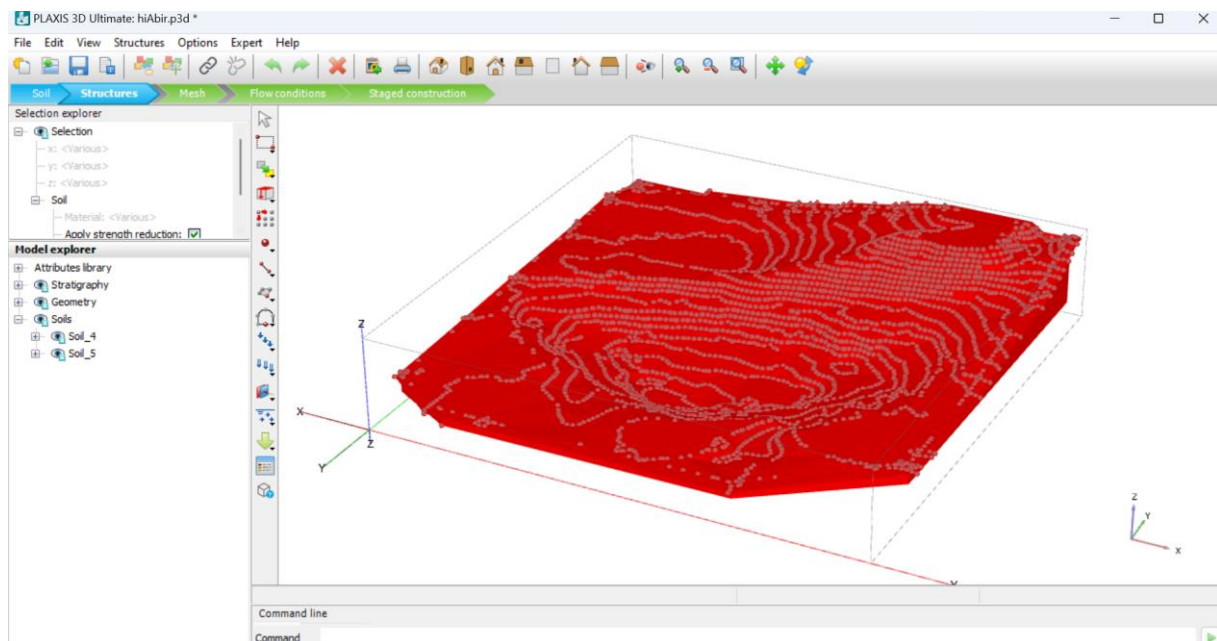
Fig IV.47: Define the Geometry-import topographic file.
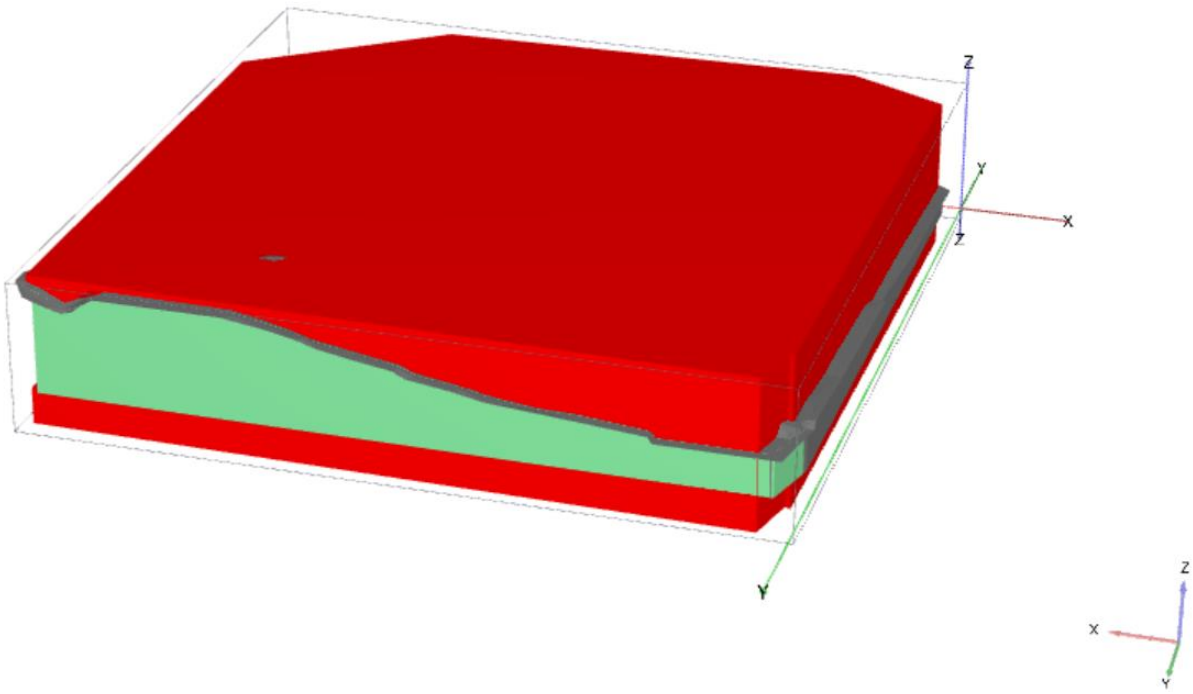
Fig IV.48: Define structures.

-Check geometry:
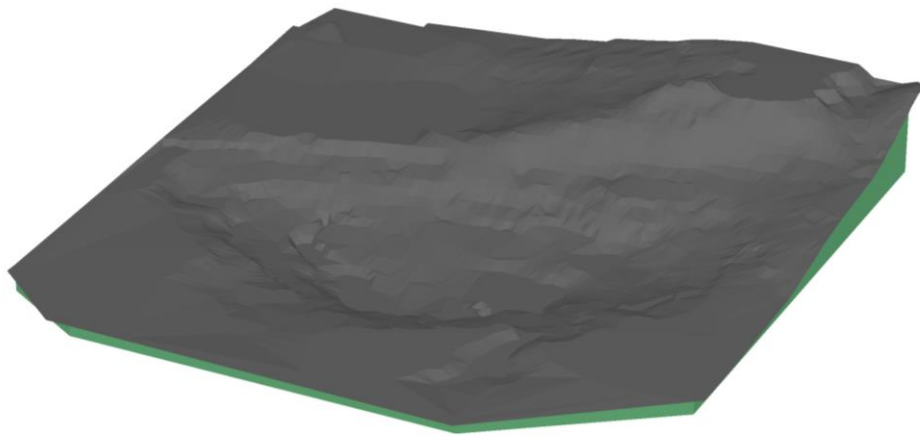
Fig IV.49: Mine structure combining and isolation and geometry checking**.**

-Input Material:
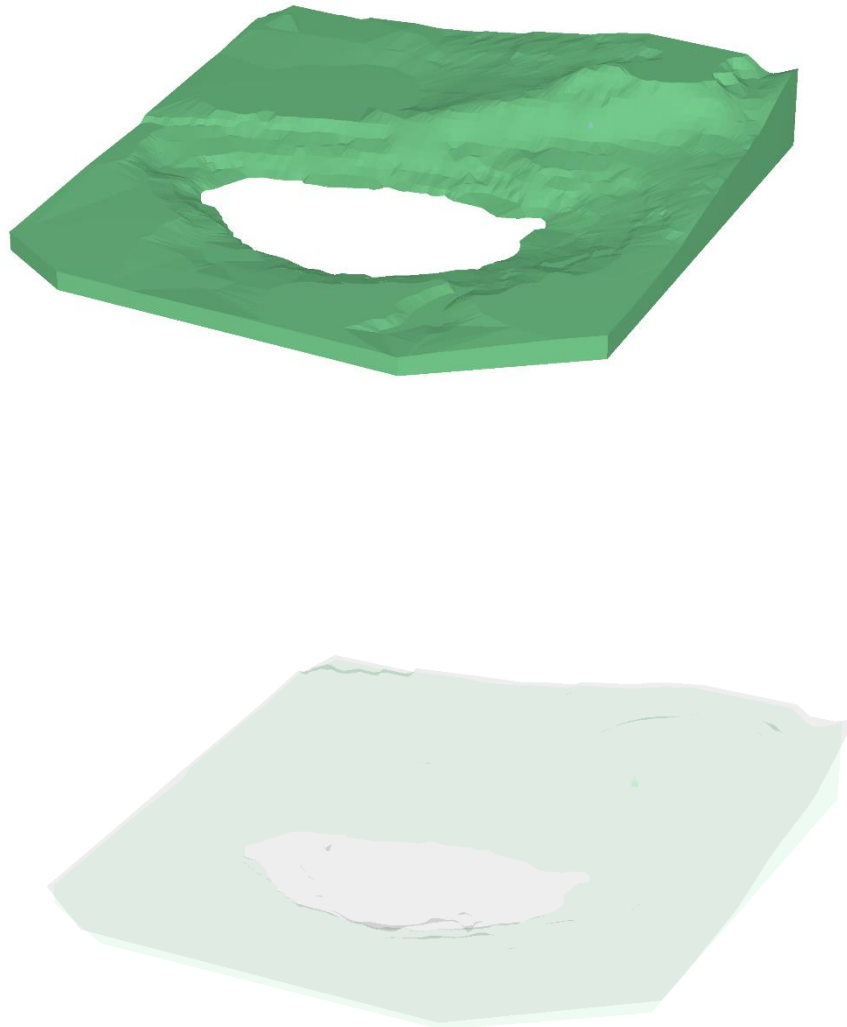
Fig IV.50 : Input Material properties.

-Mesh generating:

Connectivity plot
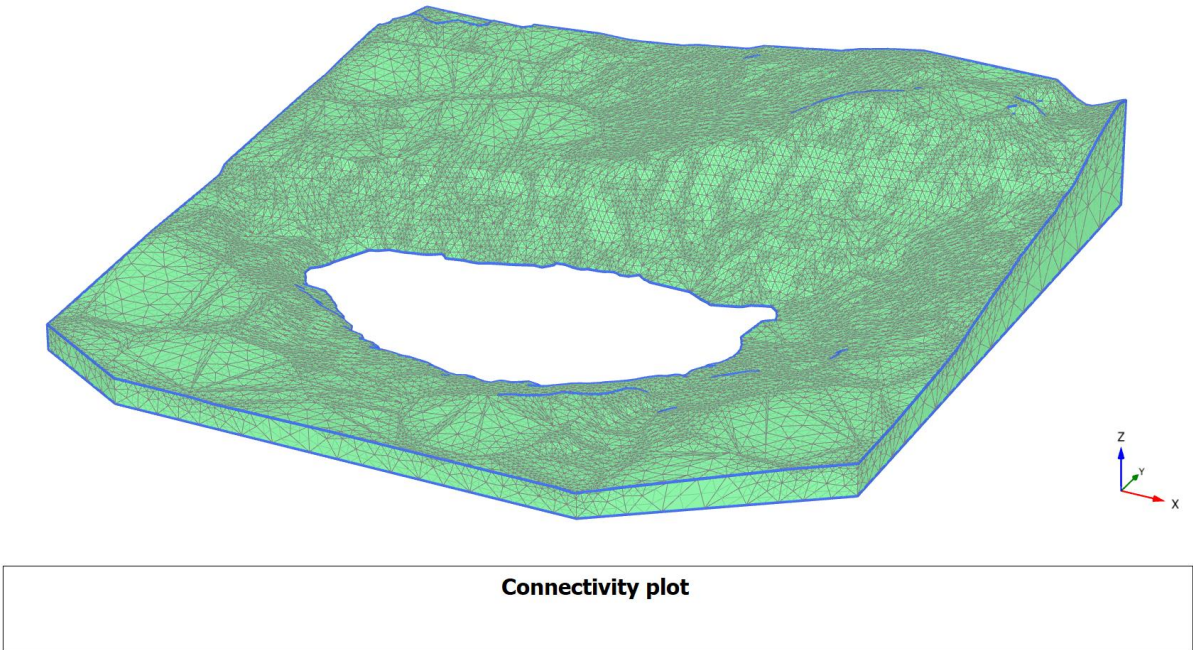
Fig IV.51: Mesh generating.

- **Output results**

Elevation (scaled up 0.200 times)

Maximum value = 230.0 m (Element 2263 at Node 67500)

Minimum value = 40.00 m (Element 21 at Node 91)

Elevation (scaled up 0.200 times)

Maximum value = 230.0 m (Element 2263 at Node 67500)

Minimum value = 40.00 m (Element 21 at Node 91)
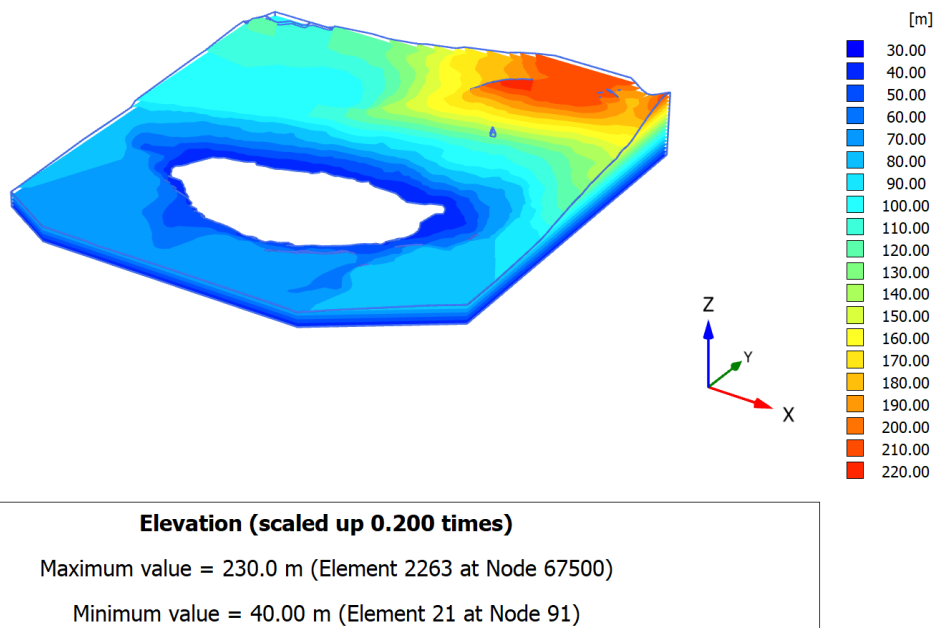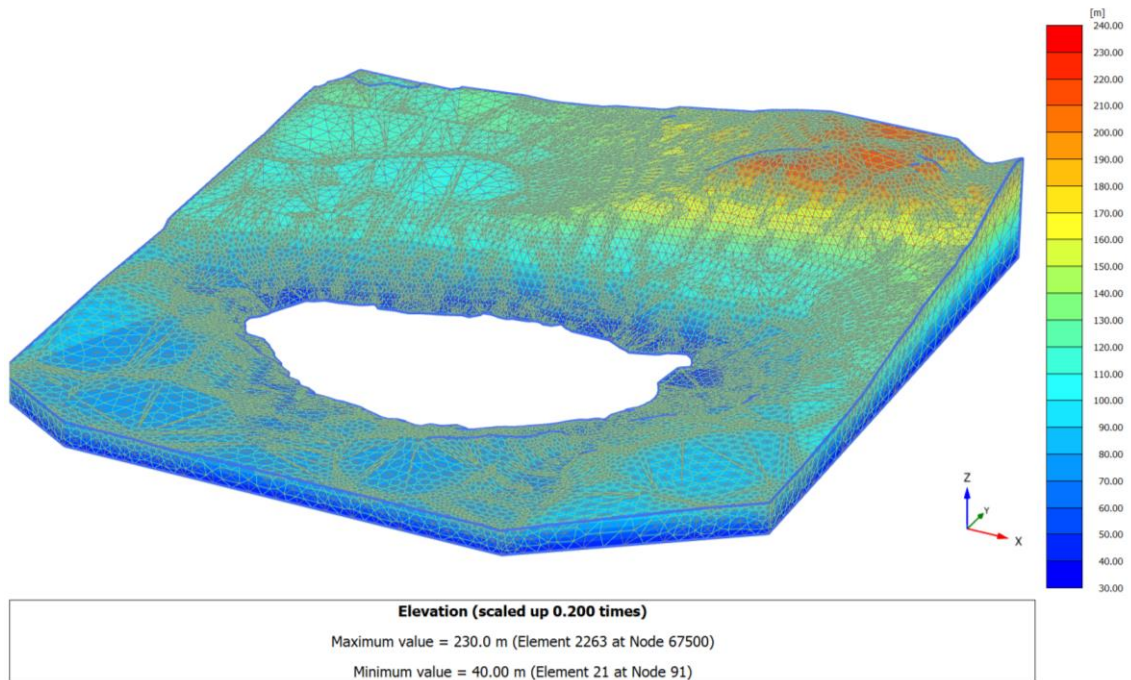
Fig IV.52: Deformation vs elevations mapping.

-Staged Construction (Calculations):

has been effectuated in two phases of calculation.

 - Initial phase: using Gravity loading calculation type.

 - First phase: the safety factor of the first phase.
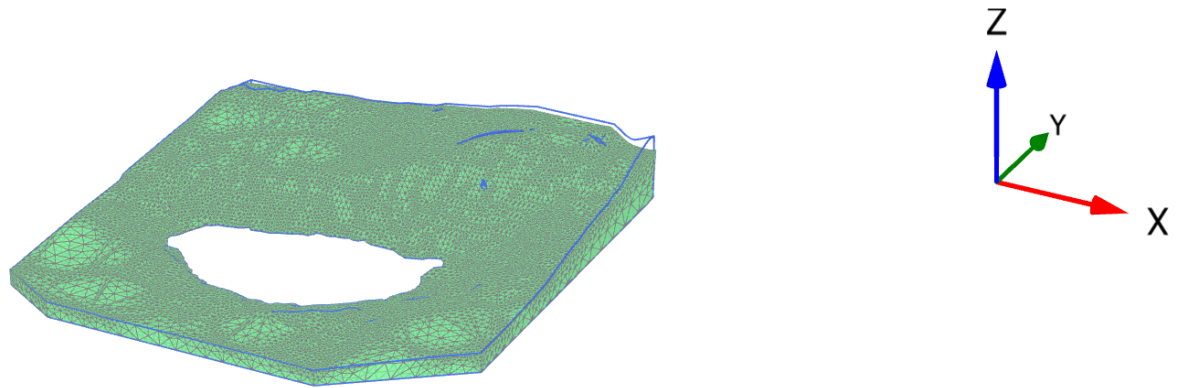
Deformed mesh |u| (scaled up 100 times)

Maximum value = 0.4530 m (at Node 5342)

Fig IV.53: Deformation mesh (Node 5342).
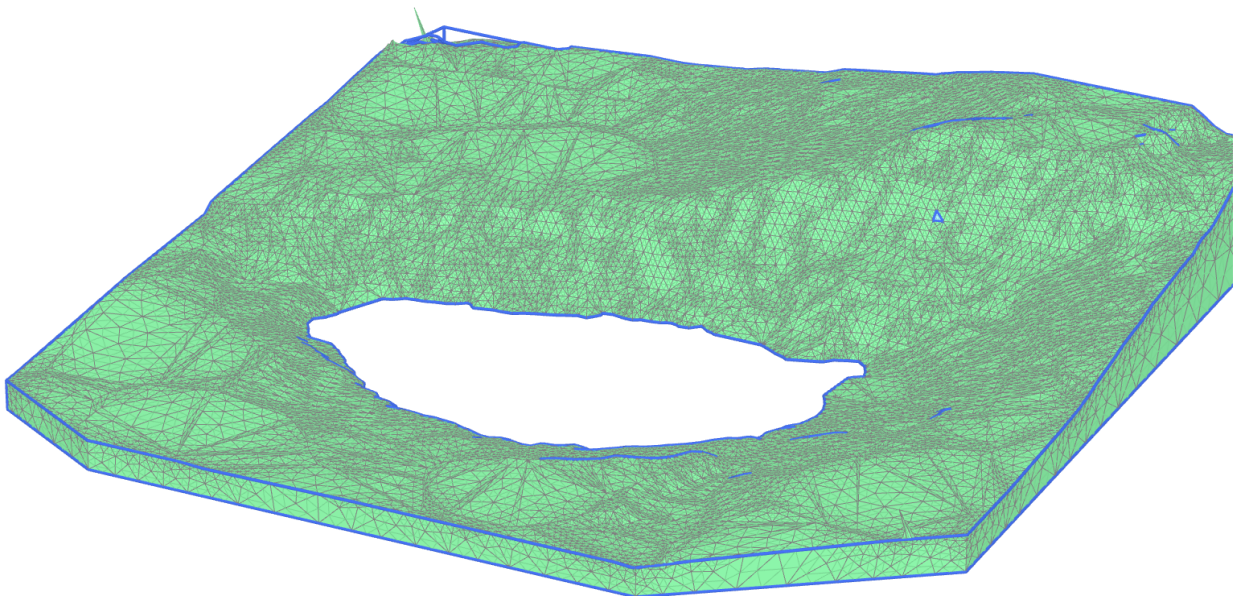
Deformed mesh |u| (scaled up 50.0 times)

Maximum value = 1.127 m (at Node 17708)

Fig IV.54: Deformation mesh (Node 17708).
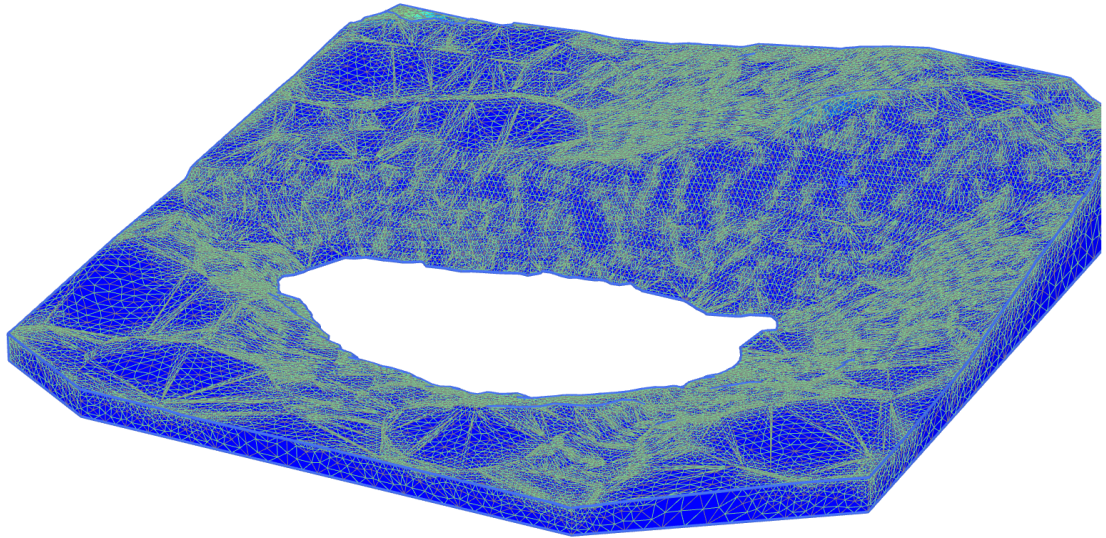
Total displacements |u| (scaled up 50.0 times)
Maximum value = 1.127 m (Element 57829 at Node 17708)

Fig IV.55: Toal displacement |u|.
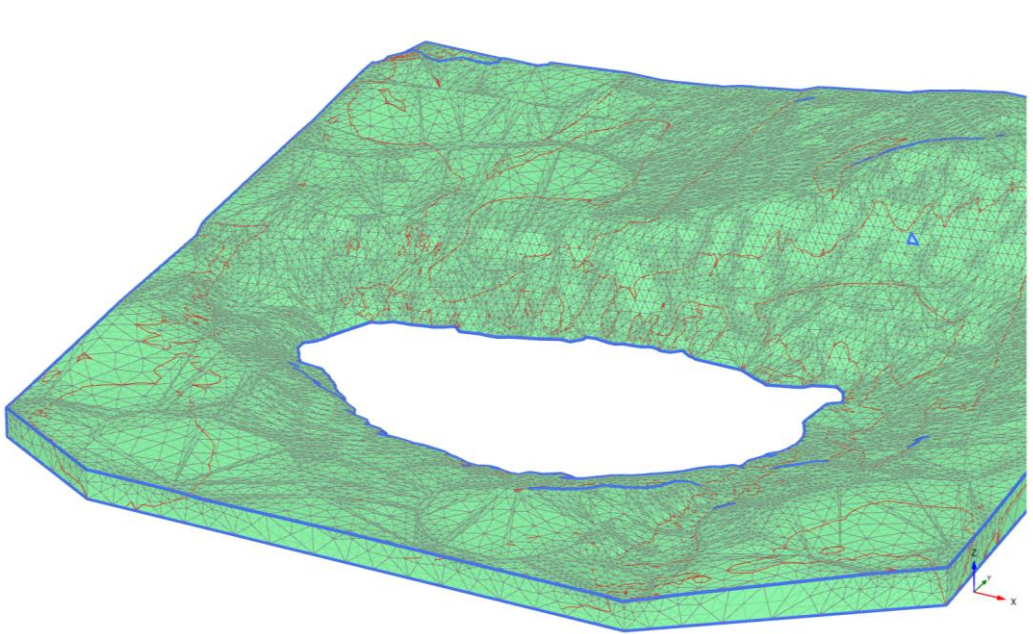
Total displacements u_z (scaled up 50.0 times)
Maximum value = 0.8540 m (Element 57829 at Node 17708)
Minimum value = -0.5876 m (Element 31592 at Node 52463)

Fig IV.56: Toal displacement |uz|.
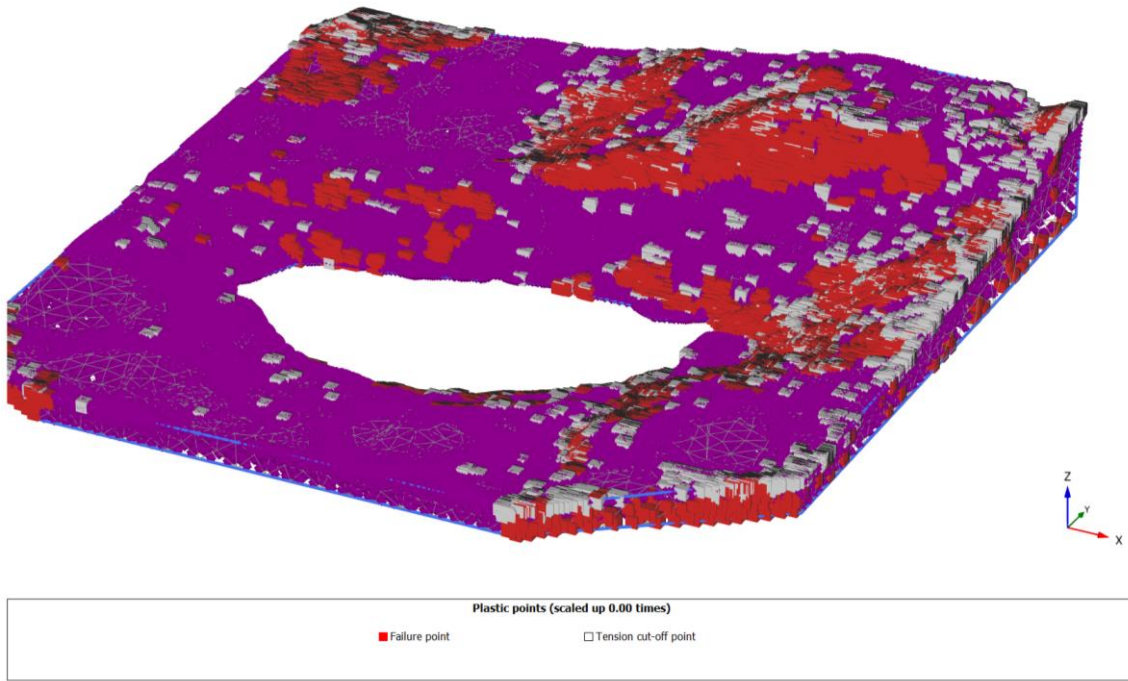
Fig IV.57: Plastic point.

-Cross section creating:
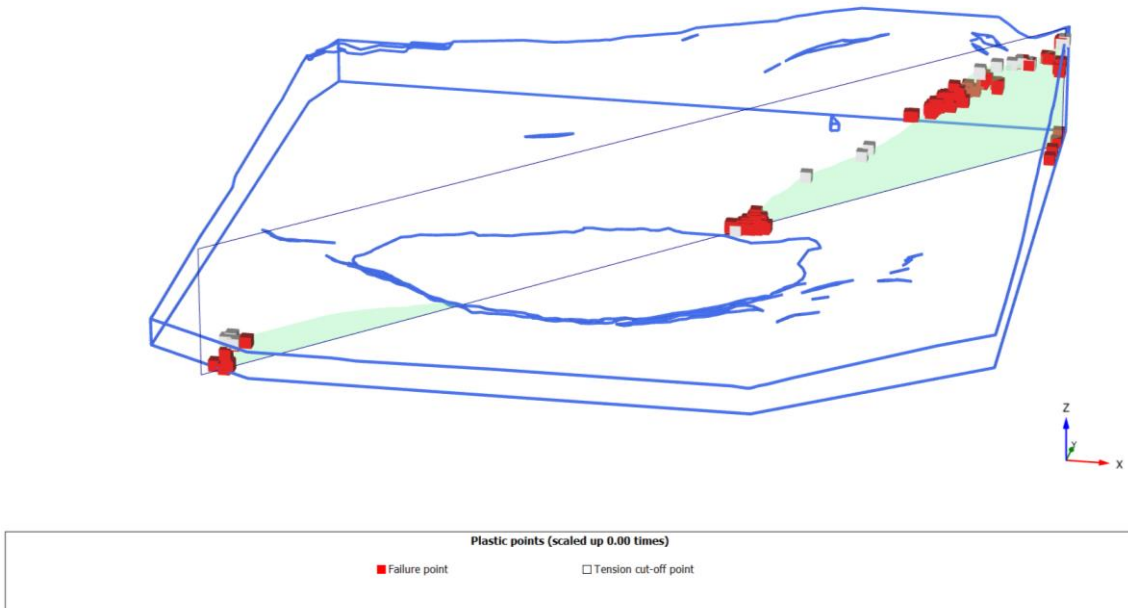
Fig IV.58: Cross section creating.

- **Curve**: factor of safety is critical in gravity equilibrium analysis as shown on (Fig IV.59) change dramatically in different steps over the total surface of the open pit mine in Kef essnoun.
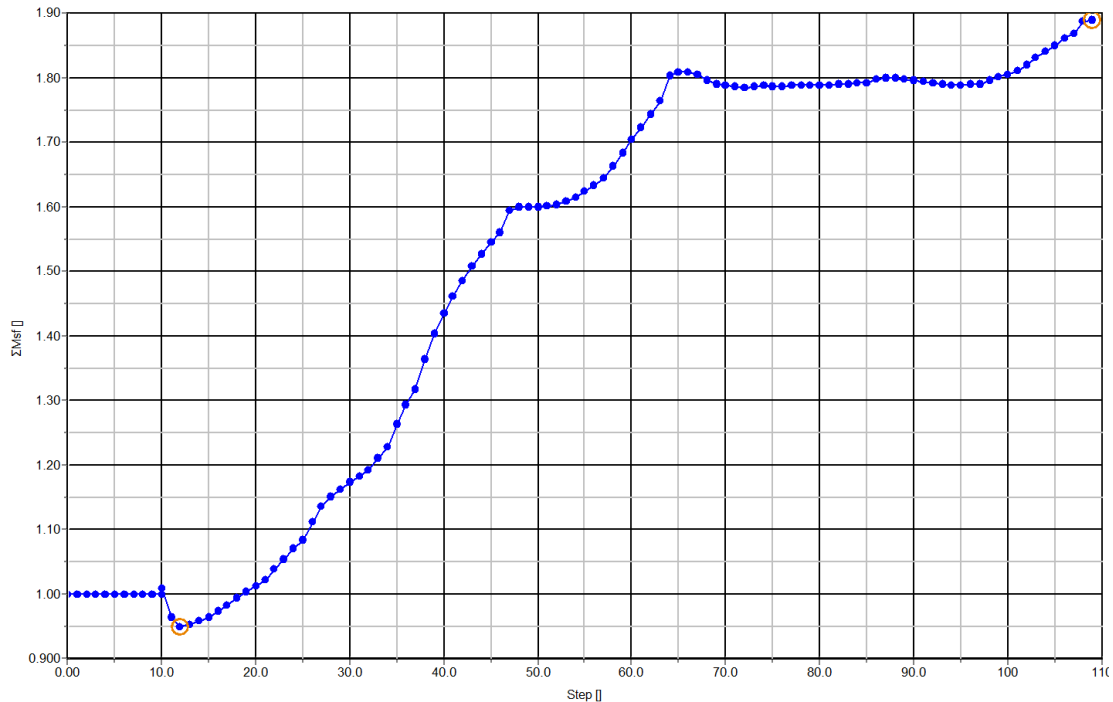
Fig IV.59: Curve represent the change of Fs.

Conclusion

The geotechnical modeling conducted at the Kef Essnoun mine provides valuable insights into the behavior of soil and rock masses, crucial for ensuring the safety and stability of civil engineering structures within the mining environment. Through meticulous analysis and simulations, several key results and values were obtained.

Material properties were meticulously defined for different layers within the mine, such as the limestone, marl, and phosphate layers. For instance, the saturated unit weight (γsat) of the limestone layer was found to be 27.0 kN/m³, with a corresponding Young's modulus (E') of 5.600E6 kN/m². Similar properties were identified for the marl and phosphate layers.

Staged construction calculations were performed in five phases, each contributing to the understanding of stability under various conditions. These phases encompassed gravity loading, plastic phase calculation, and rainfall-induced scenarios. Throughout these stages, safety factors and deformation characteristics were carefully monitored and analyzed.

The results and discussion highlighted significant findings from each phase of the analysis. Initial phases indicated marginal stability, with subsequent phases showing temporary improvements in safety factors and periods of stabilization. Rainfall-induced fluctuations in stability were observed, with notable drops in safety factors indicating potential instabilities.

The curve analysis further elucidated the trends observed during the modeling process. Factor of Safety (Fs) curves depicted initial stability, temporary improvements, and subsequent fluctuations induced by rainfall. Displacement-time curves revealed gradual increases in displacement during stable phases and sudden jumps during potential failure events.

Additionally, the analysis of safety factors revealed crucial insights into the stability of the mine structure. Initial stability conditions were characterized by safety factors close to 1.0, indicating marginal stability. Temporary improvements during certain phases were marked by safety factors reaching peaks of around 1.2, suggesting enhanced stability. However, subsequent phases showed fluctuations in safety factors, with some periods indicating drops below 1.0, signifying potential instability and the need for remedial measures.

Overall, numerical modeling using Plaxis 3d provide deep analysis, prediction and visualization in 3d of structures and materials. It has been concluded that the safety factor of the open pit mine is highly affected by the density, lineament sets (joints and beddings…) and rainfall. It is recommended that efficiently using the combination of the new developed softwares features allowing facilities of exporting and importing files between each other in the used software. It allows sophisticated and very close results that meet the requirement of open pit mining.

The integration of these results and values into the geotechnical modeling framework provides a comprehensive understanding of stability trends, material behavior, and deformation characteristics within the Kef Essnoun mine. These insights are crucial for informed decision-making regarding engineering design and safety measures within the mining environment

General conclusion

This study investigated into the slope bench stability of the north slope at the Kef Essnoun open-pit mine, focusing on geological, geotechnical, and especially hydrological impact factors. The research entailed a thorough investigation, including descriptive geological cross-sections, tectonic and discontinuity surveys, rock mass classification and characterization, and the examination of water effects resulting from rainfall.

Theoretical insights underscored the paramount importance of understanding and predicting slope stability to mitigate risks associated with ground movements, particularly in large-scale mining operations. Djebel Onk mining complex, a vital asset for SOMIPHOS, operates within a region characterized by significant geological, hydrological, and climatic features.

From a point of geological view, the area comprises phosphate deposits from the Upper Thanetian age, structured into asymmetric anticlines and synclines, with notable faults and complex stratigraphy spanning from the Upper Cretaceous to Quaternary periods. Hydrologically, various aquifer complexes, particularly the Eocene limestone, support mining operations. Climatically, Djebel Onk experiences a subarid to arid climate with cold winters, hot summers, and low annual precipitation, averaging 300 mm, impacting mining activities and necessitating meticulous water management. These features collectively shape the operational and environmental strategies of the Djebel Onk mining complex.

To comprehend slope stability and avert failure, a comprehensive approach involving field investigations, laboratory research, and detailed site analysis is imperative. The study of the north-western slope of Kef Essnoun entailed determining the physico-mechanical properties of the rock mass, critical for designing effective stabilization measures.

Geomechanical classifications such as RQD, RMR, SMR, and GSI provided insights into the quality and stability of the rock mass. RQD values indicated good quality for Danian-Montian Limestone (84-85%) and fair quality for Ypresian Limestone (70-72%) and phosphates (73%), while marls were of poor quality (45%). RMR values showcased good quality for Danian-Montian Limestone (71) and Ypresian Limestone (67), medium quality for phosphates (64), and poor quality for marls (39). SMR classification underscored the marly interface as a probable cause of instability, with marls receiving the lowest score (35.4). The GSI index ranged from 70 to 80 for limestones, suggesting a reduction in rock mass strength under different geological conditions.

The findings underscored the significance of detailed geomechanical analysis for predicting rock behavior and ensuring safe mining operations, necessitating specific interventions to stabilize the slope and prevent future failures.

Moreover, geological and geotechnical modeling of the Kef Essnoun open pit mine provided critical insights into the interactions between geological structures, hydrological conditions, and slope stability. Utilizing advanced tools such as Dips 7.0 for discontinuity analysis and ArcGIS for detailed mapping, the study offered a comprehensive understanding of the geotechnical behavior at the site.

Hydrological analysis identified significant interactions between geological structures and water inflow, indicating potential runoff and percolation issues. Various streams and drainage patterns emphasized the importance of considering hydrological factors in slope stabilization measures. Combining information from both hill shade and watershed maps provides a comprehensive understanding of the mining site's topography and hydrology. This integration helps in designing a mining plan that optimizes resource extraction while minimizing risks related to slope stability, water management, and environmental impacts.

The stability of the open pit slope benches in the large phosphate mine in the Kef Essnoun area is mainly controlled by their orientation in relation to the geological structures of the two main discontinuity groups. It is highly recommended that the design of the slopes should therefore be highly dependent on the orientation of the pit slopes relative to these structural features, while also taking into account the orientations of the main stream and branch patterns in the entire basin of the Kef Essnoun area is critical. Although there is no piezometric data indicating the presence of significant pore pressures within the open pit walls, numerical simulations show that rainfall significantly reduces safety factors in many scenarios throughout the large open pit mine.

In summary, the integration of geological, geotechnical, and hydrological data offers a comprehensive understanding of slope stability at the Kef Essnoun mine. Continuous monitoring and targeted risk mitigation measures are crucial to ensuring safety and operational sustainability within the mining environment. The geotechnical modeling framework provided valuable insights into material behavior, stability trends, and deformation characteristics, facilitating informed decision-making regarding engineering design and safety measures within the mining environment.

References

References

Abu-Ali, R., & El-Kammar, A. (2024). Other Fuel and Strategic Resources in North Africa: Oil Shale and Rare Earth Elements. In *The Geology of North Africa* (pp. 517-527). Cham: Springer International Publishing.

Akpan, A. E., Ekwok, S. E., & Ebong, E. D. (2016). Seasonal reversals in groundwater flow direction and its role in the recurrent Agwagune landslide problem: a geophysical and geological appraisal. *Environmental Earth Sciences*, *75*, 1-17.

Aksoy, H. Ü. S. E. Y. İ. N., & Ercanoglu, M. U. R. A. T. (2007). Fuzzified kinematic analysis of discontinuity-controlled rock slope instabilities. *Engineering Geology*, *89*(3-4), 206-219.

Amarasinghe, M. P., Kulathilaka, S. A. S., Robert, D. J., Zhou, A., & Jayathissa, H. A. G. (2024). Risk assessment and management of rainfall-induced landslides in tropical regions: A review. *Natural Hazards*, *120*(3), 2179-2231.

Azarafza, M., Akgün, H., Ghazifard, A., Asghari-Kaljahi, E., Rahnamarad, J., & Derakhshani, R. (2021). Discontinuous rock slope stability analysis by limit equilibrium approaches–a review. *International Journal of Digital Earth*, *14*(12), 1918-1941.

Benabid, I. (2024). Shallow landslides of the Souk Ahras region: influence of soil geotechnical properties and rainfall (Doctoral dissertation, University Echahid Cheikh Larbi-Tebessi-Tebessa).

Bezzi, N., Aifa, T., Hamoudi, S., & Merabet, D. (2012). Trace elements of Kef Es Sennoun natural Phosphate (Djebel Onk, Algeria) and how they affect the various Mineralurgic modes of treatment. *Procedia Engineering*, *42*, 1915-1927.

Bhaduri, A., & Bhaduri, A. (2018). Creep and Stress Rupture. *Mechanical Properties and Working of Metals and Alloys*, 257-316.

Biswakarma, P., Joshi, V., Puniya, M. K., & Rafique, M. F. (2023). Analyses of Different Slope Failures along the Road Sections of West Sikkim, India using Rock Mass Classification and Kinematic Analysis Approach. *Journal of the Geological Society of India*, *99*(7), 975-985.

Boucif, R., Filippov, L. O., Maza, M., Benabdeslam, N., Foucaud, Y., Marin, J., ... & Bouzidi, N. (2024). Optimizing liberation of phosphate ore through high voltage pulse fragmentation. *Powder Technology*, 119549.

Brideau, M. A., & Roberts, N. J. (2022). Landslides in bedrock. In *Landslide Hazards, Risks, and Disasters* (pp. 43-97). Elsevier.

Brideau, M. A., & Roberts, N. J. (2015). Mass movement in bedrock. In *Landslide Hazards, Risks, and Disasters* (pp. 43-90). Academic Press.

Cageao, P. P. (2014). *Fluid-particle interaction in geophysical flows: debris flows* (Doctoral dissertation, University of Nottingham).

Cao, B., Wang, S., Bai, R., Zhao, B., Li, Q., Lv, M., & Liu, G. (2023). Boundary optimization of inclined coal seam open-pit mine based on the ISSA–LSSVR coal price prediction method. Scientific Reports, 13(1), 7527.

Chen, J., Wang, L., & Che, A. (2022, August). Failure Mechanism Analysis of Loess Slope Under the Coupling Effect of Rainfall and Earthquake Using Shaking Table Test. In Conference on Performance-based Design in Earthquake. Geotechnical Engineering (pp. 1289-1296). Cham: Springer International Publishing.

Corominas, J., Mavrouli, O., & Ruiz-Carulla, R. (2017). Rockfall occurrence and fragmentation. In *Advancing Culture of Living with Landslides: Volume 1 ISDR-ICL Sendai Partnerships 2015-2025* (pp. 75-97). Springer International Publishing.

Cui, H., Medina, V., Hürlimann, M., & Ji, J. (2024). Fast physically-based probabilistic modelling of rainfall-induced shallow landslide susceptibility at the regional scale considering geotechnical uncertainties and different hydrological conditions. *Computers and Geotechnics*, *172*, 106400.

Coussot, P. (2017). *Mudflow rheology and dynamics*. Routledge.

Das, P., Patwa, D., & Bharat, T. V. (2022). Influencing factors on the simulation of rainfall-induced landslide prediction based on case study. Bulletin of Engineering Geology and the Environment, 81(5), 194.

Dass Amiour, M., Mezghache, H., & Elouadi, B. (2013). The use of three physico-chemical methods in the study of the organic matter associated with the sedimentary phosphorites in Djebel Onk Basin, Algeria. *Arabian Journal of Geosciences*, *6*, 309-319.

De Blasio, F. V. (2011). *Introduction to the physics of landslides: lecture notes on the dynamics of mass wasting*. Springer Science & Business Media.

Deere, D. (1988). The rock quality designation (RQD) index in practice. In *Rock classification systems for engineering purposes*. ASTM International.

Deere, D. U., & Deere, D. W. (1989). *Rock quality designation (RQD) after twenty years* (No. 89). US Army Engineer Waterways Experiment Station.

d'Organisation, C. Le 1er Colloque International sur la géologie de la Chaîne des Maghrébides et des régions voisines (CIGCM 2016) Du 4 au 6 décembre 2016. Sétif, Algérie.

Duncan, J.M. (1996). Soil slope stability analysis. In Turner & Schuster (eds.), Landslides: Investigation and Mitigation (Special Report 247). National Academy Press, Washington, D.C., 337-371.

Eberhardt, E. (2003). Rock slope stability analysis–utilization of advanced numerical techniques. *Earth and Ocean sciences at UBC*, *41*.

Erik Eberhardt 2013. University of British Columbia

Fantone, I., Grieco, G., & Cavallo, A. (2015). Evaluation of heterogeneous sulfide: rich mine tailings as secondary raw materials: a case study in the Mirdita District (Northern Albania).

Feng, K., Huang, D., & Wang, G. (2021). Two-layer material point method for modeling soil–water interaction in unsaturated soils and rainfall-induced slope failure. *Acta Geotechnica*, *16*(8), 2529-2551.

FROM THE DJEBEL ONK DEPOSITS. *Geologica Macedonica*, *37*(2), 99-109.

Gallage, C., Abeykoon, T., & Uchimura, T. (2021). Instrumented model slopes to investigate the effects of slope inclination on rainfall-induced landslides. Soils and Foundations, 61(1), 160-174.

Gischig, V., Amann, F., Moore, J. R., Loew, S., Eisenbeiss, H., & Stempfhuber, W. (2011). Composite rock slope kinematics at the current Randa instability, Switzerland, based on remote sensing and numerical modeling. *Engineering Geology*, *118*(1-2), 37-53.

Graba, Z., Hamoudi, S., Bekka, D., Bezzi, N., & Boukherroub, R. (2015). Influence of adsorption parameters of basic red dye 46 by the rough and treated Algerian natural phosphates. *Journal of Industrial and Engineering Chemistry*, *25*, 229-238.-

G. P. PRIAN, Ph. CORTIEL1993.

Gu, D., & Huang, D. (2016). A complex rock topple-rock slide failure of an anaclinal rock slope in the Wu Gorge, Yangtze River, China. *Engineering Geology*, *208*, 165-180.

Guo, Y., Liu, H., Sun, Y., & Ren, Y. (2024). Virtual human pose estimation in a fire education system for children with autism spectrum disorders. *Multimedia Systems*, *30*(2), 1-15.

Hamad, A., Hadji, R., Bâali, F., Houda, B., Redhaounia, B., Zighmi, K., ... & Hamed, Y. (2018). Conceptual model for karstic aquifers by combined analysis of GIS, chemical, thermal, and isotopic tools in Tuniso-Algerian transboundary basin. *Arabian Journal of Geosciences*, *11*(15), 409.

Harris, C., Kern-Luetschg, M., Christiansen, H. H., & Smith, F. (2011). The role of interannual climate variability in controlling solifluction processes, Endalen, Svalbard. *Permafrost and Periglacial Processes*, *22*(3), 239-253.

Ho, T. C., Pradhan, B., Pham, B. T., Nhu, V. H., & Revhaug, I. (2016). GIS-based modeling of rainfall-induced landslides using data mining-based functional trees classifier with AdaBoost, Bagging, and MultiBoost ensemble frameworks. *Environmental Earth Sciences*, *75*, 1-22.

Hoek, E. & Bray, J.W. (1991). Rock Slope Engineering. Elsevier Science Publishing: New York, 358 pp.

Hoek, E., Marinos, P., & Benissi, M. (1998). Applicability of the Geological Strength Index (GSI) classification for very weak and sheared rock masses. The case of the Athens Schist Formation. *Bulletin of Engineering Geology and the Environment*, *57*, 151-160.

Huang, D., Gu, D. M., Song, Y. X., Cen, D. F., & Zeng, B. (2018). Towards a complete understanding of the triggering mechanism of a large reactivated landslide in the Three Gorges Reservoir. *Engineering Geology*, *238*, 36-51.

Huang, R. (2012). Mechanisms of large-scale landslides in China. *Bulletin of Engineering Geology and the Environment*, *71*, 161-170.

Hudson, J.A. & Harrison, J.P. (1997). Engineering Rock Mechanics: an Introduction to the Principles. Elsevier Science: Oxford, 444 pp.

Hungr, O., & Amann, F. (2011). Limit equilibrium of asymmetric laterally constrained rockslides. *International Journal of Rock Mechanics and Mining Sciences*, *48*(5), 748-758.

Hungr, O., Leroueil, S., & Picarelli, L. (2014). The Varnes classification of landslide types, an update. *Landslides*, *11*, 167-194.

Jarna, A., Bang-Kittilsen, A., Haase, C., Henderson, I. H. C., Høgaas, F., Iversen, S., & Seither, A. (2015). 3-Dimensional geological mapping and modeling activities at the geological survey of Norway. *The International Archives of the Photogrammetry, Remote Sensing and Spatial Information Sciences*, *40*, 11-16.

Jason Goetz 2015: Mapping landslide hazard on Vancouver Island.

Kang, H. S., & Kim, Y. T. (2017). Rheological properties of loose sands subjected to upward flow. *Canadian Geotechnical Journal*, *54*(5), 664-673.

Kechiched, R., Laouar, R., Bruguier, O., Salmi-Laouar, S., Kocsis, L., Bosch, D., ... & Larit, H. (2018). Glauconite-bearing sedimentary phosphorites from the Tébessa region (eastern Algeria): Evidence of REE enrichment and geochemical constraints on their origin. Journal of African Earth Sciences, 145, 190-200.

Koch, K. J. (2024). *Midwest Bedrock: The Search for Nature's Soul in America's Heartland*. Indiana University Press.

KS Kalenchuk - 2010 - library-archives.canada.ca.

L. R. (2014). Ecological mitigation of hillslope instability: ten key issues facing researchers and practitioners. *Plant and Soil*, *377*, 1-23.

Lann, T., Bao, H., Lan, H., Zheng, H., & Yan, C. (2024). Hydro-mechanical effects of vegetation on slope stability: A review. *Science of the Total Environment*, 171691.

Laubscher, D. H. (1990). A geomechanics classification system for the rating of rock mass in mine design. *Journal of the Southern African Institute of Mining and Metallurgy*, *90*(10), 257-273.

Lechner, A. M., Baumgartl, T., Matthew, P., & Glenn, V. (2016). The impact of underground longwall mining on prime agricultural land: a review and research agenda. *Land Degradation & Development*, *27*(6), 1650-1663.

Lee, D. T. T. (2016). Effect of rainfall on tree stability (Doctoral dissertation).

Lee, J. G., Selvakumar, A., Alvi, K., Riverson, J., Zhen, J. X., Shoemaker, L., & Lai, F. H. (2012). A -watershed-scale design optimization model for stormwater best management practices. *Environmental Modelling & Software*, *37*, 6-18.

Leslie Smith–Guelph, Ontario, Canada, 2021 Hydrogeology and Mineral Resource Development.

Li, Q., Wang, Y., Li, X., & Gong, B. (2024). Rainfall–Mining Coupling Effects on Slope Failure Mechanism and Evolution Process: A Case Study of Open-Pit to Underground Mining. *Water*, *16*(5), 740.

Lima, S. L., Blackwell, B. F., DeVault, T. L., & Fernández-Juricic, E. (2015). Animal reactions to oncoming vehicles: a conceptual review. *Biological Reviews*, *90*(1), 60-76.

Lu, W., Xiao, Z., Chen, Y., Sun, J., & Chen, F. (2024). Spatiotemporal Characteristics and Rainfall Thresholds of Geological Landslide Disasters in ASEAN Countries. Atmosphere, 15(5), 599.-Stefan Scheidler 2019Integration of Geological Structures into Regional-Scale Groundwater Models.

Liu, W., Agusdinata, D. B., & Myint, S. W. (2019). Spatiotemporal patterns of lithium mining and environmental degradation in the Atacama Salt Flat, Chile. *International Journal of Applied Earth Observation and Geoinformation*, *80*, 145-156.

Liu, G., Meng, H., Song, G., Bo, W., Zhao, P., Ning, B., & Xu, X. (2024). Numerical simulation of wedge failure of rock slopes using three-dimensional discontinuous deformation analysis. *Environmental Earth Sciences*, *83*(10), 310.

Makhlouf, A., Quaranta, G., & Kardache, R. (2019). Energy consumption and greenhouse gas emission assessment in the Algerian sector of fertilisers production with life cycle assessment. *International Journal of Global Warming*, *18*(1), 16-36.

Malla, Birasa, Dahal, B K (2022) Effect of Rainfall on Stability of Soil Slope.

Marinos, P., & Hoek, E. (2000, November). GSI: a geologically friendly tool for rock mass strength estimation. In *ISRM international symposium* (pp. ISRM-IS). ISRM.

Marndi, B. (2011). *Stability of slopes in iron ore mines* (Doctoral dissertation).

Mandal, S., & Maiti, R. (2015). *Semi-quantitative approaches for landslide assessment and prediction* (pp. 57-93). Singapore: Springer.

Mavrouli, O., Núñez-Andrés, M. A., Buill, F., Lantada, N., & Corominas, J. (2024). Correlation between rockfall frequency and overhang geometrical attributes. *Landslides*, 1-15.

Matsuoka, N. (2010). Solifluction and mudflow on a limestone periglacial slope in the Swiss Alps: 14 years of monitoring. *Permafrost and periglacial processes*, *21*(3), 219-240.

Miranda, T., Correia, A. G., Santos, M., Ribeiro e Sousa, L., & Cortez, P. (2011). New models for strength and deformability parameter calculation in rock masses using data-mining techniques. *International Journal of Geomechanics*, *11*(1), 44-58.

Nazimko, V., & Zakharova, L. (2017). Cluster behavior of the ground during its irreversible movement. *Acta geodynamica et geomaterialia*, *14*(188), 45-49.

Nettour, D., Chettibi, M., Bouhadja, A., & Bulut, G. (2018). Determination of physicochemical parameters of Djebel Onk phosphate flotation

Nichol, S. L. (2000). *Examination of toppling behaviour in large rock slopes using the UDEC computer code* (Doctoral dissertation, University of British Columbia).

Ogila, W. A. M. (2021). Analysis and assessment of slope instability along international mountainous road in North Africa. Natural hazards, 106(3), 2479-2517. ISO 690

Ornella, T. N., & Fan, Q. (2024). Fertilizer Production in Africa as a Way to Minimise Fertilizer Importation Cost. *Open Access Library Journal*, *11*(1), 1-13.

Ortigao, J. A. R., & Sayao, A. (Eds.). (2013). *Handbook of slope stabilisation*. Springer Science & Business Media.

Palmstrom, A., & Broch, E. (2006). Use and misuse of rock mass classification systems with particular reference to the Q-system. *Tunnelling and underground space technology*, *21*(6), 575-593.

Pan, Z., Connell, L. D., Camilleri, M., & Connelly, L. (2010). Effects of matrix moisture on gas diffusion and flow in coal. *Fuel*, *89*(11), 3207-3217.

Pánek, T. (2020). Landslides and related sediments. *Encyclopedia of Geology,* 708-728.

Pathan, S. M., Pathan, A. G., Siddiqui, F. I., Memon, M. B., & Soomro, M. H. A. A. (2022). Open pit slope stability analysis in soft rock formations at Thar Coalfield Pakistan. *Archives of Mining Sciences*, *67*(3).

Qiao, P., Wang, S., Li, J., Zhao, Q., Wei, Y., Lei, M., ... & Zhang, Z. (2023). Process, influencing factors, and simulation of the lateral transport of heavy metals in surface runoff in a mining area driven by rainfall: A review. Science of the Total Environment, *857*, 159119.

Raghuvanshi, T. K. (2019). Plane failure in rock slopes–A review on stability analysis techniques. *Journal of King Saud University-Science*, *31*(1), 101-109.

Raghuvanshi, T. K. (2019). Plane failure in rock slopes–A review on stability analysis techniques. *Journal of King Saud University-Science*, *31*(1), 101-109.

Roccati, A., Paliaga, G., Luino, F., Faccini, F., & Turconi, L. (2020). Rainfall Threshold for shallow landslides initiation and analysis of long-term rainfall trends in a Mediterranean area. *Atmosphere*, *11*(12), 1367.

ROMANA, M. R. (1993). A Geomechanical classification for slopes: slope mass rating. In *Rock testing and site characterization* (pp. 575-600). Pergamon.

Romana, M. (1991, September).SMR classification. In *ISRM Congress* (pp. ISRM-7CONGRESS). ISRM.

RK, U., Singh, R., Ahmad, M., & TN, S. (2011). Stability analysis of cut slopes using continuous slope mass rating and kinematic analysis in Rudraprayag district, Uttarakhand. *Geomaterials*, *2011*.

R. RAOUDSEP, 1978.

Sari, M. (2019). Stability analysis of cut slopes using empirical, kinematical, numerical and limit equilibrium methods: case of old Jeddah–Mecca road (Saudi Arabia). *Environmental Earth Sciences*, *78*(21), 621.

SB Hecht, A Cockburn - 2010 - FCF Earney, JE Green - Critical Reviews in Environmental Science 1977 - Taylor & Francis.

Sengani, Fhatuwani &Mulenga, François 2020 Application of Limit Equilibrium Analysis and Numerical Modeling in a Case of Slope Instability

Shao, X., Xu, C., Li, L., Yang, Z., Yao, X., Shao, B., ... & Xu, X. (2024). Spatial analysis and hazard assessment of Large-scale ancient landslides around the reservoir area of Wudongde Hydropower Station, China. *Natural Hazards*, *120*(1), 87-105.

Shibkov, A. A., Gasanov, M. F., Zheltov, M. A., Zolotov, A. E., & Ivolgin, V. I. (2016). Intermittent plasticity associated with the spatio-temporal dynamics of deformation bands during creep tests in an AlMg polycrystal. *International Journal of Plasticity*, *86*, 37-55.

Sidle, R. C., & Bogaard, T. A. (2016). Dynamic earth system and ecological controls of rainfall-initiated landslides. *Earth-science reviews*, *159*, 275-291.

Smith, J., & Doe, A. (2018). Modern Mining Techniques. 3rd ed. Mining Publications.

Smith, J., & Doe, A. (2018). Rock Mechanics and Slope Stability. 2nd ed. Geotechnical Publishing House.

Smith, J. V., & Arnhardt, C. (2016). Distinguishing between single and double plane sliding of tetrahedral wedges using the circle method. *Engineering geology*, *211*, 98-101.

Stokes, A., Douglas, G. B., Fourcaud, T., Giadrossich, F., Gillies, C., Hubble, T., ... & Walker,

Tahri, T., Narsis, S., Souici, Z. C., Bezzi, N., Sekiou, O., Trirat, T., ... & Bellucci, S. (2023). MINERALOGICAL AND CHEMICAL CHARACTERISTICS OF PHOSPHATES **Tien Bui, D., Take, W. A., & Beddoe, R. A. (2014).** Base liquefaction: a mechanism for shear-induced failure of loose granular slopes. *Canadian Geotechnical Journal*, *51*(5), 496-507.

Utili, S., & Crosta, G. B. (2015). Analysis tools for mass movement assessment. In *Landslide Hazards, Risks, and Disasters* (pp. 479-503). Elsevier.

Vick, L. M., Böhme, M., Rouyet, L., Bergh, S. G., Corner, G. D., & Lauknes, T. R. (2020). Structurally controlled rock slope deformation in northern Norway. *Landslides*, *17*, 1745-1776.

Visse, L. D. (1952). Genèse des gîtes phosphatés du Sud-Est algéro-tunisien. *XIX^< eme> Congr. Intern. Alger, 1^< ere> serie, 1952*, *27*.

Vuille, M., Carey, M., Huggel, C., Buytaert, W., Rabatel, A., Jacobsen, D., ... & Sicart, J. E. (2018). Rapid decline of snow and ice in the tropical Andes–Impacts, uncertainties and challenges ahead. *Earth-science reviews*, *176*, 195-213.

Wang, M., Liu, K., Yang, G., & Xie, J. (2017). Three-dimensional slope stability analysis using laser scanning and numerical simulation. *Geomatics, Natural Hazards and Risk*, *8*(2), 997-1011.

Wang, J., & Vanapalli, S. (2024). A framework for estimating the matric suction in unsaturated soils using multiple artificial intelligence techniques. International Journal for Numerical and Analytical Methods in Geomechanics.

Wei, K., Liu, Y., Wang, A., Fang, Q., & Wang, C. Experimental Study on the Dynamic Response and Pore-Fracture Structure Evolution of Deep Coal Reservoirs Under Stress Release. Available at SSRN 4791468.

Wolter, A., Stead, D., & Clague, J. J. (2014). A morphologic characterisation of the 1963 Vajont Slide, Italy, using long-range terrestrial photogrammetry. *Geomorphology*, *206*, 147-164.

Yang, K. H., Uzuoka, R., Lin, G. L., & Nakai, Y. (2017). Coupled hydro-mechanical analysis of two unstable unsaturated slopes subject to rainfall infiltration. *Engineering Geology*, *216*, 13-30.

Yang, H., & Adler, R. F. (2008). Predicting global landslide spatiotemporal distribution: integrating landslide susceptibility zoning techniques and real-time satellite rainfall estimates. International Journal of Sediment Research, 23(3), 249-257.

Zhao, B., Su, L., Wang, Y., Li, W., & Wang, L. (2023). Insights into some large-scale landslides in southeastern margin of Qinghai-Tibet Plateau. *Journal of Rock Mechanics and Geotechnical Engineering*, *15*(8), 1960-1985.

Zhao, Y., Xu, M., Guo, J., Zhang, Q., Zhao, H., Kang, X., & Xia, Q. (2015). Accumulation characteristics, mechanism, and identification of an ancient translational landslide in China. *Landslides*, *12*, 1119-1130.

Zhang, L., Li, J., Li, X., Zhang, J., & Zhu, H. (2016). Rainfall-induced soil slope failure. *Florida: Taylor&Francis Group*.

范付松. (2015). *TOPPLING FAILURE AND ROCK BURST ANALYSIS USING THE IMPROVED NMM AND DDA SIMULATION TECHNIQUES* (Doctoral dissertation, 九州大学).

Webography

(website1) data:image/png;base64

(website 2) https://www.nbcnews.com/news/world/massive-mine-collapse-china-missing-rcna71920

(website 3) https://www.usgs.gov/media/images/creep

(website 4) https://besafenet.net/hazards/landslides/

(website 5) https://www.scribd.com/document/325024389/Types-of-Landslides-docx

(website 6) https://www.researchgate.net/figure/Modes-of-failure-in-rock-slopes-after-Hoek-and-Bray-1-_a-Plane-b-wedge-c_fig1_264086457

(website 7) https://www.researchgate.net/figure/Schematic-diagrams-of-main-toppling-failure-modes-a-flexural-b-blocky-and-c_fig1_345674302

Appendix

Degree	Term	Evaluation Criteria	Examples
R6	Extremely Resistant	The geologist's hammer does not chip the sample.	Basalt, diabase, gneiss, granite, fresh quartzite
R5	Very Resistant	The sample must receive numerous blows from the geologist's hammer before fracturing.	Amphibolite, gneiss, basalt, gabbro, gneiss, granodiorite, limestone, marble, rhyolite, tuff
R4	Resistant	The sample must receive more than one blow from the geologist's hammer before fracturing.	Limestone, marble, schist, fine sandstone, metamorphic schist, sedimentary schist, fine sandstone
R3	Moderately Resistant	The sample cannot be scratched or peeled with a knife but can be fractured with a single blow from the geologist's hammer.	Argillite, coal, concrete, metamorphic schist, sedimentary schist, fine sandstone
R2	Friable	The sample can be easily flaked with a knife; making a mark.	Chalk, halite, potash
R1	Very Friable	The sample crumbles if struck with a sharp blow from the point of a geologist's hammer; it can be flaked with a knife.	Extremely altered/degraded rock
R0	Extremely Friable	The sample is marked under the pressure of a fingernail.	

Table: rock strength estimation criterion.

Table:

Term	Description	degree
Fresh	No visible sign of rock material weathering; perhaps slight discolouration on major discontinuity surfaces.	I
Slightly weathered	Discolouration indicates weathering of rock material and discontinuity surfaces. All rock material may be discoloured by weathering.	II
Moderately weathered	Less than half of the rock material is decomposed or disintegrated to a soil. Fresh or discoloured rock is present either as a continuous framework or as core stones.	III
Highly weathered	More than half of the rock material is decomposed or disintegrated to a soil. Fresh or discoloured rock is present either as a discontinuous framework or as core stones.	IV
Completely weathered	All rock material is decomposed and/or disintegrated to soil. The original mass structure is still largely intact.	V
Residual soil	All rock material is converted to soil. The mass structure and material fabric is destroyed. There is a large change in volume, but the soil has not been significantly transported.	VI

Quantification of weathering.

	Type of failure	Auxiliary angles		Very favorable	Favorable	Normal	Unfavorable	Very unfavorable
Paralellism	P	A=	$\|\alpha_j - \alpha_s\|$					
	T		$\|\alpha_j - \alpha_s - 180\|$	$> 30°$	$30 - 20°$	$20 - 10°$	$10 - 5°$	$< 5°$
	W		$\|\alpha_i - \alpha_s\|$					
	P/T/W	F_1		0.15	0.40	0.70	0.85	1.00
Dip angle	P/W	B=	β_j or β_i	$< 20°$	$20 - 30°$	$30 - 35°$	$35 - 45°$	$> 45°$
	P/W	F_2		0.15	0.40	0.70	0.85	1.00
	T					1.00		
Dip relationship	P	C=	$\beta_j - \beta_s$	$> 10°$	$10 - 0°$	$0°$	$0 - (-10)°$	$< (-10)°$
	W		$\beta_i - \beta_s$					
	T		$\beta_j + \beta_s$	$< 110°$	$110 - 120°$	$> 120°$	-	-
	P/T/W	F_3		0	-6	-25	-50	-60

Excavation method (F_4)			
Natural slope	+15	Blasting or mechanical	0
Presplitting	+10	Deficient blasting	-8
Smooth blasting	+8		

Table: Slope Mass Rating systeme.

Table : Classification RMR .

	PARAMETER		Range of values						
1	Strength of intact rock material	Point-load strength index:					For this low range - uniaxial compressive test is preferred		
		Point Load	> 10 M Pa	4 - 10 M Pa	2 - 4 M Pa	1 -2 M Pa	-		
		Uniaxial comp. strength	> 250 MPa	100-250 MPa	50-100 Mpa	25 - 50 MPa	10-25	3-10	<3 (unit M Pa)
		Rating	15	12	7	4	2	1	0
2	RQD Rock Quality Designation		90 - 100 %	75 - 90 %	50 - 75 %	25 - 50 %	< 25 %		
	Rating		20	17	13	8	3		
3	Spacing of discontinuities		> 200 cM	60 - 200 cM	20-60 cM	6-20 cM	<6 cM or <60 mm		
	Rating		20	15	10	8	5		
4	Condition of discontinuities		Very rough surfaces Not continuous No separation Unweathered wall rock (hard wall)	Slightly rough surfaces Separation < 1 mm, Slightly weathered walls (hard wall)	Slightly rough surfaces Separation < 1 mm Highly weathered walls (soft wall)	Slickenside surfaces or Gouge < 5 mm thick or Separation 1-5 mm Continuous	Soft gouge >5 mm thick or Separation > 5 mm Continuous		
	Rating		30	25	20	10	0		
5	Ground water	Inflow per 10 m tunnel length (l/m)	Non	<10	10 – 25	25 – 125	> 125		
		(Joint water press)/ (Major principal V).	0	0 - 0,1	0,1 - 0,2	0,2 - 0,5	> 0,5		
		General conditions	Completely	Dry	Wet	Dripping	Flowing		
		Rating	15	10	7	4	0		